

ANISOTROPIC EFFECTS FOLLOWING
INNER SHELL IONIZATION

BY

SAMUEL CRAIG McFARLANE, B.Sc.

Thesis submitted to the University of Stirling for
for the degree of Doctor of Philosophy.

Physics Department,
University of Stirling,
Stirling.

ProQuest Number: 13917076

All rights reserved

INFORMATION TO ALL USERS

The quality of this reproduction is dependent upon the quality of the copy submitted.

In the unlikely event that the author did not send a complete manuscript and there are missing pages, these will be noted. Also, if material had to be removed, a note will indicate the deletion.



ProQuest 13917076

Published by ProQuest LLC (2019). Copyright of the Dissertation is held by the Author.

All rights reserved.

This work is protected against unauthorized copying under Title 17, United States Code
Microform Edition © ProQuest LLC.

ProQuest LLC.
789 East Eisenhower Parkway
P.O. Box 1346
Ann Arbor, MI 48106 – 1346

ABSTRACT

This thesis looks into the possibility that X radiation following inner shell ionization by electron impact might be polarized. There has been some speculation on this point: one published conclusion (Cooper and Zare, 1968) is that the polarization must be zero; another conclusion (Mehlhorn, 1968) is that the polarization need not be zero and can be substantially polarized. By application of the Bethe and Born collision theories (Chapters 4 and 5), it will be shown that both these assertions are wrong: a non-zero polarization can exist, but will be extremely small, even in the region of high impact energies. This work (McFarlane, 1972) has been indirectly confirmed by measurements of the related phenomenon of the angular distribution of Auger electrons following inner shell ionization by electrons (Cleff and Mehlhorn, 1971). By extending the Bethe theory to include relativistic corrections after the manner of Møller (1932) it is shown (Chapter 6) that the polarization approaches its high energy limit only very slowly.

The thesis also looks at other anisotropic processes following electron and photon impact. Chapter 7 deals with

the related problem of Auger electron angular distributions following inner shell photoionization. Chapter 8 postulates a directional correlation between photoelectrons and Auger electrons. Chapter 9 shows that the spin of a photoelectron is correlated with its direction of ejection, if there is significant fine structure interaction in the bound state.

An appendix is concerned with the high energy limit of the form of anisotropies, and shows that this limit is more subtle than has been realized. An analytic, compact expression for the line polarization is hence derived and tested successfully against experiment and a more complicated theory.

ACKNOWLEDGMENTS:

Several people have helped me towards completing the work in this thesis, and I should like to thank them. The number of colleagues at Stirling who have helped me in many discussions is too large to list individually. In particular, however, I should like to thank Dr. A. Dickinson for a critical reading of part of the manuscript and for his willingness to discuss and clarify many points. My sincere thanks go to Mr. A. Clark for his help with computer programming and for his readiness to perform many small tasks associated with the preparation of the typescript. Mrs. C. Phillips has typed a none-too-clear manuscript with speed and skill. I have been fortunate to have as my supervisor Professor I.C. Percival. I thank him for his wise direction, assistance and encouragement, and for the example of his own approach to theoretical physics. I wish to acknowledge the award of an S.R.C. Research Studentship, during which much of the present work was performed.

Finally, I wish to thank my wife Fiona for her forbearance, which has been much tried in the past few years.

CONTENTS

<u>Chapter 1</u>	Preliminaries	
1.	Introduction	1
2.	The Radiative Problem	7
 <u>Chapter 2</u>	 A Cross Section Transformation Relation for Inner Shell Ionization.	
1.	Deriving the Relation	11
2.	Physical Interpretation	15
3.	Coupling to Angular Momenta in Outer Shells.	20
 <u>Chapter 3</u>	 The Dipole Approximation	
1.	Dipole Matrix Element: One-Electron Problem	22
2.	Dipole Matrix Element: Many-Electron Problem	27
 <u>Chapter 4</u>	 The Bethe Theory	
1.	Preliminary Remarks - Threshold Polarization.	40
2.	The Bethe Limit	43

Chapter 4 (continued)

3. An Improved Bethe Theory I: 52
Direction of Momentum Transfer
4. An Improved Bethe Theory II: 60
Non-Dipole Transitions

Chapter 5: The Born Approximation:

1. Theory 68
2. Results 74

Chapter 6: Relativistic Modification of the
Bethe Theory

1. Introductory Remarks 81
2. The Need for Modifying the Møller 82
Formula
3. An Outline of Møller's Method 87
4. Adapting the Møller Formula 93

Chapter 7: Anisotropy Following Inner Shell Photoionization

1. Introduction 100
2. Calculations and Results 101
3. Comments 106

Chapter 8: Directional Correlation in Inner
Shell Photoionization.

1. Theory 111
2. Results

Chapter 9: Correlation between Spin Polarization and Angle of Photoejection

1. General Case: Arbitrary Angle of Ejection. 128
2. Special Case: Ejection Along Quantization Axis. 133
3. Results. 135

Appendix: The Form of Anisotropies in the High-Energy Limit of the Born Approximation. 140

References: 154

CHAPTER 1

PRELIMINARIES

1. Introduction

This thesis will touch on various topics which can all be assembled under the heading: the study of anisotropic processes following electron- and photon-atom collisions. A justification for such a study may be put forward as follows:

- (a) Knowledge of angular distributions can be vital in obtaining accurate total cross sections. For example, polarization corrections must be applied to excitation cross sections obtained by optical measurements. (An account of how such corrections may be made is contained in the review by Moiseiwitsch and Smith, 1968). Hence it is necessary to know the polarization of the emitted light as a function of collision energy.
- (b) The quantum-mechanical amplitude for an anisotropic process of the type dealt with here can be factorized into a radial and an angular part (Wigner-Eckart theorem). The latter depends only on the rotational symmetry of the problem and can be treated by standard Racah methods (see, for example, Edmonds, 1960). The former contains the detailed

information on the structure and interaction. To take an example from nuclear physics, the angular distribution between two radiations emitted successively from a nucleus depends partly on symmetry properties, i.e. on the angular momenta of the states involved, and partly on the detailed structure of the states. A classical example is the motion of a particle in a central field. The symmetry of the interaction leads to a plane orbit and conservation of angular momentum, while the exact shape of the orbit depends upon the detailed form of the central interaction. To return to the radial amplitudes, anisotropic processes give information on the ratio of their squared moduli, whereas total cross sections depend usually on the sum of the squared moduli. The types of measurement can thus be complementary.

- (c) As long ago as 1933, Massey and Mohr calculated angular distributions of electrons ejected in collisions of fast electrons with hydrogen atoms. No experimental information was (or, to the writer's knowledge, is yet) available to check against their calculations. However, this kind of situation is changing, and experimental measurements of differential cross sections are increasingly becoming available. Such experiments will be mentioned as appropriate in the text. Hence the interest in anisotropic processes seems likely to increase.

The kind of process dealt with here, then, is the inelastic collision of a photon or an electron with an atom resulting in the removal of a bound electron from an inner shell of the atom. (An appendix deals with the polarization of outer shell radiation following electron excitation).

When a photon is absorbed by an atom it thereby gives up its angular momentum to the atom, and hence the latter may be left in a non-spherically symmetric state. Thus when the excited atoms relax, the anisotropy can be reflected in a non-uniform distribution of the relaxation products (e.g. photons or Auger electrons). Notice that use of unpolarized radiation does not preclude the introduction of anisotropy, for no angular momentum may be transferred to the atom in the direction of the beam. It is necessary that a collimated beam of radiation be used (but not, for some types of anisotropy, sufficient).

In collisions of electrons with atoms (and molecules) the anisotropy can usefully be thought of as arising from the receipt by the atom of a momentum transfer, $\hbar \mathbf{k}$, which is not isotropically distributed. For a given angle of scattering the direction $\hat{\mathbf{k}}$ is uniquely defined. However, if the angle of scattering is not detected, the direction $\hat{\mathbf{k}}$ is in effect averaged, even for a fixed velocity of impact. The

customary picture, due to Bethe (1933), is of the variation of \hat{k} from being parallel to the direction of incidence at the threshold excitation energy, to being perpendicular to this direction in the limit of high energies. Hence the anisotropy gradually makes a transition between two limiting forms as the collision energy is varied. We shall make a more thorough analysis of the variation of \hat{k} in connection with Bethe's theory.

Finally, we give a resumé of the contents of the thesis.

The remaining section of this chapter derives expressions for the polarization of the characteristic X-ray lines when the atom has been left with a vacancy in an inner shell, the vacancy distribution being known.

Chapter 2 derives a relation which relates the cross sections for ionization from the "fine structure" states ($n l j m_j$) to those for the "uncoupled" states ($n l m$).

Chapter 3 obtains expressions for dipole matrix elements (bound \rightarrow free) which are useful both for photoionization and electron ionization (Bethe theory).

Chapter 4 applies the Bethe theory to inner shell ionization by electrons. In the process a prescription is obtained for the treatment of the direction $\hat{\mathbf{K}}$ which is of wider application (see Appendix).

Chapter 5 applies the Born approximation to L-shell ionization. It is shown that earlier treatments of this problem must be modified owing to their choice of quantization axis. The polarization of some X-ray lines is calculated in this way as a function of collision energy. Also, comparison is made with some experimental results on the angular distribution of Auger electrons ejected from the L_3 -shell of argon by electrons (Cleff and Mehlhorn, 1971).

Chapter 6 modifies the Bethe theory to take into account the effect of relativity in the motion of the incident and bound particles. In effect, this requires the adaptation of Møller's theory (1930).

Chapter 7 calculates the asymmetry coefficient of the angular distribution of Auger electrons following photoionization. Some earlier calculations of a similar type are commented on.

Chapter 8 postulates a correlation between the direction of photoelectrons and that of the resultant Auger electrons following the inner shell photoeffect. The nature of the correlation is estimated and an experiment to investigate the effect is suggested.

Chapter 9 shows that the photoelectrons which originate from individual fine structure levels will be partially spin-polarized, the degree of spin polarization depending markedly on the direction of ejection. In particular, the polarization of forward-ejected photoelectrons may be obtained solely from a consideration of angular momentum.

Finally, the Appendix considers two opposing views of the form of anisotropies in the high energy limit of electron impact. One is these is vindicated (with qualifications) and the other shown to be erroneous. In the process, a very simple analytic formula, giving the polarization of optical radiation excited by electron impact as a function of collision energy, is derived. It depends on a single, well-known collisional parameter which is related to the differential scattering cross section. The simple formula is shown to compare well with the Born approximation as applied to helium excitation by Ariens and Carrière (1970).

2. The Radiative Problem

The problem dealt with in this section may be stated as follows: given a certain vacancy distribution following inner shell ionization, what will be the resultant polarization of the X-ray lines emitted when these vacancies are filled by radiative transitions from higher shells?

Due to the complete analogy between the parts played by the electron and the vacancy respectively, the radiative problem of Percival and Seaton (1958; called PS hereafter) is equivalent to that treated here. However, two of the transitions we wish to consider - $L_3 \rightarrow M_4, M_5$ ($2^2 p_{3/2} \rightarrow 3^2 d_{3/2, 5/2}$) - are not tabulated by Percival and Seaton, and we will derive the appropriate expression for the polarization of these lines here. The third transition - $L_3 \rightarrow M_1$ ($2^2 p_{3/2} \rightarrow 3^2 s_{1/2}$) is tabulated by Percival and Seaton; we will derive this also as a check on our algebra.

We begin by defining our axis of magnetic quantization to be the direction of the incoming electrons. The percentage polarization of the radiation is

$$P = 100 \frac{I'' - I^\perp}{I'' + I^\perp} \quad (1.2.1)$$

where I'' and I^\perp are the radiation intensities, in a direction perpendicular to the quantization axis Oz , with electric vectors respectively parallel and perpendicular to Oz . By a generalization of the argument given by Percival and Seaton, we may write for P :

$$P = 100 \frac{3K_z - K}{K_z + K} \quad (1.2.2)$$

K_z is the rate coefficient for emission of photons characteristic of a dipole aligned along the Z-axis, K is the total rate coefficient for emission of all photons. They are defined by the relations

$$K_z = \frac{\nu}{A} \sum_{\alpha, \beta} A_z(\alpha \rightarrow \beta) Q(\alpha) \quad (1.2.3)$$

$$K = \nu \sum_{\alpha} Q(\alpha) \quad (1.2.4)$$

Here α represents the substates of the ionized level and β those of the level to which the vacancy makes its transition, subsequent to ionization. $Q(\alpha)$ is the ionization cross section for the initial substate α . A_z is the radiative transition probability for emission of a Z-photon:

$$A_z(\alpha \rightarrow \beta) = C |\langle \beta | z | \alpha \rangle|^2 \quad (1.2.5)$$

where C is a multiplicative constant which need not concern us here. A is the radiative transition probability summed over polarizations.

Now since X-ray levels exhibit fine structure, we must consider a transition of the type $(j m_j \rightarrow j' m_{j'})$. The necessary cross section transformation relation to express the $Q(j m_j)$ in terms of the $Q(l m)$ is established in the following chapter. It is

$$Q(j m_j) = \frac{1}{2} \sum_{m, m_s} [j] \begin{pmatrix} l & \frac{1}{2} & j \\ m & m_s & -m_j \end{pmatrix}^2 Q(l, m) \quad (1.2.6)$$

where the factor of $\frac{1}{2}$ arises because $Q(l m m_s)$ is independent of m_s , and we have put $[j] = 2j + 1$. Using the Wigner-Eckart theorem, we have

$$A_z(j m_j \rightarrow j' m_{j'}) = \begin{pmatrix} j & 1 & j' \\ m_j & 0 & -m_{j'} \end{pmatrix}^2 [j] A(j \rightarrow j') \quad (1.2.7)$$

where

$$A(j \rightarrow j') = \sum_{m_{j'}, \mu} A_\mu(j m_j \rightarrow j' m_{j'}) \quad (1.2.8)$$

In obtaining (1.2.7) we have used the fact that \mathbf{z} may be considered as a component of an irreducible tensor operator. Using (1.2.6) and (1.2.7) in (1.2.3) gives

$$K_z = \frac{\nu}{2} \cdot \frac{A(j \rightarrow j')}{A(j)} [j'] [j] \\ \cdot \sum_{m_j, m_{j'}} \sum_{m_s, m_s} \sum_{\mu} \begin{pmatrix} j & 1 & j' \\ m_j & 0 & -m_{j'} \end{pmatrix}^2 \begin{pmatrix} l & \frac{1}{2} & j \\ m & m_s & -m_j \end{pmatrix}^2 Q(lm) \quad (1.2.9)$$

Also,

$$K = \frac{\nu}{2} \frac{A(j \rightarrow j')}{A(j)} \cdot \frac{[j]}{[l]} \sum_m Q(lm) \quad (1.2.10)$$

By employing (1.2.2), (1.2.9) and (1.2.10) we may calculate

$P(j \rightarrow j')$ in terms of the $Q(lm)$. We find

$$P(L_3 \rightarrow M_1) = 300 \frac{Q_0 - Q_1}{5Q_0 + 7Q_1} \quad (1.2.11a)$$

$$P(L_3 \rightarrow M_4) = 300 \frac{Q_1 - Q_0}{4Q_0 + 11Q_1} \quad (1.2.11b)$$

$$P(L_3 \rightarrow M_5) = 100 \frac{Q_0 - Q_1}{7Q_0 + 13Q_1} \quad (1.2.11c)$$

where Q_0 and Q_1 abbreviate $Q(2p, 0)$ and $Q(2p, \pm 1)$.

The first of these agrees with the tables of Percival and

Seaton.

CHAPTER 2

A CROSS SECTION TRANSFORMATION RELATION
FOR INNER SHELL IONIZATION

1. Deriving the Relation

In the theory of atomic line polarization by electron impact, one calculates cross sections for excitation to individual magnetic substates of the upper level. We may designate these cross sections $Q(\alpha SL M_S M_L)$, α being any other quantum numbers needed to specify the state fully. If the upper level has well-defined fine structure, one must express cross sections $Q(\alpha SL J M_J)$ in terms of those with definite M_L . The necessary relation was obtained by Percival and Seaton (1958) and can be written

$$Q(\alpha SL J M_J) = \sum_{M_S M_L} [J] \begin{pmatrix} S & L & J \\ M_S & M_L & -M_J \end{pmatrix}^2 \cdot Q(\alpha SL M_S M_L) \quad (2.1.1)$$

where we have used Wigner's $3j$ -symbol and the abbreviation

$[J] = 2J + 1$. Now Percival and Seaton emphasize that this relation is valid only so long as three assumptions remain valid. These are:

- (a) that LS-coupling holds (i.e. the spin-orbit interaction is weak);
- (b) that the initial state of the atom has zero orbital angular momentum;
- (c) and that the interaction potential producing the transition does not involve spin co-ordinates.

The related phenomenon of polarization of characteristic X-rays excited by electron impact, the study of which forms a major part of this thesis, has attracted some attention in the literature quite recently; relevant references are contained in Chapter 5. Since X-ray levels invariably exhibit well-developed fine structure - the "spin doublets" of X-ray spectroscopy - one must therefore express the cross section for ionization of the atom from the spin-orbital characterized by the set of one-electron quantum numbers $(n \ell j m_j)$ in terms of the set $(n \ell m m_s)$. The published papers mentioned above have in fact employed a relation for this purpose. It is

$$Q(n \ell j m_j) = \sum_{m m_s} \binom{\ell \ s \ j}{m \ m_s - m_j}^2 [j] Q(n \ell m m_s) \quad (2.1.2)$$

Now this second relation has been employed without proof - the similarity to (2.1.1) shows that it has been merely extended to include the second situation. The validity of

such an extension is not self-evident; nor are the constraints (corresponding to the conditions (a), (b) and (c) placed on the use of (2.1.1) by Percival and Seaton) on the use of (2.1.2) obvious. For one thing, it is clearly not true that LS-coupling holds for X-ray levels. We will now show that (2.1.2) can be used for the stated purpose - in fact, the proof is very simple. But the above remarks should make it plain that (2.1.1) and (2.1.2) refer to two quite distinct physical situations, so that the one cannot simply be inferred from the other.

We denote by $(\underline{\kappa}, m_s')$ the wave vector and spin state of the ejected electron. In the same way the incident and scattered electron is labelled by $(\underline{k}_0, m_{s_0})$ and $(\underline{k}_1, m_{s_1})$ respectively. Hence we represent the process by the transition amplitude

$$T(nl_j m_j) = \langle \underline{\kappa}, m_s'; \underline{k}_1, m_{s_1} | T(nl_j m_j; \underline{k}_0, m_{s_0}) \rangle \quad (2.1.3)$$

It will be necessary to adopt assumption (c) above - that the interaction is spin - independent - so that total spin and orbital angular momenta will be separately conserved. Uncoupling the spin and orbital angular momenta of the bound electron, we write:

$$T(nl j m_j) = \sum_{m m_s} \begin{pmatrix} l & s & j \\ m & m_s - m_j & \end{pmatrix} [j]^{1/2} (-1)^{l+s-m_j} \cdot \langle \tilde{\kappa}, m_s'; \tilde{\kappa}_1, m_{s_1} | T | n l m m_s; \tilde{\kappa}_0, m_{s_0} \rangle \quad (2.1.4)$$

Conservation of total spin imposes the constraint

$$m_s + m_{s_0} = m_{s_1}' + m_{s_1} \quad (2.1.5)$$

The cross section is proportional to the squared modulus of (2.1.4). We see that cross terms will arise in m and m_s . However, the conservation condition (2.1.5) eliminates cross terms in m_s , and the remaining cross terms vanish as a result of the condition

$$m_j = m + m_s \quad (2.1.6)$$

imposed by the 3j-symbol. Thus we have

$$|T(nl j m_j)|^2 = \sum_{m m_s} \begin{pmatrix} l & s & j \\ m & m_s - m_j & \end{pmatrix}^2 [j] |T(nl m m_s)|^2 \quad (2.1.7)$$

and (2.1.2) follows immediately. We see that the fact that the spin component m_s' of the ejected electron is a good quantum number is essential to the existence of (2.1.2).

This corresponds to the imposition of the constraint (b) in the case of discrete excitation. In other words, (2.1.1) and (2.1.2) hold because in the former case there is no spin-orbit interaction in the initial state, in the latter

there is none in the final state.

As for condition (a) above, the question of LS-coupling, we see that it does not arise for inner shell ionization, where the ionized subshell is initially complete and therefore there is only a single vacancy in the shell after ionization. The Pauli vacancy principle tells us that this vacancy behaves like a single electron in an otherwise empty subshell.

2. Physical Interpretation

In the previous section we saw that the relations (2.1.1) and (2.1.2) hold only so long as there is no spin-orbit interaction in one of the two states connected by the collisional interaction. It is possible to present a physical interpretation of this rule as follows. The physical content of the two transformation relations is, in effect, that no interference takes place between the amplitudes represented on the right hand side of each relation. In Figure 2.1 a schematic diagram has been drawn of the collisional transition $n^2 S_{1/2} \rightarrow n'2 P_{3/2}$. The degenerate magnetic substates have been shown as separate for convenience. We can think of the transition as being

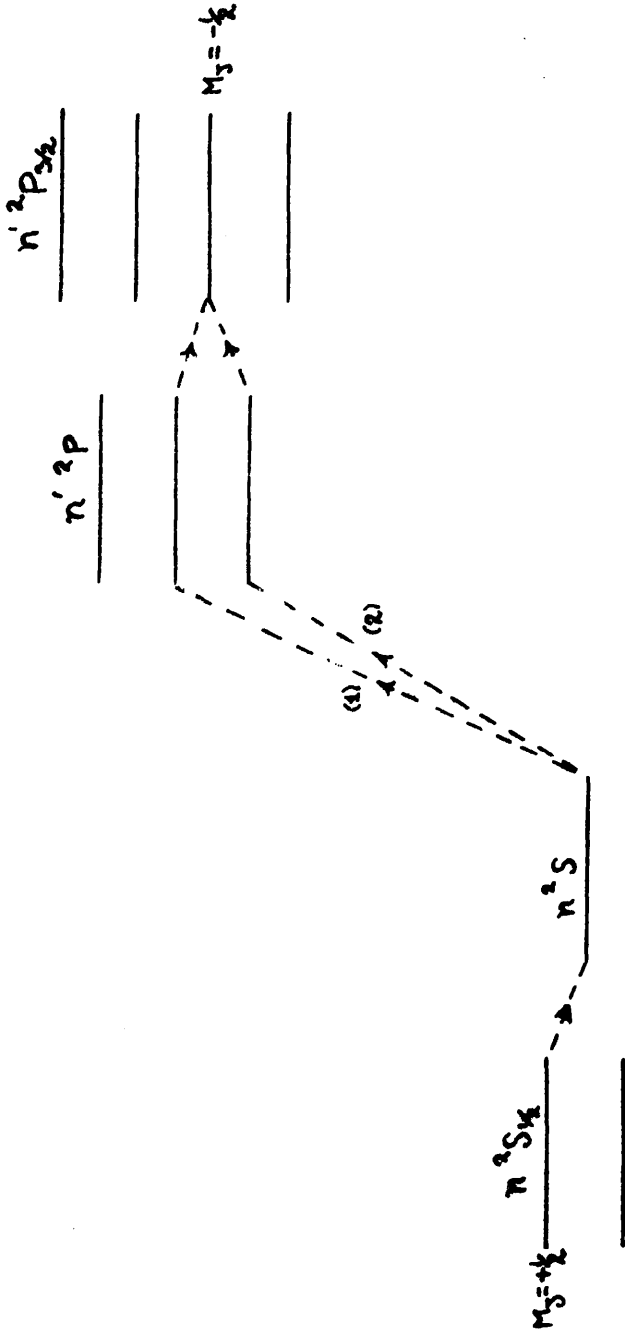


Fig. (2.1)

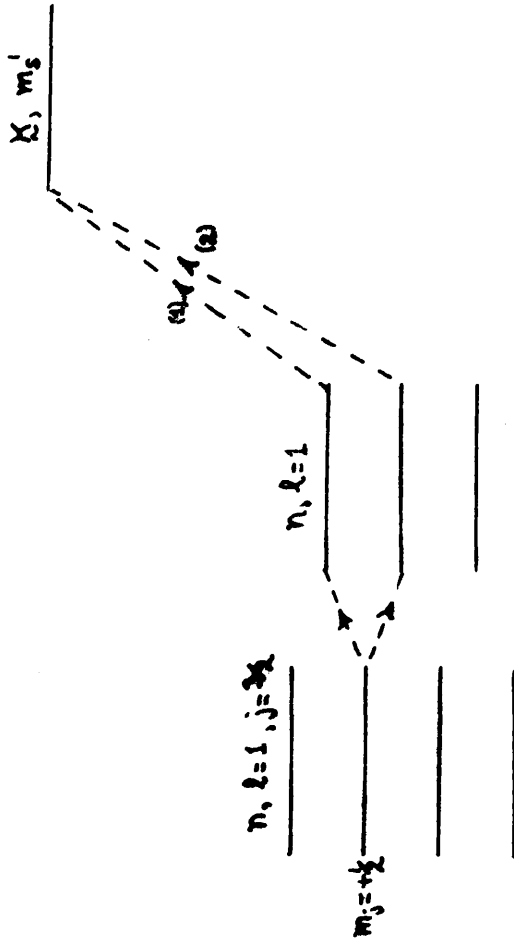


Fig. (2.3)

accomplished in three distinct stages: first, the spin-orbit interaction in the ground state takes the atom into a state of definite M_L ; secondly, the collisional interaction causes a transition to an excited state of definite M_J ; and thirdly, the spin-orbit interaction in the excited state takes the atom into a state of definite M_J . In particular we have shown the transition ($n^2 S_{\frac{1}{2}}, M_J = +\frac{1}{2} \longrightarrow n^2 P_{\frac{3}{2}}, M_J = -\frac{1}{2}$). There exist two possible paths the transition may take, subject to the conservation of angular momentum: via upper states with $M_L = 0$ and $M_L = -1$ respectively. However, the amplitudes for these two paths may not interfere if it is possible, in principle, to determine which was taken in any particular case without disturbing the process. This rule is a consequence of the Uncertainty Principle and is basic to quantum mechanics. A discussion of this point may be found in Feynman and Hibbs (1965, Chapter 1). To use their terminology, the two paths represent exclusive (as against interfering) alternatives, because they could have been separately identified by the information available. If we use a spin-polarized electron beam and detect the spin component of the scattered electron, we know from spin conservation the change in spin component of the atom, ΔM_S . Measurement of the initial and final orientations

of the atom gives us ΔM_J . Hence, since $\Delta M_L = \Delta M_J - \Delta M_S$ we know which of the two paths was actually taken in a given instance. Note that preparation of beam and target in no way limits the discussion, since unpolarized beams and randomly-orientated targets can be represented by statistical ensembles of prepared systems.

Figure 2.2 by contrast illustrates the transition

$(n^2 P_{3/2}, M_J = -\frac{1}{2} \rightarrow n' 2 P_{3/2}, M_J = +\frac{1}{2})$. Here we can still determine ΔM_L , but paths (1) and (2) both have $\Delta M_L = +1$ and are therefore interfering alternatives.

Figure 2.3 shows that no interfering alternatives arise for the case of ionization, since we are faced again with exclusive alternatives.

3. Coupling to Angular Momenta in Outer Shells

A contingency which would upset the simple situation corresponding to (2.1.2) would be if the angular momentum of the vacancy were to couple to another source of angular momentum - that of a partially filled outer shell. However, such coupling would lead to a further splitting of the X-ray doublets and could be observed experimentally. In

fact, the idea that such higher multiplicities could arise was propounded as far back as 1926 by Coster and Mulder, but has never been observed in the Kor L groups, due probably to the large natural widths of the lines. Van der Tuuk (1927) has observed what appear to be unresolved multiplets in the M series lines of the rare earths. Thus it seems reasonable to treat the atom in an inner shell ionization process as if its initial angular momentum were zero, in accordance with assumption (b) of § 2.1.

CHAPTER 3

THE DIPOLE APPROXIMATION

1) Dipole Matrix Element: One-Electron Problem

In the following chapters of this thesis we shall see that the same matrix elements - those of the components of the position operator, \underline{r} - occur both in the treatment of photoionization and in the treatment of electron-atom collisions at high energy known as the Bethe approximation (see, for instance, Mott & Massey, 1965, p.497). Therefore it seemed appropriate to evaluate these matrix elements prior to a consideration of either of these theories and to call on the results whenever necessary.

It simplifies the use of tensor operator theory if we express r in terms of its spherical components, $r C_{\mu}^1$ ($\mu = 0, \pm 1$). These are related to the Cartesian components by

$$r C_0^1 = z \quad , \quad r C_{\pm 1}^1 = \frac{1}{\sqrt{2}} (x \pm iy) \quad (3.1.1.)$$

We require the matrix elements of these operators between initial and final states $|\psi_i\rangle$ and $|\psi_f\rangle$ where

$$|\psi_i\rangle = R_{n\ell'}(r) |l'm'\rangle \quad (3.1.2)$$

represents the bound state of the electron and is therefore an eigenstate of angular momentum; and

$$|\Psi_f\rangle = 4\pi \sum_{l,m} (i)^l e^{-i\delta_l} Y_{l,m}^*(\hat{\kappa}) Y_{l,m}(\hat{r}) G_{\kappa l}(r) \quad (3.1.3)$$

represents the ejection of the electron in the direction $\hat{\kappa}$ with momentum $\hbar\kappa$, and thus is not an eigenstate of angular momentum. $G_{\kappa l}(r)$ is the radial wavefunction divided by κr and δ_l is the phase shift (Coulomb + non-Coulomb) of the l th partial scattered wave. The normalization of $G_{\kappa l}(r)$ need not be discussed here, concerned as we shall be with relative transition probabilities. It will be convenient to rewrite (3.1.3) as

$$|\Psi_f\rangle = \sum_{l,m} a(l,m) Y_{l,m}(\hat{r}) G_{\kappa l}(r) \quad (3.1.4)$$

where

$$a(l,m) = 4\pi (i)^l e^{-i\delta_l} Y_{l,m}^*(\hat{\kappa}) \quad (3.1.5)$$

The dipole matrix element for the transition may now be written:

$$\langle \Psi_f | r C_{\mu}^1 | \Psi_i \rangle = \sum_{l,m} a(l,m) R_{\kappa,l} \langle l m | C_{\mu}^1 | l' m' \rangle \quad (3.1.6)$$

$R_{\kappa,l}$ is the radial dipole integral

$$R_{\kappa,l} = \int_0^{\infty} r^3 R_{n l'}(r) G_{\kappa l}(r) dr \quad (1.7)$$

By application of the Wigner-Eckart theorem

$$\langle \ell m | C_{\mu}^1 | \ell' m' \rangle = (-1)^{\ell-m} \langle \ell || C^1 || \ell' \rangle \cdot \begin{pmatrix} \ell' & 1 & \ell \\ m' & \mu & -m \end{pmatrix} \quad (3.1.8)$$

where the reduced matrix element

$$\langle \ell || C^1 || \ell' \rangle = (-1)^g \ell_{>}^{1/2} \quad (3.1.9)$$

and $g = (\ell' - \ell + 1)/2$, $\ell_{>}$ being the greater of ℓ and ℓ' . Thus (3.1.6) becomes

$$\langle \Psi_f | r C_{\mu}^1 | \Psi_i \rangle = \sum_{\ell, m} a(\ell, m) (-1)^{\ell-m+g} \ell_{>}^{1/2} \cdot R_{X, \ell} \begin{pmatrix} \ell' & 1 & \ell \\ m' & \mu & -m \end{pmatrix} \quad (3.1.10)$$

The transition probability is obtained by squaring (3.1.10):

$$\begin{aligned} \bar{P}(n \ell' m' \rightarrow X) &= |\langle \Psi_f | r C_{\mu}^1 | \Psi_i \rangle|^2 \\ &= \sum_{\ell_1, \ell_2} a(\ell_1, m+\mu) a^*(\ell_2, m+\mu) \\ &\quad \cdot (-1)^{\ell_1+\ell_2+g_1+g_2} \ell_{1>}^{1/2} \ell_{2>}^{1/2} R_{X, \ell_1} R_{X, \ell_2} \\ &\quad \cdot \begin{pmatrix} \ell' & 1 & \ell_1 \\ m' & \mu & -m'-\mu \end{pmatrix} \begin{pmatrix} \ell' & 1 & \ell_2 \\ m' & \mu & -m'-\mu \end{pmatrix} \end{aligned} \quad (3.1.11)$$

where the properties of the 3j-symbol have been used to eliminate two summations. We make use of the convenient quantity \bar{P} , where $P = \alpha \bar{P}$ is the exact transition probability and α is left undefined at this stage. We now integrate over all directions of ejection and use the orthonormality property of spherical harmonics. Thus (3.1.11) becomes

$$\begin{aligned} \bar{P}(n\ell'm' \rightarrow \kappa) &= \int |\langle \Psi_f | r C_{\mu}^1 | \Psi_i \rangle|^2 d\omega(\hat{\kappa}) \\ &= (4\pi)^2 \sum_{\ell} \ell > \mathcal{R}_{\kappa, \ell}^2 \left(\begin{array}{ccc} \ell' & 1 & \ell \\ m' & \mu & -m' - \mu \end{array} \right)^2 \end{aligned} \quad (3.1.12)$$

The summation over ℓ is limited by the selection properties of the 3j-symbol to the terms $\ell = \ell' + 1$ and $\ell = \ell' - 1$. Hence we have, on dropping the primes,

$$\begin{aligned} \bar{P}(n\ell m \rightarrow \kappa) &= (4\pi)^2 \left\{ (\ell+1) \mathcal{R}_{\kappa, \ell+1}^2 \right. \\ &\quad \left. \cdot \left(\begin{array}{ccc} \ell & 1 & \ell+1 \\ m & \mu & -m-\mu \end{array} \right)^2 + (\ell) \mathcal{R}_{\kappa, \ell-1}^2 \left(\begin{array}{ccc} \ell & 1 & \ell-1 \\ m & \mu & -m-\mu \end{array} \right)^2 \right\} \end{aligned} \quad (3.1.13)$$

If there is an appreciable spin-orbit interaction in the initial state, we must describe the bound electron by means of the quantum numbers $(n \ell j m_j)$. Hence to evaluate the dipole matrix element we first make the expansion

$$\begin{aligned}
 |\Psi_i\rangle &= \Psi(n \ell j m_j) \\
 &= \sum_{m, m_s} R_{n\ell}(r) | \ell m \rangle \chi_{m_s}^{\frac{1}{2}} \\
 &\quad \cdot (-1)^{\ell - \frac{1}{2} + m_j} [j]^{\frac{1}{2}} \begin{pmatrix} \ell & \frac{1}{2} & j \\ m & m_s & -m_j \end{pmatrix} \quad (3.1.14)
 \end{aligned}$$

where $[j] = 2j + 1$. $|\Psi_f\rangle$ is unchanged apart from multiplication by its spin function $\chi_{m_s'}^{\frac{1}{2}}$. Evaluating the dipole matrix element as before we find that

$$\begin{aligned}
 &\langle \Psi_f | r C_{\mu}^1 | \Psi_i \rangle_{\text{coupled}} \\
 &= \sum_m (-1)^{\ell - \frac{1}{2} + m_j} [j]^{\frac{1}{2}} \begin{pmatrix} \ell & \frac{1}{2} & j \\ m & m_j - m & -m_j \end{pmatrix} \quad (3.1.15)
 \end{aligned}$$

$$\langle \Psi_f | r C_{\mu}^1 | \Psi_i \rangle_{\text{uncoupled}}$$

where we have summed over final spin m_s' . On squaring the matrix element and integrating over angles of ejection we can show that

$$\begin{aligned}
 \bar{P}(n \ell j m_j \rightarrow \kappa) &= (2j + 1) (4\pi)^2 \sum_m \begin{pmatrix} \ell & \frac{1}{2} & j \\ m & m_j - m & -m_j \end{pmatrix}^2 \\
 &\cdot \left\{ (\ell + 1) R_{\kappa, \ell + 1}^2 \begin{pmatrix} \ell & 1 & \ell + 1 \\ m & \mu & -m - \mu \end{pmatrix}^2 + (\ell) R_{\kappa, \ell - 1}^2 \begin{pmatrix} \ell & 1 & \ell - 1 \\ m & \mu & -m - \mu \end{pmatrix}^2 \right\} \quad (3.1.16)
 \end{aligned}$$

2.- Dipole Matrix Element: Many-Electron Problem

In this section we generalize the considerations of the previous section to atoms containing many electrons. In such atoms the electron which is removed by the ionization process will initially be coupled to the other electrons via spin-orbit and electrostatic interactions. Also, we must take account of the indistinguishability of the electrons; this means that, as fermions, they must be represented by a wavefunction which is antisymmetric under exchange of particles. Accordingly, we shall construct such N-particle wavefunctions for the extreme cases of L S and j-j coupling, and use them to recalculate the dipole matrix element.

We assume that the initial and final states may be represented as a Slater determinant of spin-orbitals, the radial wavefunctions being calculated in the central field approximation.

(a) j-j Coupling

Here the good quantum numbers are l_1, l_2, \dots, l_N , j_1, j_2, \dots, j_N , S_1, S_2, \dots, S_N , J, M_J (along with $N - 2$ quantum numbers representing intermediate stages in the coupling of the j's to form J). We write the initial state wavefunction as

$$|\Psi_i\rangle = \frac{1}{\sqrt{N!}} \sum_{\mathcal{P}} (-1)^{\mathcal{P}} \mathcal{P} \Psi(\alpha J M_J)$$

(3.2.1)

where \mathcal{P} is the permutation operator and α represents the remaining $4N-2$ quantum numbers. The final state wavefunction may be written as

$$|\Psi_f\rangle = \frac{1}{\sqrt{N!}} \sum_{\mathcal{P}} \sum_{\ell, m} (-1)^{\mathcal{P}} \mathcal{P} a(\ell, m) \Psi(\alpha'' J'' M_J) \cdot \mathcal{Q}(n \ell m m_s) \quad (3.2.2)$$

where $a(\ell, m)$ is as given by (3.1.5). Ψ represents the state of the ion and \mathcal{Q} that of the ejected electron. We now expand the N -particle wavefunction $|\Psi_i\rangle$ in terms of its $(N-1)$ -particle parent wavefunctions:

$$|\Psi_i\rangle = \sum_{\substack{\alpha', J', n', \ell', j' \\ n', \ell', j'}} |\alpha' J', n' \ell' j'; \alpha J M_J\rangle \cdot \langle \alpha' J', n' \ell' j' | \alpha J \rangle \quad (3.2.3)$$

where

$$|\alpha' J', n' \ell' j'; \alpha J M_J\rangle = \sum_{M_J', m_j'} \Psi(\alpha' J' M_J') \mathcal{Q}(n' \ell' j' m_j') \cdot (-1)^{J' - j' + M_J} \begin{pmatrix} J' & j' & J \\ M_J' & m_j' & -M_J \end{pmatrix} [J]^{1/2} \quad (3.2.4)$$

Note that in this expression the (N-1)-particle functions

$\Psi(\alpha' J' M_J')$ are understood to be antisymmetrized. The quantity $\langle \alpha' J', n' l' j' | \} \alpha J \rangle$, the weighting coefficient in the expansion (3.2.3), is known as the fractional parentage coefficient. Since the parent wavefunctions are orthonormal, the matrix element of a one-electron operator may receive contributions only when initial and final states possess a parent in common. Thus $|\Psi_i\rangle$ as written in (3.2.3) consists of a series of products of (N-1)-particle functions with one-particle functions, whereas $|\Psi_f\rangle$ consists of only one such product. Hence a non-zero contribution to the dipole matrix element occurs only when $\alpha' = \alpha''$, $J' = J''$, $M_J' = M_J''$ (or, in other words, when the "core" of non-jumping electrons does not change its quantum numbers). Hence the contributing terms in the expansion of $|\Psi_i\rangle$ are

$$\sum_{n'l'j'} \Psi(\alpha'' J'' M_J'') \varphi(n'l'j' M_J - M_J'')$$

$$\cdot (-1)^{J'' - j' + M_J} [J]^{1/2} \begin{pmatrix} J'' & j' & J \\ M_J'' & M_J - M_J'' & -M_J \end{pmatrix} \quad (3.2.5)$$

$$\cdot \langle \alpha'' J'', n' l' j' | \} \alpha J \rangle$$

At this point it should be noted that we shall use the Pauli

approximation to the exact Dirac wavefunction for the bound electron in evaluating the dipole matrix element (see Bethe and Salpeter (1957) p.148). In the Dirac theory, the radial eigenfunction depends on j and the argument presented here breaks down. The Pauli wavefunctions will constitute a good approximation only so long as $Z\alpha \approx Z/137$ is not comparable to unity. It is worth mentioning also that the Pauli solutions approximate those of Dirac more closely for $j = l + \frac{1}{2}$, since we shall be particularly concerned with the level arising from ionization of the L_3 -subshell ($n = 2$, $l = 1$, $j = \frac{3}{2}$).

The dipole matrix element is thus

$$\begin{aligned}
 & \langle \Psi_f | \sum_j r_j C_{\mu}^1 | \Psi_i \rangle \\
 &= \sum_{l,m} \sum_{m',m_s'} \sum_{n,l',j'} a^*(l,m) \langle \alpha'' J'', n'l'j' | \{ \alpha J \rangle \\
 & \cdot R_{x,\ell} \langle \ell || C_{\mu}^1 || \ell' \rangle [J]^{1/2} [j']^{1/2} (-1)^{\ell' - \frac{1}{2} + J'' - j' - M_J''} \\
 & \cdot \begin{pmatrix} \ell' & 1 & \ell \\ m' & \mu & -m \end{pmatrix} \begin{pmatrix} J'' & j' & J \\ M_J'' & M_J - M_J'' & -M_J \end{pmatrix} \begin{pmatrix} \ell' & \frac{1}{2} & j' \\ m' & m_s' & -M_J + M_J'' \end{pmatrix} \quad (3.2.6)
 \end{aligned}$$

where the expansion

$$\begin{aligned}
 & \Phi(n'l'j' M_J - M_J'') \\
 &= \sum_{m', m_s'} \Phi(n'l'm'm_s') \begin{pmatrix} l' & \frac{1}{2} & j' \\ m' & m_s' & -M_J + M_J'' \end{pmatrix} \\
 & \quad \cdot [j']^{\frac{1}{2}} (-1)^{l' - \frac{1}{2} + M_J - M_J''}
 \end{aligned} \tag{3.2.7}$$

has been used.

The reduced matrix element $\langle l \| \zeta^1 \| l' \rangle$ is given in (3.1.9). We now make use of the assumption that we need only consider the ejection of equivalent electrons, so that the summations over n', l' , and j' in (3.2.6) vanish. This will avoid cross-terms arising in these quantum numbers. Taking the squared modulus of (3.2.6) and integrating over all angles of ejection we find

$$\begin{aligned}
 & \bar{P}(\alpha J \rightarrow \alpha'' J'' M_J'', X) \\
 &= (2j+1)(4\pi)^2 \langle \alpha'' J'', n l j | \zeta^1 | \alpha J \rangle^2 \\
 & \cdot \sum_{M_J} \sum_{m, m_s} \begin{pmatrix} J'' & j & J \\ M_J'' & M_J - M_J'' & -M_J \end{pmatrix}^2 \begin{pmatrix} l & \frac{1}{2} & j \\ m & m_s & -M_J + M_J'' \end{pmatrix}^2 \\
 & \cdot \left\{ (l+1) R_{X, l+1}^2 \begin{pmatrix} l & 1 & l+1 \\ m & \mu & -m-\mu \end{pmatrix}^2 + (l) R_{X, l-1}^2 \begin{pmatrix} l & 1 & l-1 \\ m & \mu & -m-\mu \end{pmatrix}^2 \right\}
 \end{aligned} \tag{3.2.8}$$

where we have averaged over initial atomic orientations M_J ;

summed over final spin orientations m_s ; and dropped the primes on the initial one-electron orbital.

Now the form of (3.2.8) as compared with (3.1.17) implies that by taking account of the coupling to the other electrons we will in general reduce the degree of anisotropy in the final orientation of the atom. However, for the important case of a completely filled subshell ($J = M_J = 0$) prior to ionization, (3.2.8) reduces to (3.1.17), apart from a factor of $(2j+1)$, (which arises because of the implicit assumption here that the probability of finding an electron in the orbital $(n \ell_j m_j)$ is $(2j+1)^{-1}$, whereas in the previous section it is unity). One might have expected such a result from the "Pauli vacancy principle".

(b) LS coupling

In this case, the good quantum numbers are $l_1, l_2, \dots, l_N,$
 s_1, s_2, \dots, s_N , L, S, J and M_J (along with $2N - 4$
intermediate quantum numbers). The initial state wavefunction is

$$|\Psi_i\rangle = \frac{1}{\sqrt{N!}} \sum_P (-1)^P P \Psi(\alpha L S J M_J) \quad (3.2.9)$$

The final state wavefunction is

$$|\Psi_f\rangle = \frac{1}{\sqrt{N!}} \sum_P \sum_{\ell, m} (-1)^P P \alpha(\ell, m) \cdot \Psi(\alpha'' L'' S'' J'' M_J'') \varphi(n \ell m m_s) \quad (3.2.10)$$

Again we may expand $|\Psi_i\rangle$, an N-particle wavefunction, in terms of a series of (N-1)-particle parent wavefunctions:

$$|\Psi_i\rangle = \sum_{\substack{\alpha', L', S', \\ n', \ell'}} |\alpha' L' S', n' \ell'; \alpha L S J M_J\rangle \cdot \langle \alpha' L' S', n' \ell' | \alpha L S \rangle \quad (3.2.11)$$

where

$$\begin{aligned} & |\alpha' L' S', n' \ell'; \alpha L S J M_J\rangle \\ &= \sum_{M', m'} \sum_{M_s', m_s'} \sum_{M, M_s} \Psi(\alpha' L' S' M' M_s') \varphi(n' \ell' m' m_s') \\ & \cdot \begin{pmatrix} L' & \ell' & L \\ M' & m' & -M \end{pmatrix} \begin{pmatrix} S' & s' & S \\ M_s' & m_s' & -M_s \end{pmatrix} \begin{pmatrix} L & S & J \\ M & M_s & -M_J \end{pmatrix} \\ & \cdot ([L][S][J])^{\frac{1}{2}} (-1)^{L' - \ell' + M + S' - s' + M_s + L - S + M_J} \end{aligned} \quad (3.2.12)$$

The $\Psi(\alpha' L' S' M' M_s')$ are understood to be antisymmetrized. Noticing that the final state (N-1)-particle

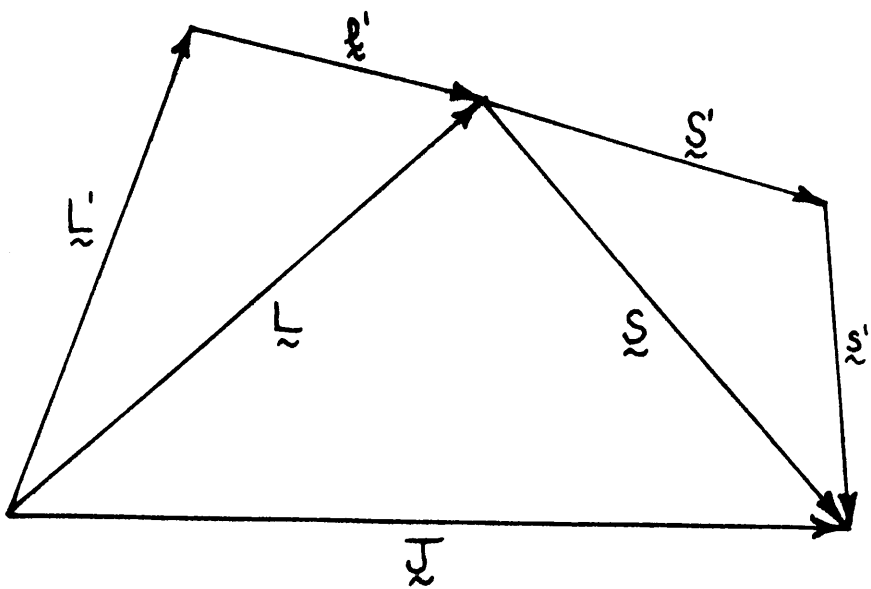
functions are expressed in the $(L S J M_J)$ coupling scheme, we may now express the $\Psi(\alpha' L' S' M' M'_S)$ in terms of the wavefunctions $\Psi(\alpha' L' S' J' M'_J)$ and proceed as for j-j coupling. However, an alternative and more elegant procedure is to use the following expansion in place of (3.2.12):

$$\begin{aligned}
 & |\alpha' L' S', n' l'; \alpha L S J M_J\rangle \\
 = & \sum_{J', j'} \left\{ \begin{array}{ccc} L' & S' & J' \\ l' & s' & j' \\ L & S & J \end{array} \right\} |\alpha' L' S', n' l'; \alpha J' j' J M_J\rangle \\
 & \cdot ([J'] [j'] [L] [S])^{\frac{1}{2}}
 \end{aligned} \tag{3.2.13}$$

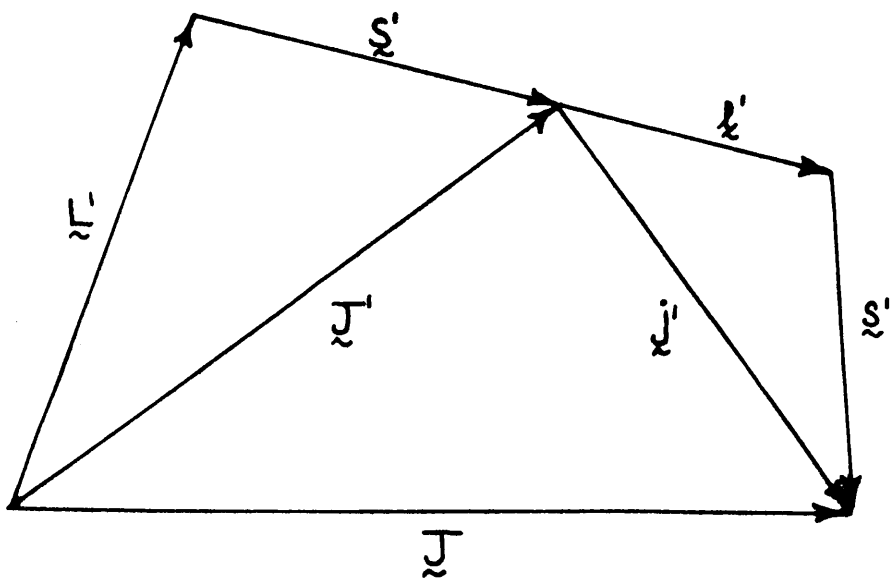
where

$$\begin{aligned}
 & |\alpha' L' S', n' l'; \alpha J' j' J M_J\rangle \\
 = & \sum_{M'_J, m'_j} \Psi(\alpha' L' S' J' M'_J) \Phi(n' l' j' m'_j) \\
 & \cdot \begin{pmatrix} J' & j' & J \\ M'_J & m'_j & -M_J \end{pmatrix} (-1)^{J'-j'+M_J} [J]^{\frac{1}{2}}
 \end{aligned} \tag{3.2.14}$$

The transformation (3.2.13) relates two possible methods of coupling the four angular momenta \underline{L}' , \underline{l}' , \underline{S}' and \underline{s}' to form a fifth, \underline{J}' . The two schemes are indicated diagrammatically opposite. By means of (3.2.13), the eigenvectors of Scheme (a) are related to those of Scheme (b). It is well



(a)



(b)

Fig. (3.1)

known that the coefficients of such a transformation must be the $9j$ - symbols (see Messiah, 1961, p.1066).

Substitution of (3.2.13) and (3.2.14) in (3.2.11) gives

$$\begin{aligned}
 |\Psi_i\rangle = & \sum_{\substack{\alpha', L', S', \\ n', l'}} \sum_{J', j'} \sum_{M_J', m_J'} \Psi(\alpha' L' S' J' M_J') \\
 & \cdot \varphi(n' l' j' m_J') \langle \alpha' L' S', n' l' | \{L S\} \\
 & \cdot \left\{ \begin{array}{ccc} L' & S' & J' \\ l' & s' & j' \\ L & S & J \end{array} \right\} \begin{pmatrix} J' & j' & J \\ M_J' & m_J' & -M_J \end{pmatrix} \quad (3.2.15) \\
 & \cdot ([J][J'][j][L][S])^{1/2} (-1)^{J-j'+M_J}
 \end{aligned}$$

By the same reasoning as before, the only terms in (3.2.15) which contribute to the dipole matrix element are

$$\begin{aligned}
 & \sum_{n' l' j'} \Psi(\alpha'' L'' S'' J'' M_J'') \varphi(n' l' j' M_J - M_J'') \\
 & \cdot \left\{ \begin{array}{ccc} L'' & S'' & J'' \\ l' & s' & j' \\ L & S & J \end{array} \right\} \langle \alpha'' L'' S'', n' l' | \{L S\} \\
 & \cdot \begin{pmatrix} J'' & j' & J \\ M_J'' & M_J - M_J'' & -M_J \end{pmatrix} ([J][J''][j][L][S])^{1/2} (-1)^{J''-j'+M_J} \quad (3.2.16)
 \end{aligned}$$

It is interesting to note the similarity of (3.2.16) to (3.2.5), the corresponding expression for j-j coupling. They differ only by a multiplicative factor which is independent of M_J and M_J'' , the initial and final orientations of the atom respectively.

Once more we assume that the ejected electrons are equivalent initially; which means for LS-coupling that the summations over n' and l' (but not j') vanish. From this point the evaluation of the transition probability proceeds as before and yields

$$\begin{aligned}
 & \bar{P}(\alpha L S J \rightarrow \alpha'' L'' S'' J'' M_J'', X) \\
 &= (4\pi)^2 [L][S][J''] \langle \alpha'' L'' S'', n l | \{ L S \}^2 \\
 & \cdot \sum_{j, j'} \left\{ \begin{array}{ccc} L'' & S'' & J'' \\ l & s & j \\ L & S & J \end{array} \right\} \left\{ \begin{array}{ccc} L'' & S'' & J'' \\ l & s & j' \\ L & S & J \end{array} \right\} [j][j'] \\
 & \cdot \sum_{M_J} \sum_{m_s, m_s} \left(\begin{array}{ccc} J'' & j & J \\ M_J'' & M_J - M_J' & -M_J \end{array} \right)^2 \left(\begin{array}{ccc} l & s & j \\ m & m_s & -M_J + M_J'' \end{array} \right) \left(\begin{array}{ccc} l & s & j' \\ m & m_s & -M_J + M_J'' \end{array} \right) \\
 & \cdot \left\{ (\ell+1) R_{X, \ell+1}^2 \left(\begin{array}{ccc} \ell & 1 & \ell+1 \\ m & \mu & -m-\mu \end{array} \right)^2 \right. \\
 & \quad \left. + (\ell) R_{X, \ell-1}^2 \left(\begin{array}{ccc} \ell & 1 & \ell-1 \\ m & \mu & -m-\mu \end{array} \right)^2 \right\} \quad (3.2.17)
 \end{aligned}$$

A more complicated result equivalent to (3.2.17) has been obtained by Flügge, Mehlhorn and Schmidt (1972) by a simple extension of the work of Cooper and Zare (1968). The latter start from an expansion of the final state many-electron wavefunction $|\psi_f\rangle$, and hence their procedure appears rather different from that outlined above, which seems to be shorter and more elegant to the present writer. One arrives at an expression equivalent to (3.2.17) by squaring equation (2) of Flügge et al. It is thus apparent that the method given here leads to a more economical result, since the alternative expression involves copious numbers of cross-terms in unobserved magnetic quantum numbers and is altogether more cumbersome. The equivalence of the two formulae can be demonstrated by the application of the standard relation for 9j-symbols:

$$\sum_b (2b+1) \begin{pmatrix} a & b & c \\ \alpha & \beta & \gamma \end{pmatrix} \begin{pmatrix} b & e & h \\ \beta & \epsilon & \eta \end{pmatrix} \begin{Bmatrix} a & b & c \\ d & e & f \\ g & h & i \end{Bmatrix} \\ = \sum_{\varphi \nu \delta \rho} \begin{pmatrix} c & f & i \\ \gamma & \varphi & \nu \end{pmatrix} \begin{pmatrix} a & d & g \\ \alpha & \delta & \rho \end{pmatrix} \begin{pmatrix} d & e & f \\ \delta & \epsilon & \varphi \end{pmatrix} \begin{pmatrix} g & h & i \\ \rho & \eta & \nu \end{pmatrix} \quad (3.2.18)$$

By comparison, the only cross-terms arising in (3.2.17) are those involving j . Since $S = \frac{1}{2}$, the values taken by j are limited by

the triangular relationships as follows:

$$j = l \pm \frac{1}{2} \quad (3.2.19a)$$

$$J + J'' \geq j \geq |J - J''| \quad (3.2.19b)$$

We see therefore that the double summation over j and j' in (3.2.17) never involves more than four terms. In fact, if

$$l = J + J'' + \frac{1}{2} \quad (3.2.20a)$$

or

$$l = |J - J''| - \frac{1}{2} \quad (3.2.20b)$$

only one $9j$ -symbol need be evaluated, and no cross-terms remain.

Comparing (3.2.17) and (3.2.8), we see that the two coupling schemes in general give different relative probabilities for the different final atomic orientations M_J'' . As one would expect, though, for ejection from a filled subshell, LS-coupling, jj-coupling and the one-electron model all give the same results.

CHAPTER 4

THE BETHE THEORY

1. Preliminary Remarks - Threshold Polarization

In the theory of the polarization of atomic line radiation by electron impact, one distinguishes three different situations regarding the collision problem:

- (a) At threshold: At the threshold excitation energy, the relative probability of exciting the different magnetic substates of the upper level may be calculated purely from a consideration of angular momentum conservation, no detailed knowledge of the collision process thus being necessary.
- (b) Near threshold: In this region, reliable calculations of the collision cross sections are most difficult to obtain, so that experimental measurements and the above threshold law provide an important test for collision theories.
- (c) Far from threshold: Here the theoretical calculations are

simpler. The most important and most frequently employed of such theories is the Born approximation. The question of interest is how close to threshold one may apply the Born theory without encountering significant deviations from experiment. However, the situation is complicated at high energies by "cascade" population of the upper level.

In the following sections we shall be concerned with calculating the relative vacancy population of the magnetic substates of the excited level produced by the removal of an electron from a hitherto complete inner shell. It is of interest to compare the problem with that of outer shell excitation for each of the three cases distinguished above.

(a) At threshold: At the ionization threshold, the scattered and ejected electrons have zero velocity and therefore zero orbital angular momentum. As we choose our quantization axis along the direction of incidence and recall that a complete subshell has $L = M = 0$, the total orbital A.M. component along the Z-axis is zero prior to the collision. Hence only vacancy states with zero A.M. component in this direction may be excited by ionization at threshold. However, the situation is complicated by the existence of discrete unfilled levels below the ionization continuum. These levels may be filled as

a result of the collisional excitation, and hence obscure the threshold law deduced above. Strictly then, the threshold energy will be that required to excite an electron to the first unoccupied outer level. Only if this level is an S-state ($L = 0$) will the above selection rule still hold. If $L = 0$, we have merely $\Delta M = 0$ for the transition, a restriction which will not lead to large inequalities in the vacancy population over the magnetic substates. Even if the first unoccupied outer level should be an S-state, the situation is complicated by the fact that the outer energy levels may be so close compared with the energy spread in the incident electron beam that any large threshold polarization is effectively smeared out.

(b) Near threshold: Again, the situation is more complex than for the outer shell case, due to the absence of a well-defined selection rule and the importance of the discrete excitations in this region.

(c) Far from threshold: Here it should be permissible to neglect the influence of discrete excitations, and to estimate the ionization cross sections accurately at such high energies.

The considerations outlined above induce us to begin our investigations with the high energy region, where one expects the calculations to be simpler, and also where one might expect to find large polarizations resulting from inner-shell transitions, by analogy with the optical case (see Percival and Seaton (1958) p.133).

The remaining sections of this chapter apply the Bethe theory to this problem. Although worked out in considerable detail in Bethe's monumental paper (1930), the theory has not been fully appreciated or exploited until recently. An interesting review of the Bethe theory has recently been given by Inokuti (1971).

The following chapter extends the results to lower energies using the Born approximation.

2. The Bethe Limit

The Born approximation leads to the well-known transition matrix element

$$\langle f | \exp(i\mathbf{k}\cdot\mathbf{r}) | i \rangle \quad (4.2.1)$$

At sufficiently high energies of impact, the bulk of all ionizing collisions are due to small angle, "glancing" collisions,

that is, collisions involving small momentum transfer $\hbar \underline{k}$. Hence we may perform what is known as the Bethe approximation, and replace the exponential in the Born matrix element by the first two terms in its expansion:

$$\exp(i \underline{k} \cdot \underline{r}) \approx 1 + i \underline{k} \cdot \underline{r} \quad (4.2.2)$$

so that

$$|\langle f | \exp(i \underline{k} \cdot \underline{r}) | i \rangle|^2 \approx |\langle f | \underline{k} \cdot \underline{r} | i \rangle|^2 \quad (4.2.3)$$

The scalar product $\underline{k} \cdot \underline{r}$ can be expanded as follows:

$$\underline{k} \cdot \underline{r} = kr \sum_{\mu} C_{\mu}^{1*}(\theta_k, \varphi_k) C_{\mu}^1(\theta, \varphi) \quad (4.2.4)$$

The C_{μ}^1 are the spherical tensor components defined by equation (3.1.1). (θ_k, φ_k) and (θ, φ) are the polar angles of \underline{k} and \underline{r} respectively in a coordinate system where the Z-axis coincides with the direction of the incidence of the electron. Equation (4.2.4) allows us to write

$$\langle f | \underline{k} \cdot \underline{r} | i \rangle = k \sum_{\mu} C_{\mu}^{1*}(\theta_k, \varphi_k) \cdot \langle f | r C_{\mu}^1(\theta, \varphi) | i \rangle \quad (4.2.5)$$

We can simplify (4.2.5) further by the assumption that \underline{k} is virtually perpendicular to \underline{k}_0 , the wave vector of the incoming electron, so that we may set $\theta_k = \frac{\pi}{2}$. The validity

of this approximation will be scrutinized in the following section. Using this fact we have

$$\langle f | \underline{k}, \underline{r} | i \rangle \approx K \left\{ e^{i\varphi_k} \langle f | r C_{+1}^1(\theta, \varphi) | i \rangle + e^{-i\varphi_k} \langle f | r C_{-1}^1(\theta, \varphi) | i \rangle \right\} \quad (4.2.6)$$

Since we do not detect the azimuthal angle φ_k , we must average over this variable. Hence we obtain

$$\begin{aligned} & \frac{1}{2\pi} \int_0^{2\pi} |\langle f | \underline{k}, \underline{r} | i \rangle|^2 d\varphi_k \\ &= K^2 \left\{ |\langle f | r C_{+1}^1(\theta, \varphi) | i \rangle|^2 + |\langle f | r C_{-1}^1(\theta, \varphi) | i \rangle|^2 \right\} \quad (4.2.7) \end{aligned}$$

We now identify $|i\rangle$ as the bound state of an electron specified by the quantum numbers $(n \ell m)$, and $|f\rangle$ as the continuum state representing an ejected electron of momentum

$\hbar \underline{k}$. On integrating (4.2.7) over all directions of ejection, using (3.1.14) and inserting explicit values for 3j-symbols, one finds

$$\begin{aligned} & \frac{1}{2\pi} \iint |\langle f | \underline{k}, \underline{r} | i \rangle|^2 d\varphi_k d\omega(\underline{k}) \\ &= K^2 \left\{ R_{x, \ell+1}^2 \frac{(\ell+1)(\ell+2) + m^2}{2(2\ell+3)(2\ell+1)} + R_{x, \ell-1}^2 \frac{\ell(\ell-1) + m^2}{2(2\ell+1)(2\ell-1)} \right\} \quad (4.2.8) \end{aligned}$$

Now the total cross section is given by the relationship

$$Q(n\ell m \rightarrow \kappa) = \frac{4\pi a_0^2}{E/R_{\ell}} \int_{K_{\min}}^{K_{\max}} \frac{d(K^2)}{K^4} \cdot \frac{K^2}{a_0^2} \cdot \frac{1}{2\pi} \iint |\langle f | \kappa, \hat{x} | i \rangle|^2 d\varphi_K d\omega(\hat{x}) \quad (4.2.9)$$

where we have

$$K_{\min} = k_0 - k_1 \quad (4.2.10a)$$

$$K_{\max} = k_0 + k_1 \quad (4.2.10b)$$

We follow the customary practice in the Bethe approximation of putting

$$K_{\min} = \frac{m \Delta E}{\hbar^2 k_0} \quad (4.2.11)$$

It is also customary to disregard the kinematic upper limit

K_{\max} , replacing it with the value K_0 , called the "momentum transfer cut off". Here we shall put

$$K_0 = \left(\frac{2m \Delta E}{\hbar^2} \right)^{1/2} \quad (4.2.12)$$

and ignore all collisions resulting in larger momentum transfers.

It will later become clear that this practice is consistent with

the other approximations made in this section, in particular

setting $\theta_{\kappa} = \frac{\pi}{2}$.

Using (4.2.8), (4.2.9), (4.2.11) and (4.2.12), and integrating over K , one obtains

$$Q(nlm \rightarrow \kappa) = \frac{4\pi a_0^2}{E \frac{Z^2 R_y}{\kappa}} \ln \left(\frac{4E}{\Delta E} \right) \cdot \left\{ \mathcal{R}_{\kappa, l+1}^2 \frac{(l+1)(l+2)+m^2}{2(2l+3)(2l+1)} + \mathcal{R}_{\kappa, l-1}^2 \frac{l(l-1)+m^2}{2(2l+1)(2l-1)} \right\} \quad (4.2.13)$$

Finally, we must also integrate over all possible energy transfers ΔE . This is equivalent to an integration over κ , since

$$\Delta E = I_{nl} + \frac{\hbar^2 \kappa^2}{2m} \quad (4.2.14)$$

where I_{nl} is the ionization energy of the nl -subshell.

Note that the argument of the logarithm in (4.2.13) is dependent on ΔE , but since this dependence occurs in a logarithmic term it is usual to simplify the integration by putting $\Delta E \approx I_{nl}$ in this part of the integrand. Thus one has finally

$$Q|ml| = Q(nlm \rightarrow \text{continuum}) = \frac{4\pi a_0^2}{E \frac{Z^2 R_y}{\kappa}} \ln \left(\frac{4E}{I_{nl}} \right) \cdot \left\{ \int \mathcal{R}_{\kappa, l+1}^2 dx \cdot \frac{(l+1)(l+2)+m^2}{2(2l+3)(2l+1)} + \int \mathcal{R}_{\kappa, l-1}^2 dx \cdot \frac{l(l-1)+m^2}{2(2l+1)(2l-1)} \right\} \quad (4.2.15)$$

It is apparent that the cross section (4.2.15) factorises into a part dependent on collision energy E , and a part dependent on m , the magnetic quantum number. Hence the ratio $Q^{l'm'}/Q^{lm'}$ in which we are interested is independent of E . For the particular case of ionization from a $2p$ subshell, we have

$$Q_0/Q_1 = \frac{\frac{1}{5} \int R_{Xd}^2 dx}{\frac{7}{30} \int R_{Xd}^2 dx + \frac{1}{6} \int R_{Xs}^2 dx} \quad (4.2.16)$$

To obtain a numerical value for the ratio we must now make some assumption about the wavefunctions to be used in evaluating the R_{Xl+1} . If we take them to be hydrogenic and use the data of Bethe and Salpeter (1957 p.350) we find

$$Q_0/Q_1 = 0.814 \quad (4.2.17)$$

Note that the ratio is also independent of Z' . Using results derived earlier (see Chapter 1, (1.2.11a,b,c)) we obtain estimates of P_∞ , the high energy limit of the polarization, for three lines of the L series.

$$P_\infty(L_2) = P_\infty(M_1 \rightarrow L_3) = -5.04\% \quad (4.2.18a)$$

$$P_\infty(L_{\alpha_1}) = P_\infty(M_5 \rightarrow L_3) = -1.00\% \quad (4.2.18b)$$

$$P_\infty(L_{\alpha_2}) = P_\infty(M_4 \rightarrow L_3) = +3.91\% \quad (4.2.18c)$$

These polarizations are small, whereas P_{∞} for many optical transitions is large. It is possible to gain some physical insight into this result as follows:

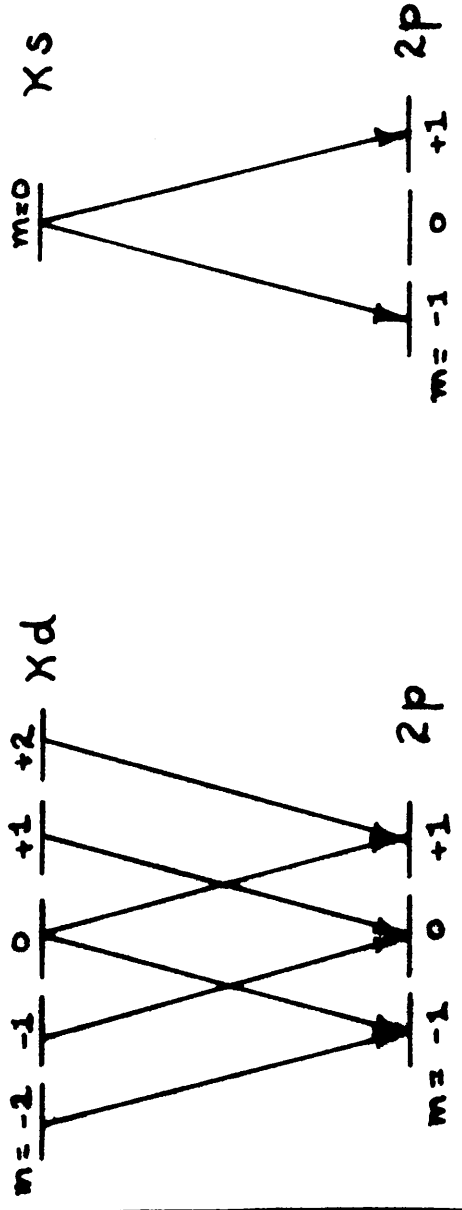
If the collision energy becomes sufficiently large, the momentum transfer will take place virtually at right angles to the direction of incidence. This means that any transitions which result from the collision must obey the selection rule

$$\Delta m = \pm 1 \quad (4.2.19)$$

This is true both for optical excitation and for inner shell ionization. In the latter case, the only transitions into the continuum in the Bethe limit are those which are optically allowed:

$$\Delta l = \pm 1 \quad (4.2.20)$$

With the aid of these two selection rules we can illustrate the situation diagrammatically. In figure 4.1(a) we see that, notwithstanding the selection rule, transitions from all magnetic substates into the continuum are possible. In figure 4.1.(b), however, transitions from the state ($2p, m=0$) are forbidden. If only this latter case were important, the vacancy distribution after the collision would be highly unequal and the polarization of the characteristic X rays large. That the polarization is in fact small is a result of the inequality



(b)

(a)

Fig. (4.1)

$$R_{xd}^2 \gg R_{xs}^2 \quad (4.2.21)$$

when the radial eigenfunctions are hydrogenic. Thus the question arises as to whether the inequality (4.2.21) could be reversed in a case where different wavefunctions were appropriate - particularly since the sensitivity of the integrands in (4.2.21) to small changes in the form of the radial eigenfunctions is well known from the related study of photoionization. In fact, it is known that for certain atoms one has the phenomenon known as the "Cooper minimum" in the photoionization cross section as a function of photon energy. This is due to the vanishing of R_{xd} for certain values of χ . Anisotropy following photoionization will be dealt with separately in Chapter 7. However, the integration over χ tends to mask this behaviour, and it appears likely that (4.2.21) will be obeyed by any physically realistic wavefunctions.

The Bethe theory, as we mentioned earlier, is capable of a greater degree of sophistication than that which we have deployed up to this point. The following sections therefore will seek to improve on the situation, re-examining in the process the assumptions on which this section is based.

3. An Improved Bethe Theory I: Direction of Momentum Transfer

The version of the Bethe theory employed in the preceding section is useful for three reasons: firstly, it allows us to predict P_{∞} , the high energy limit of the polarization of the characteristic X radiation; secondly, it provides a check on the more accurate Born cross sections to be calculated in the following chapter; and lastly, it provides us with the simple physical picture which results from the selection rule $\Delta m = \pm 1$ (see Fig.(4.1)).

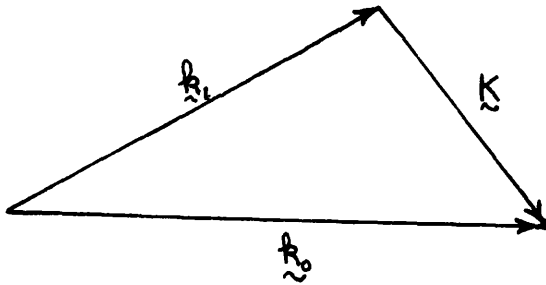
However, as a source of realistic cross sections - even for the region well above threshold - the theory is inadequate. Its inadequacy stems from the neglect of terms of order E^{-1} in the cross section with respect to the $E^{-1} \ln E$ term. A more realistic form for the total cross section would be

$$Q = \frac{A}{(E/I_{ne})} \ln(4E/I_{ne}) + \frac{B}{(E/I_{ne})} \quad (4.3.1)$$

Of course if E is sufficiently large one expects the logarithmic term in (3.5.1) to dominate; but if $B \gg A$ then the non-logarithmic term will be important even for very large E . A study of this problem has been made by Schram & Vriens (1965). They show that, for the ionization of a hydrogenic atom

from the 2p-state, the ratio $B/A = 10.177$. Hence the possibility exists that the simple calculations of the preceding ^{section} are nowhere valid, since for E such that the non-logarithmic terms is negligible, one may be well into the relativistic region - particularly since one is dealing with processes where the ionization threshold is high. The question of relativistic corrections will be dealt with in Chapter 6. In this section and the next we calculate the term of order E^{-1} in the cross sections $Q(2p, m \rightarrow \text{ionization continuum})$. One contribution comes from the close collisions - more specifically, from those transitions involving momentum transfers $> \hbar K_0$, where K_0 is the so-called "momentum transfer cutoff factor", to be defined below. This contribution is well-known and is dealt with in Bethe's original (1930) paper. A further contribution, peculiar to ionization from (or excitation to) states with well-defined magnetic quantum number m , arises from the removal of the assumption that θ_K , the angle between the momentum transfer vector $\hbar \underline{K}$ and the incident electron momentum $\hbar \underline{k}_0$, is $\pi/2$. This assumption is made in the previous section and in all Bethe literature known to the present writer. In other words, we shall show that setting $\theta_K = \pi/2$ is equivalent for these cross sections to the neglect of a term of order E^{-1} .

Consider the situation as presented in the diagram:



We have

$$\cos \theta_K = \frac{K^2 + k_0^2 - k_1^2}{2 k_0 K} \quad (4.3.2)$$

From conservation of energy this may be rewritten

$$\cos \theta_K = \frac{K^2 + \frac{2m\Delta E}{\hbar^2}}{2 k_0 K} \quad (4.3.3)$$

The Bethe procedure is to split the integration over K into two ranges, $K_{\min} \rightarrow K_0$ and $K_0 \rightarrow K_{\max}$, where K_{\min} and K_{\max} are the kinematic limits and K_0 is chosen so that the dipole approximation, $\exp(i\mathbf{k}\cdot\mathbf{r}) \simeq 1 + i\mathbf{k}\cdot\mathbf{r}$, is valid throughout the lower range:

$$K_0 \ll \alpha_{nl} \quad (4.3.4)$$

where α_{nl} is the reciprocal orbit size of the nl -subshell.

Equation (4.3.4) may thus be rewritten:

$$K_0 \ll \left(\frac{2m E_{nl}}{\hbar^2} \right)^{1/2} \quad (4.3.5)$$

Now E_{nl} is the ionization energy of the $n\ell$ -subshell, so that $E_{nl} \leq \Delta E$, the energy transfer to the atom in an ionizing collision, and we may write:

$$K_0^2 \ll \frac{2m \Delta E}{\hbar^2} \quad (4.3.6)$$

Use of (4.3.6) in conjunction with (4.3.3) leads to the conclusion that in the dipole range $K_{min} \rightarrow K_0$ one has

$$\begin{aligned} \cos \Theta_K &\approx \frac{m \Delta E}{\hbar^2 A_0 K} \\ &\approx \frac{K_{min}}{K} \end{aligned} \quad (4.3.7)$$

so we see that $\Theta_K = 0$ when $K = K_{min}$, and if $K_0 \gg K_{min}$ we have

$\Theta_K = \pi/2$. Hence the integrand in this region of the integration may not be simplified by assigning a fixed value to Θ_K .

K_0 can be chosen such that

$$K_{min}^2 \ll K_0^2 \ll \frac{2m \Delta E}{\hbar^2} \quad (4.3.8)$$

only if

$$\frac{2m \Delta E}{\hbar^2 K_{min}^2} \gg 1 \quad (4.3.9)$$

Since

$$\frac{2m \Delta E}{\hbar^2 K_{\min}^2} \approx \frac{4E}{\Delta E} \quad (4.3.10)$$

condition (4.3.8) can be satisfied in the range of energies to which the Bethe applies.

Hence we can write

$$(\cos^2 \theta_K)_{K=K_0} \ll 1 \quad (4.3.11)$$

Now, for $K = K_{\max} \approx 2K_0$

$$\cos \theta_K \approx \frac{4K_0^2 + 2m \Delta E / \hbar^2}{4K_0^2} \approx 1 \quad (4.3.12)$$

Equations (4.2.11) and (4.2.12) appear to suggest that assigning a fixed value to θ_K in the upper region would also be unjustified. However, it is well known that the contribution to the cross section is negligible unless $K^2 \ll K_0^2$ i.e. we can choose a second cut-off K_1 such that

$$\frac{2m \Delta E}{\hbar^2} \ll K_1^2 \ll K_0^2 \quad (4.3.13)$$

and integrate only from K_0 to K_1 .

Now

$$(\cos^2 \theta_K)_{K=K_1} \approx \frac{K_1^2}{4K_0^2} \ll 1 \quad (4.3.14)$$

So we see from (4.3.11) and (4.3.14) that no significant error is sustained in the upper integration region by setting

$\theta_K = \frac{\pi}{2}$. We shall call on this result in the following

section. Meanwhile, we shall re-evaluate the dipole

contribution taking into account the variation of θ_K .

Assuming that \underline{k} is contained in the XZ-plane, we may write

$$\begin{aligned} \langle \underline{x} | \underline{k} \cdot \underline{r} | n l m \rangle &= K \sin \theta_K \langle \underline{x} | x | n l m \rangle \\ &+ K \cos \theta_K \langle \underline{x} | z | n l m \rangle \end{aligned} \quad (4.3.15)$$

We now square, integrate over $\hat{\underline{x}}$, and evaluate angular factors:

$$\begin{aligned} &\int |\langle \underline{x} | \underline{k} \cdot \underline{r} | n l m \rangle|^2 d\omega(\hat{\underline{x}}) \\ &= K^2 \sin^2 \theta_K \left\{ \frac{(\ell+1)(\ell+2)+m^2}{2(2\ell+3)(2\ell+1)} \mathcal{R}_{x,\ell+1}^2 \right. \\ &\quad \left. + \frac{\ell(\ell-1)+m^2}{2(2\ell+1)(2\ell-1)} \mathcal{R}_{x,\ell-1}^2 \right\} \\ &+ K^2 \cos^2 \theta_K \left\{ \frac{(\ell+1)^2 - m^2}{(2\ell+3)(2\ell+1)} \mathcal{R}_{x,\ell+1}^2 + \frac{\ell^2 - m^2}{(2\ell+1)(2\ell-1)} \mathcal{R}_{x,\ell-1}^2 \right\} \end{aligned} \quad (4.3.16)$$

Now

$$\int_{K_{\min}}^{K_0} d(K^2) K^{-2} \cos^2 \theta_K = 1 + \frac{\Delta E}{2E} \ln \frac{2\hbar^2 K_0^2 E}{m(\Delta E)^2} + O(E^{-1}) \quad (4.3.17)$$

Since we retain terms of order at least E^{-1} in the total cross section, only the first term on the right of (4.3.17) makes a significant contribution. Note that this term is independent of the cut-off parameter K_0 .

The differential cross section in the dipole region is

$$dQ_{\text{distant}} = \frac{4\pi a_0^2}{E/R_y \cdot \Delta E/R_y} \cdot (K_0)^{-4} d(K^2 a_0^2) \int |\langle \chi | \mathbf{K} \cdot \mathbf{r} | n l m \rangle|^2 d\omega(\hat{\mathbf{x}}) \quad (4.3.18)$$

Use of (4.3.16), (4.3.17) and (4.3.18) allows us to perform the integration over \mathbf{K} , upon which we find:

$$Q_{\text{distant}} = \frac{4\pi a_0^2}{E/R_y \cdot \Delta E/R_y} \cdot \left[\left(\ln \frac{2\hbar^2 E K_0^2}{m \Delta E^2} - 1 \right) \cdot \frac{1}{2} \left\{ \frac{(\ell+1)(\ell+2)+m^2}{(2\ell+3)(2\ell+1)} \mathcal{R}_{\chi, \ell+1}^2 + \frac{\ell(\ell-1)+m^2}{(2\ell+1)(2\ell-1)} \mathcal{R}_{\chi, \ell-1}^2 \right\} + \left\{ \frac{(\ell+1)^2 - m^2}{(2\ell+3)(2\ell+1)} \mathcal{R}_{\chi, \ell+1}^2 + \frac{\ell^2 - m^2}{(2\ell+1)(2\ell-1)} \mathcal{R}_{\chi, \ell-1}^2 \right\} \right] \quad (4.3.19)$$

The dependence on the cut-off parameter K_0 will vanish when the non-dipole contribution is added to (4.3.19).

It may be shown without difficulty that the additional term of order E^{-1} vanishes on performance of a summation over m . To demonstrate that it is non-negligible, note that the

argument of the logarithm may be written

$$\left(k_0^2 / 2m\Delta E / \hbar^2 \right) \left(\frac{E}{\Delta E} \right) \quad (4.3.20)$$

Since the first factor is small compared to unity (see (4.3.6)), the logarithm may not be large compared to unity until E is very much larger than ΔE indeed.

The presence of the E^{-1} term above is a result of kinematical considerations; hence we might expect it to be of importance for any discussion of the form of anisotropies in the high-energy limit of the Born approximation. In fact, the only recognition of its importance known to the writer is that of Zare (1967) in his calculations of the angular distribution of products in the electron impact dissociation of H_2^+ . Zare points out that the form of the Born integrand is such as to weight strongly small values of k , of the order of k_{min} . Since for $k = k_{min}$ we have $\Theta_k = 0$, as demonstrated above, the effect of setting $\Theta_k = \frac{\pi}{2}$ is to make the form of the anisotropy approach its high energy limit too rapidly. Zare supports his case by theoretical and experimental examination of the above-mentioned angular distribution. However, he does not consider the Bethe cross section (4.3.1), which gives us in analytic form the high-energy behaviour of the Born cross

section, so his arguments remain more qualitative than those presented here. Zare also makes an incorrect extension of his argument in which he asserts that the form of anisotropies will not, in general, reach that value predicted by setting $\theta_k = \frac{\pi}{2}$, no matter how high the impact energy; on the basis of this he suggests that some of the results of Percival and Seaton (1958) are in error. In an appendix to this work it is demonstrated that Zare's reasoning is mistaken and that, in fact, the results of Percival and Seaton are correct. However, it is shown also that for the case of optically-allowed excitations, the approach to the Percival and Seaton limit will be slower than for optically-forbidden excitations.

4. An Improved Bethe Theory II: Non-Dipole Transitions

We now evaluate the remaining contribution of order E^{-1} to the Bethe cross section formula (3.5.1). It arises from the region $k_0 \rightarrow k_{\max}$, where the simplification

$\exp(i\mathbf{k} \cdot \mathbf{r}) \approx 1 + i\mathbf{k} \cdot \mathbf{r}$ is inapplicable. To this end, we define the generalized oscillator strength $f_{\epsilon}(k)$ as follows:

$$f_{\epsilon}(k) = \int |\langle \mathbf{x} | \exp(i\mathbf{k} \cdot \mathbf{r}) | nlm \rangle|^2 d\omega(\hat{\mathbf{x}}) \quad (4.4.1)$$

$$f_{\epsilon}(k) = \int |\langle \mathbf{x} | \exp(i\mathbf{k} \cdot \mathbf{r}) | nlm \rangle|^2 d\omega(\hat{\mathbf{x}})$$

$$\cdot \epsilon \cdot \left(\frac{ka_0}{Z} \right)^{-2}$$

Here ϵ is the convenient parameter $\frac{\Delta E}{Z^2 R_y}$. The contribution from the "close" collisions to the total cross section is thus

$$Q_{\text{close}} = \frac{4\pi a_0^2}{Z^4} g^{-1} \epsilon^{-1} \int_{K_0}^{K_{\text{max}}} f_{\epsilon}(K) d \ln(K^2) \quad (4.4.2)$$

where $g = \frac{E}{Z^2 R_y}$ is a convenient scaled unit of impact energy.

The integral in (4.4.2) will have to be performed numerically, so that we must make the limits of integration explicit. We follow the well-established procedure of setting $K_{\text{max}} = \infty$ and thus ignoring the kinematic limit, on the grounds that the additional contribution arising thereby may be neglected. As for the lower limit, we avoid the ascription of an explicit value to K_0 by the following method, equivalent to that of Miller and Platzman (1957): we write

$$\begin{aligned} & \int_{K_0}^{\infty} f_{\epsilon}(K) d \ln(K^2) \\ & \approx \int_{K_0}^0 f_{\epsilon}(0) d \ln(K^2) - \int_{-\infty}^0 (f_{\epsilon}(0) - f_{\epsilon}(K)) d \ln(K^2) \\ & \quad + \int_0^{\infty} f_{\epsilon}(K) d \ln(K^2) \quad (4.4.3) \\ & = -f_{\epsilon}(0) \ln(K_0^2) - I_1 + I_2 \end{aligned}$$

where

$$I_1 = \int_{-\infty}^0 (f_{\epsilon}(0) - f_{\epsilon}(K)) d \ln(K^2) \quad (4.4.4a)$$

and

$$I_2 = \int_0^{\infty} f_{\epsilon}(K) d \ln(K^2) \quad (4.4.4b)$$

We see that all dependence on the cut-off parameter K_0 will vanish when the contribution from (4.3.19) is taken into account. The replacement of the exact lower limit in I_1 , by $-\infty$ is justified, since the integrand is negligible for $-\infty \leq K \leq K_0$.

The $f_{\epsilon}(K)$ must be obtained before I_1 and I_2 can be evaluated. In the present work, we use $f_{\epsilon}(K)$ evaluated with hydrogenic wavefunctions for the states $(2p, m=0)$ and $(2p, m=\pm 1)$. These come from the Born approximation calculations of the following chapter, Equations (5.1.9a) and (5.1.9b). It will be noticed that these expressions involve θ_K , the momentum transfer direction, and thus depend implicitly on the impact energy E . However, we may effect an important simplification by remembering (see Section 4.3) that in those regions of integration in I_1 and I_2 for which the integrand is significant, small error is sustained by setting $\theta_K = \pi/2$.

Hence we have

$$f_{\epsilon}^{\text{nlm}}(k) = \sum_{nlm} \left\{ 1 - \exp\left(-\frac{2\pi z'}{\kappa a_0}\right) \right\}^{-1} \quad (4.4.5)$$

$$\cdot \exp\left\{ -\frac{2z'}{\kappa a_0} \arctan\left(\frac{2\kappa a_0 / n z'}{(\frac{\kappa a_0}{z'})^2 - (\frac{\kappa a_0}{z'})^2 + \frac{1}{n^2}}\right) \right\}$$

where $\hbar \kappa$ is the momentum of the ejected electron and

$$\sum_{2p,0}^{\text{nlm}} = \frac{4\epsilon}{15\{(\epsilon-d)^2 + d\}^4} \quad (4.4.6a)$$

$$\cdot \{4(\epsilon-d)^2 + (28d+3)(\epsilon-d) + 24d^2 + 18d\}$$

$$\sum_{2p,\pm 1}^{\text{nlm}} = \frac{2\epsilon}{15\{(\epsilon-d)^2 + d\}^5} \quad (4.4.6b)$$

$$\cdot \{11(\epsilon-d)^4 + (92d+7)(\epsilon-d)^3 + (216d^2+76d)(\epsilon-d)^2 + (108d^2+3d)(\epsilon-d) + 24d^3 + 33d^2\}$$

Here the shorthand notation $d = \left(\frac{\kappa a_0}{z'}\right)^2$ has been employed.

The optical oscillator strengths $f_{\epsilon}(0)$ can, of course, be obtained by setting $d=0$ in equations (4.4.5), (4.4.6a) and (4.4.6b), or by using the explicit formulae for the R_{XRL} given by Bethe and Salpeter (1957).

We have thus:

$$\begin{aligned}
Q(\epsilon) &= Q(\epsilon)_{\text{close}} + Q(\epsilon)_{\text{distant}} \\
&= \frac{4\pi a_0^2}{z^4 \mathcal{E}} \left[\left(\ln \frac{4\mathcal{E}}{\epsilon^2} - 1 \right) \right. \\
&\quad - \frac{1}{2} \left\{ \frac{(\ell+1)(\ell+2)+m^2}{(2\ell+3)(2\ell+1)} \mathcal{R}_{\ell, \ell+1}^2 + \frac{\ell(\ell-1)+m^2}{(2\ell+1)(2\ell-1)} \mathcal{R}_{\ell, \ell-1}^2 \right\} \\
&\quad + \left\{ \frac{(\ell+1)^2 - m^2}{(2\ell+3)(2\ell+1)} \mathcal{R}_{\ell, \ell+1}^2 + \frac{\ell^2 - m^2}{(2\ell+1)(2\ell-1)} \mathcal{R}_{\ell, \ell-1}^2 \right\} \\
&\quad \left. + (I_2 - I_1) \right]
\end{aligned} \tag{4.4.7}$$

Since we do not in general detect the energy of ejection, we shall evaluate

$$\begin{aligned}
Q_{\text{tot}} &= \int_{\frac{1}{n^2}}^{\infty} Q(\epsilon) d\epsilon \\
&= \frac{4\pi a_0^2}{z^4 \mathcal{E}} \left[\left(\ln \frac{4\mathcal{E}}{\epsilon^2} - 1 \right) \right. \\
&\quad \cdot \frac{1}{2} \left\{ \frac{(\ell+1)(\ell+2)+m^2}{(2\ell+3)(2\ell+1)} \int_{\frac{1}{n^2}}^{\infty} \frac{\mathcal{R}_{\ell, \ell+1}^2}{\epsilon} d\epsilon + \frac{\ell(\ell-1)+m^2}{(2\ell+1)(2\ell-1)} \int_{\frac{1}{n^2}}^{\infty} \frac{\mathcal{R}_{\ell, \ell-1}^2}{\epsilon} d\epsilon \right\} \\
&\quad + \left\{ \frac{(\ell+1)^2 - m^2}{(2\ell+3)(2\ell+1)} \int_{\frac{1}{n^2}}^{\infty} \frac{\mathcal{R}_{\ell, \ell+1}^2}{\epsilon} d\epsilon + \frac{\ell^2 - m^2}{(2\ell+1)(2\ell-1)} \int_{\frac{1}{n^2}}^{\infty} \frac{\mathcal{R}_{\ell, \ell-1}^2}{\epsilon} d\epsilon \right\} \\
&\quad \left. + C_{nlm} \right]
\end{aligned} \tag{4.4.8}$$

where

$$C_{n\ell m} = \int_{\frac{1}{n^2}}^{\infty} \epsilon^{-1} d\epsilon (I_2(n\ell m; \epsilon) - I_1(n\ell m; \epsilon)) - 2 \int_{\frac{1}{n^2}}^{\infty} \epsilon^{-1} \ln \epsilon d\epsilon \quad (4.4.9)$$

The $C_{n\ell m}$ must be evaluated by numerically integrating over ϵ and K . Using formulae (4.4.5), (4.4.6a) and (4.4.6b), we have calculated

$$C_{2p,0} = 5.4240 \quad (4.4.10a)$$

and

$$C_{2p,\pm 1} = 6.0446 \quad (4.4.10b)$$

The work of Vriens & Bosen (1968) contains the (implicit) values

$$\int_{\frac{1}{4}}^{\infty} R_{yd}^2 \frac{d\epsilon}{\epsilon} = 2.29993 \quad (4.4.11a)$$

$$\int_{\frac{1}{4}}^{\infty} R_{ys}^2 \frac{d\epsilon}{\epsilon} = 0.18063 \quad (4.4.11b)$$

Hence we find

$$Q(2p,0 \rightarrow i) = \frac{4\pi a_0^2}{z^{14} \mathcal{E}} [0.45999 \ln 4 \mathcal{E} + 5.6375] \quad (4.4.12a)$$

$$Q(2p,\pm 1 \rightarrow i) = \frac{4\pi a_0^2}{z^{14} \mathcal{E}} [0.56676 \ln 4 \mathcal{E} + 5.9378] \quad (4.4.12b)$$

We shall not plot the above cross sections as a function of \mathcal{E} , reserving that for the more accurate Born cross sections of the following chapter. However, the simple analytic form of (4.4.12a) and (4.4.12b) allows us to draw some interesting conclusions. Firstly, since the magnitude of the E^{-1} term is similar for both cross sections, the effect of the corrections is strongly depolarizing. Secondly, since $B_A \sim 10$ for both cross sections, the $E^{-1} \ln E$ term will be comparable in magnitude to the E^{-1} term when $E \approx 5,000 Z^2 R_y$. Thus, even for the lightest atoms, the cross sections of Section 4.2 are unrealistic, since such energies are relativistic. Thirdly, consideration of (4.4.10a) and (4.4.10b) shows that the non-dipole contribution to the E^{-1} term in the cross section is easily the larger, the dipole contribution, however, being non-negligible.

Table (4.1) gives some idea of how slow is the approach to the high-energy limit of the cross section ratio which was calculated in § 3.4.

$\xi_G (= E/\Sigma^2 R_y)$	Q_1/Q_2
10	0.9135
50	0.9031
200	0.8957
1000	0.8853
∞	0.8116

Table (4.1)

CHAPTER 5

THE BORN APPROXIMATION

1. Theory

The Born approximation is the most widely-used collisional theory in dealing with electron-atom collisions where the incoming electron has a velocity at least several times larger than the bound electron with which it interacts. It is based on first-order perturbation theory in that both electron and atom are considered as making a transition from an initial to a final unperturbed state as a result of their mutual interaction, without passing through virtual, intermediate states as occurs when higher orders in the perturbation expansion are taken into account. For a derivation and discussion of Born's formulae, the reader is referred to standard texts such as Mott and Massey (1965) or Messiah (1961).

In the Born theory, the amplitude for a transition from an initial state $|i\rangle$ to a final state $|f\rangle$ is proportional to the matrix element

$$\langle f | \exp(i\mathbf{k}\cdot\mathbf{r}) | i \rangle \tag{5.1.1}$$

For the ionization process we wish to consider, $|i\rangle$ is a state labelled by the quantum numbers $n, l,$ and m , where the axis of magnetic quantization is parallel to the direction of the incoming electron. For the innermost shells of the heavier atoms, the deviation of the potential from Coulomb shape is small, and to a good approximation we may use hydrogenic eigenstates with the appropriate screening. $|f\rangle$ is a state of the continuous spectrum in which the atomic electron is moving in a particular direction \hat{x} with momentum $\hbar k$ in the field of a charge $+Z'e = +(Z-S)e$, where Z is the nuclear charge and S the screening factor. Obviously the charge "seen" by the ejected electron varies as it moves through the atom. Discussions of this problem can be found in the literature and in the standard references (Mott and Massey, for instance). In the present work, the same value of Z' will be employed for both bound and ejected electron wavefunctions. As mentioned earlier, the state of most interest here is the 2p state. Calculations of ionization cross sections for the 2p state of a hydrogenic system in the Born approximation have been carried out by several investigators (Bjorn 1940, Mandl 1952, Swan 1955, McCrea and McKirgan 1960, and Omidvar 1965). However, in all of these the practice has been to choose a quantization axis which is parallel to the momentum

transfer vector, $\hbar \underline{k}$. This is the obvious choice, since thereby the operator $\exp(i \underline{k} \cdot \underline{r})$ in (5.1.1) becomes simply $\exp(i k r \cos \theta) = \exp(i k z)$. It leads to no difficulty so long as the cross section is averaged over atomic orientations m , as is customary. But if we are interested in a particular value of m , the total cross section is no longer meaningful, since to obtain it we must integrate over \underline{k} , the average direction of which changes with collision energy. Hence it is plainly misleading to display graphical results for ionization cross sections for the individual m states (as is done by McCrea and McKirgan) referred to \underline{k} as axis, without making this point clear.

We shall now show how it is possible to relate the double differential cross sections with respect to energy transfer and momentum transfer in the two sets of axes and hence re-calculate the desired total cross sections. To avoid confusion, we shall label magnetic substates taken with respect to axis \underline{k} by μ , those taken with respect to (the wavevector of the incident electron) by m . If we consider these two sets of axes as coinciding when one set is rotated in the appropriate direction through an angle θ_k about their common y-axis, we obtain the following relation between the two sets of quantum states $|n \ell m\rangle$ and $|n \ell \mu\rangle$:

$$|n \ell m\rangle = \sum_{\mu} \mathcal{D}_{m\mu}^{(\ell)}(0 \theta_k 0) |n \ell \mu\rangle \quad (5.1.2)$$

where the rotation matrix element $\mathcal{D}_{m\mu}^{(\ell)}(\alpha\beta\gamma)$ is as defined by Edmonds (1960).

Hence we have

$$\begin{aligned} & \langle f | \exp(i\mathbf{k}\cdot\mathbf{r}) | n\ell m \rangle \\ &= \sum_{\mu} \mathcal{D}_{m\mu}^{(\ell)}(0\theta_k 0) \langle f | \exp(i\mathbf{k}\cdot\mathbf{r}) | n\ell \mu \rangle \end{aligned} \quad (5.1.3)$$

The cross section is proportional to

$$\begin{aligned} & |\langle f | \exp(i\mathbf{k}\cdot\mathbf{r}) | n\ell m \rangle|^2 \\ &= \sum_{\mu, \mu'} \mathcal{D}_{m\mu'}^{(\ell)*}(0\theta_k 0) \mathcal{D}_{m\mu}^{(\ell)}(0\theta_k 0) \\ & \quad \cdot \langle n\ell \mu' | \exp(-i\mathbf{k}\cdot\mathbf{r}) | f \rangle \langle f | \exp(i\mathbf{k}\cdot\mathbf{r}) | n\ell \mu \rangle \end{aligned} \quad (5.1.4)$$

The differential cross sections which Burhop and others calculate are in effect diagonal elements of the matrix defined by (5.1.4) when $n = 2$, $\ell = 1$, and $\mu = 0$ or ± 1 (apart, that is, from the rotation matrix elements). We would appear also to have to evaluate the off-diagonal elements. Fortunately, a detailed consideration of the structure shows that the contribution from such cross-terms vanishes when one integrates over all direction of ejection. Thus we may write

$$\begin{aligned} & \int |\langle f | \exp(i\mathbf{k}\cdot\mathbf{r}) | n\ell m \rangle|^2 d\omega(\hat{\mathbf{k}}) \\ &= \sum_{\mu} |\mathcal{D}_{m\mu}^{(\ell)}(0\theta_k 0)|^2 \int |\langle f | \exp(i\mathbf{k}\cdot\mathbf{r}) | n\ell \mu \rangle|^2 d\omega(\hat{\mathbf{k}}) \end{aligned} \quad (5.1.5)$$

or, alternatively,

$$f_{\Delta E}(\underline{k}; nlm) = \sum_{\mu} |D_{m\mu}^{(l)}(0 \theta_k 0)|^2 f_{\Delta E}(\underline{k}; nlm) \quad (5.1.6)$$

where

$$f_{\Delta E}(\underline{k}; nlm) = \frac{\Delta E/R_y}{(K_{a0})^2} \int | \langle f | \exp(i \underline{k} \cdot \underline{r}) | nlm \rangle |^2 d\omega(\hat{\underline{k}}) \quad (5.1.7)$$

is the quantity known as the generalized oscillator strength for the transition, ΔE being the energy transfer. $f_{\Delta E}(\underline{k})$, usually valuable on account of its independence of incident particle energy, is here dependent on the energy of the collision through θ_k , which is given by

$$\cos \theta_k = \frac{(K_{a0})^2 + \Delta E/R_y}{2 (K_{a0} (E/R_y))^{1/2}} \quad (5.1.8)$$

It is possible to plot $f_{\Delta E}(K)$ against K for different choices of ΔE , producing in this way what has become known as the "Bethe Surface" for the atom (see Inokuti, 1971). But in the present case, one has also the direction of \underline{k} to take into account; for each possible value of $\hat{\underline{k}}$ there exists a distinct Bethe surface.

Evaluating the rotation matrix elements for the 2p state yields the relations

$$f_{\Delta E}(\kappa; 2p, m=0) = \cos^2 \theta_{\kappa} f_{\Delta E}(\kappa; 2p, \mu=0) + \sin^2 \theta_{\kappa} f_{\Delta E}(\kappa; 2p, \mu=\pm 1) \quad (5.1.9a)$$

and

$$f_{\Delta E}(\kappa; 2p, m=\pm 1) = \frac{1}{2}(1 + \cos^2 \theta_{\kappa}) f_{\Delta E}(\kappa; 2p, \mu=\pm 1) + \frac{1}{2} \sin^2 \theta_{\kappa} f_{\Delta E}(\kappa; 2p, \mu=0) \quad (5.1.9b)$$

The $f_{\Delta E}(\kappa)$ for a hydrogenic system are of the general form

$$f_{\Delta E}(\kappa; n\ell\mu) = \mathcal{P}_{n\ell\mu} \left\{ 1 - \exp\left(-\frac{2\pi z'}{x a_0}\right) \right\}^{-1} \cdot \exp\left\{ -\frac{2z'}{x a_0} \arctan\left(\frac{2x a_0 / n z'}{d - \left(\frac{x a_0}{z'}\right)^2 + \frac{1}{n^2}}\right) \right\} \quad (5.1.10)$$

where $d = \left(\kappa a_0 / z'\right)^2$. We obtain from the work of Banks, Vriens and Bensen (1969) in conjunction with that of Vriens and Bensen (1968), the expressions

$$\mathcal{P}_{2p, \mu=0} = \frac{4\epsilon}{15\{(\epsilon-d)^2 + d\}} \left\{ \gamma(\epsilon-d)^4 + (64d+4)(\epsilon-d)^3 + (192d^2+54d)(\epsilon-d)^2 + 80d^2(\epsilon-d) + 15d^2 \right\} \quad (5.1.11a)$$

and

$$\mathcal{P}_{2p, \mu=\pm 1} = \frac{4\epsilon}{15\{(\epsilon-d)^2 + d\}} \left\{ 4(\epsilon-d)^2 + (28d+3)(\epsilon-d) + 24d^2 + 18d \right\} \quad (5.1.11b)$$

where $\epsilon = \frac{\Delta E}{Z^2 R_y}$. Hence by means of equations (5.1.8), (5.1.9a, b), (5.1.10), (5.1.11a) and (5.1.11b) we have defined the $f_{\Delta E}(K; 2p, m)$ in terms of q , ϵ and E . To obtain the total cross section we require the relation

$$Q = \frac{4\pi a_0^2}{(E/R_y) Z^4} \int_{q_{\min}}^{q_{\max}} \int_0^{\frac{E}{Z^2 R_y}} f_{\Delta E}(K; 2p, m) \frac{dq}{q} \frac{d\epsilon}{\epsilon} \quad (5.1.12)$$

The double integration in (5.1.12) must be performed numerically for each value of E of interest.

2. Results

The total cross sections $Q(2p, m=0 \rightarrow K)$ and $Q(2p, m=\pm 1 \rightarrow K)$, as calculated from (5.1.12) above, are shown in Figure (5.1). They are given in scaled units of $\pi a_0^2 / Z^4$. The qualitative behaviour of these cross sections is quite different from those of McCrea and McKirgan mentioned above. Whereas in the latter $Q(m=0)$ is larger than $Q(m=\pm 1)$ for all energies, the present cross sections intersect about 16 times the threshold energy and thereafter $Q(m=\pm 1)$ is the larger, the ratio slowly increasing with increasing energy.

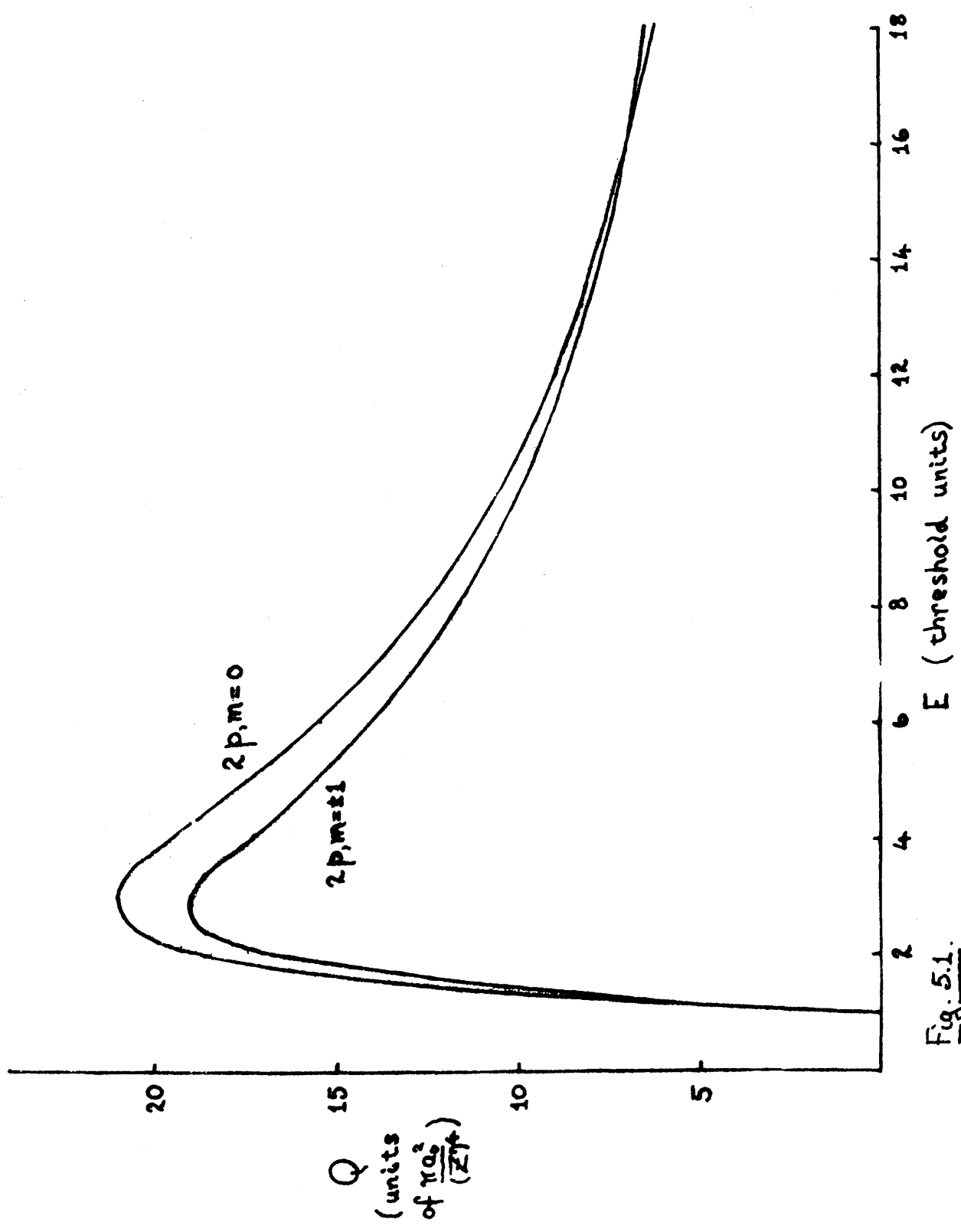
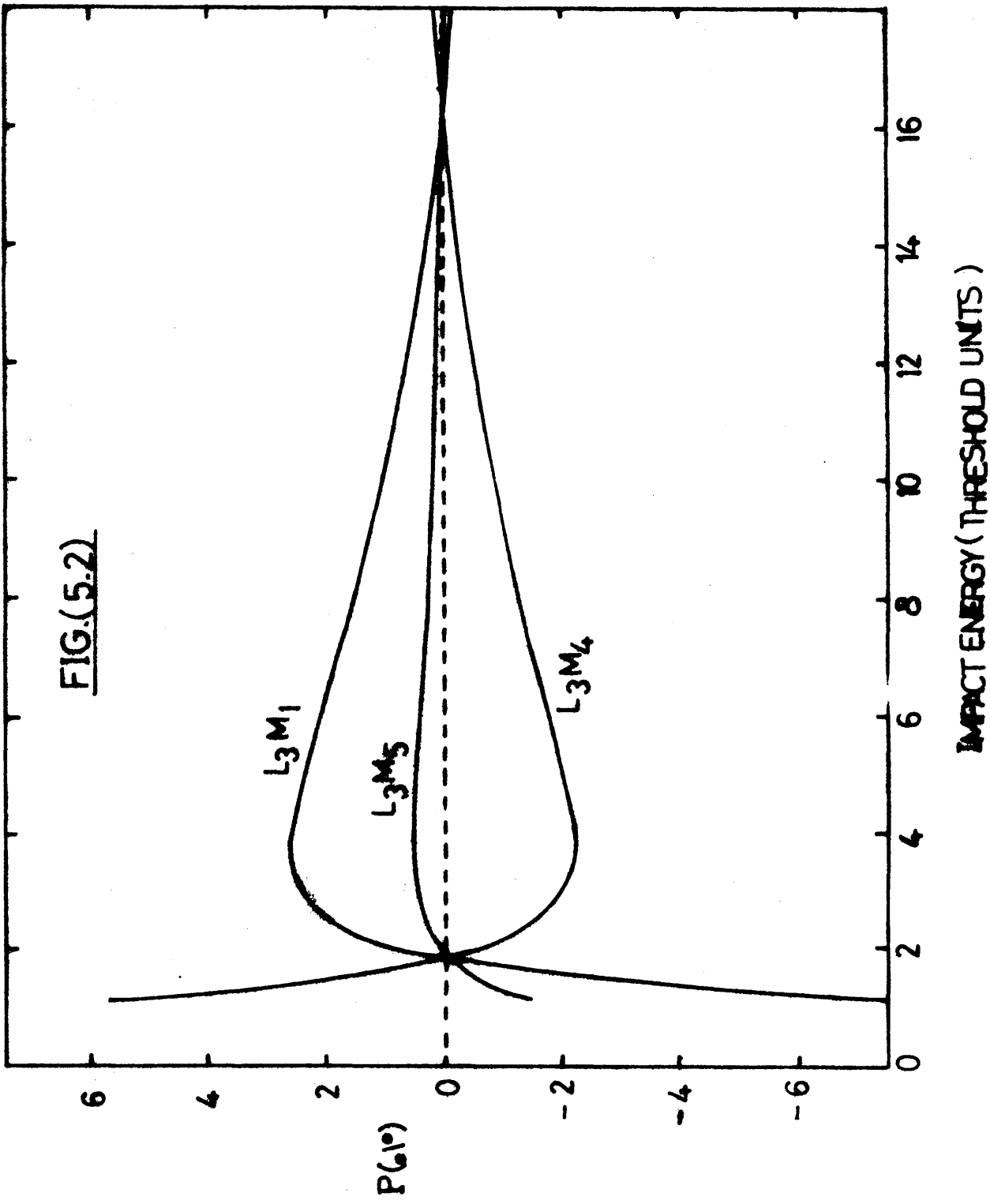


Fig. 5.1.

Figure (5.2) gives the polarization of the lines L_{β} , L_{α} , and L_{α_2} as a function of the collision energy. These curves are obtained simply by substitution of our cross section data in the formulae (1.2.11a), (1.2.11b), and (1.2.11c). Note the intersection around twice the threshold energy. This is not visible in Figure (5.1) because it occurs on the steep, low-energy side of the cross section peak. There seems to be no physical reason for this behaviour, which can probably be safely ascribed to the inadequacy of the Born approximation in this region.

At this point we mention that Figures (5.1) and (5.2) are in sharp disagreement with a calculation published by Melhorn (1968). Melhorn does not present any detailed analysis which can be compared with the above derivation. His polarization results, however, are substantially larger for all incident energies shown, do not change sign anywhere in this range, and appear to be tending to very different high energy limits. It appears that one could account for such results by assuming that the collision cross sections were referred to a momentum transfer quantization axis. This has, in fact, been confirmed by Melhorn (private communication). It is therefore surprising that the only published experimental ^{study} of X ray polarization

FIG.(5.2)



- that of Hrdý, Henins and Bearden (1970) on the L_{α} , X rays of mercury - is in fairly good agreement with the erroneous results of Melhorn.

In further support of the present results, two checks have been carried out. The cross section ratio for the Bethe limit was obtained by setting $K = 0$ in equation (5.1.12) and performing the integration over ϵ numerically. The result was

$$\frac{Q(2p, m=0 \rightarrow K)}{Q(2p, m=\pm 1 \rightarrow K)} = 0.81161 \quad (5.2.1)$$

in good agreement with (4.2.17). Also, the corresponding

$f_{AE}(K)$ in the binary encounter (classical impulse) theory (see Burgess and Percival 1968, or Vriens 1969) were calculated for the particular case $\theta_K = \frac{\pi}{2}$ and checked with the previous unpublished calculations of Banks (private communication). They are:

$$f_{AE}(K, \theta_K = \frac{\pi}{2}; 2p, m=0) = \frac{16}{5\pi} \frac{\epsilon q^{5/2}}{\{(\epsilon - q)^2 + q\}^4} \quad (5.2.2a)$$

and

$$f_{AE}(K, \theta_K = \frac{\pi}{2}; 2p, m=\pm 1) = \frac{8}{5\pi} \frac{\epsilon q^{5/2} \{9(\epsilon - q)^2 + q\}}{\{(\epsilon - q)^2 + q\}^5} \quad (5.2.2b)$$

The cross sections displayed in Figure (5.1) have been used by Cleff and Melhorn (1971) to predict Auger asymmetry parameters β (see Chapter 7) for comparison with their experimental measurements on the angular distribution of Auger electrons ejected from the L_3 level of Ar as a result of electron impact. Table 5.1 opposite shows this comparison. The latter two results are in quite good agreement, theory falling within experimental error limits. The disagreement for the first result is hardly surprising in view of the unreliability of the Born theory at this energy.

ELECTRON ENERGY (threshold units)	β theory	β experiment (± 0.03)
2	-0.03	-0.10
4	-0.07	-0.10
16	0.00	-0.02

Table (5.1)

CHAPTER 6

RELATIVISTIC MODIFICATION OF THE BETHE THEORY

1. Introductory Remarks

In this chapter we wish to see what changes have to be made to the Bethe theory when v , the velocity of the incident electron, becomes comparable to c , the velocity of light.

We first of all note that such a revised Bethe theory already exists. Møller (1932) has derived the following expression for the cross section for the transition ($n\ell \rightarrow n'\ell'$) due to the impact of an electron of velocity v on an arbitrary target atom:

$$Q(n\ell \rightarrow n'\ell') = \frac{2\pi e^4 \alpha^2}{R_y \cdot mv^2} \cdot R_{n',\ell'}^2 \cdot \left[\ln(2 C_{n',\ell'} m v^2 / R_y) - \ln(1 - \frac{v^2}{c^2}) - \frac{v^2}{c^2} \right] \quad (6.1.1)$$

where R_y is the Rydberg energy, α the fine structure constant, and $C_{n',\ell'}$ has been defined in connection with the non-relativistic Bethe theory. The assumptions on which Møller's calculations rest will be discussed later. The most important difference between (6.1.1) and the non-relativistic expressions (4.4.12a,b) is the presence of the term $-\ln(1 - \frac{v^2}{c^2})$;

this means that, whereas the expression (4.4.12) decreases monotonically with increasing incident velocity, here the cross section approaches a minimum and then increases as v approaches very close to c . The question is whether (6.1.1) can be employed for transitions of the type $(nlm \rightarrow n'l'm')$, or whether it must be further modified. In the following section, three distinct considerations are advanced which indicate that the latter course must be taken.

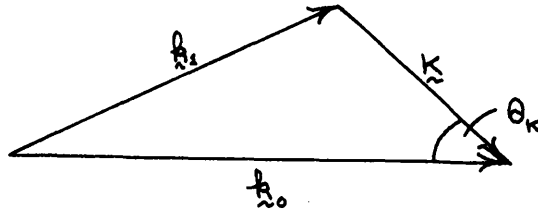
2. The Need for Modifying the Møller Formula

(a) The first consideration is purely classical, the outcome of kinematical requirements. As has been pointed out earlier, the physical reason for the variation of the cross section

$Q(nlm \rightarrow n'l'm')$ with impact velocity is the concomitant variation of the direction of momentum transfer. We now examine the change in \hat{k} as the momentum of the incoming electron, $\hbar k_0$ becomes very large.

(i) Non-relativistic case

The situation is shown vectorially in the diagram.



We are interested in the angle θ_K which \underline{K} makes with the Z-axis, chosen to be parallel to \underline{k}_0 . Geometrically we have

$$\cos \theta_K = \frac{K^2 + k_0^2 - k_1^2}{2k_0 K} \quad (6.2.1)$$

From energy conservation,

$$k_0^2 - k_1^2 = \frac{2m \Delta E}{\hbar^2} \quad (6.2.2)$$

where ΔE is the increase in energy of the atom as a result of the collision. Hence

$$\cos \theta_K = \frac{K^2 + 2m \Delta E / \hbar^2}{2k_0 K} \quad (6.2.3)$$

Now as $k_0 \rightarrow \infty$, $\cos \theta_K \rightarrow 0$, and so the momentum transfer in the high energy limit takes place perpendicular to the direction of incidence, for all K .

(ii) Relativistic case:

Equation (6.2.1) still, of course, holds, but in place of (6.2.2) we have

$$\hbar c \sqrt{K^2 + k_0^2} - \hbar c \sqrt{K^2 + k_1^2} = \Delta E \quad (6.2.4)$$

where $K = mc/\hbar$

Hence

$$k_1^2 = \left(\sqrt{K^2 + k_0^2} - \frac{\Delta E}{\hbar c} \right)^2 - K^2 \quad (6.2.6)$$

Substitution of (6.2.5) in (6.2.1) gives

$$\cos \theta_K = \frac{\left(K^2 - \left(\frac{\Delta E}{\hbar c} \right)^2 + 2 \sqrt{K^2 + k_0^2} \cdot \frac{\Delta E}{\hbar c} \right)}{2 k_0 K} \quad (6.2.6)$$

Again letting $k_0 \rightarrow \infty$, we find

$$\cos \theta_K \rightarrow \frac{\Delta E}{\hbar c K} \quad (6.2.7)$$

So we see that this time the direction of momentum transfer tends to a limit which is dependent on its magnitude, $\hbar K$.

Since we may consider ΔE to be fixed for a given inelastic transition, $\cos \theta_K$ takes its maximum value in (6.2.7)

when $K = K_{\min} = k_0 - k_1$, which is the kinematic lower

limit, taken by both Bethe and Born approximations in the integration over K .

Hence

$$\begin{aligned} K_{\min} &= k_0 - \left\{ \left(\sqrt{x^2 + k_0^2} - \frac{\Delta E}{\hbar c} \right)^2 - x^2 \right\}^{\frac{1}{2}} \\ &= k_0 - k_0 \left\{ 1 + \left(\frac{\Delta E}{\hbar c k_0} \right)^2 - 2 \frac{\sqrt{x^2 + k_0^2}}{k_0} \frac{\Delta E}{\hbar c} \right\}^{\frac{1}{2}} \end{aligned} \quad (6.2.8)$$

As $k_0 \rightarrow \infty$,

$$K_{\min} \rightarrow k_0 - k_0 \left(1 - \frac{\Delta E}{\hbar c k_0} + O(k_0^{-2}) + \dots \right)$$

Since all terms in the brackets of order (k_0^{-2}) or smaller will tend to zero as $k_0 \rightarrow \infty$, we are left with the result

$$K_{\min} \rightarrow \frac{\Delta E}{\hbar c} \quad \text{as} \quad k_0 \rightarrow \infty \quad (6.2.9)$$

Combination of (6.2.7) and (6.2.9) gives

$$(\cos \Theta_K)_{\max} \rightarrow 1 \quad \text{as} \quad k_0 \rightarrow \infty \quad (6.2.10)$$

Thus in distinction to the non-relativistic case \underline{K} is parallel to \underline{k}_0 in the limit of high energy and low momentum transfer.

It will be recalled that the Bethe method involves division of the momentum transfer integration into two ranges; the boundary between the two is given by $K = K_0$, where K_0 satisfies the inequalities

$$K_0 \ll \left(\frac{2mE_0}{\hbar^2} \right)^{\frac{1}{2}} \quad (6.2.11a)$$

$$K_0^2 \gg \left(\frac{\Delta E}{\hbar c} \right)^2 \quad (6.2.11b)$$

(6.2.11a) corresponds to the non-relativistic constraint on K_0 . The need for (6.2.11b) will become apparent below. Here E_0 is the ionisation energy of the bound electron. Use of the inequality (6.2.11b) in conjunction with (6.2.6) shows that throughout the range $K_0 \rightarrow K_{\max}$ one can put $\Theta_K = \frac{\pi}{2}$ without significant error. In the range $K_{\min} \rightarrow K_0$, however, Θ_K varies from 0 to $\frac{\pi}{2}$, so that one cannot simplify the integration over K in this range by assigning a fixed value to Θ_K . Moreover, it is from this region that the logarithmic term in the total cross section, dominant at high energies, is derived. We shall also see that in this region of K the effects of spin and retardation are appreciable.

(b) In the Møller theory, the familiar Coulomb interaction is augmented by a term representing the interaction of the spins of the incident and bound electrons. This leads eventually to the replacement of the Bethe operator $\exp(i\mathbf{k}\cdot\mathbf{r})$ by the operator

$$\exp(i\mathbf{k}\cdot\mathbf{r}) \left(1 + i \frac{\sqrt{\delta^2 - 1}}{\kappa \gamma} \frac{\partial}{\partial \mathbf{x}} \right) \quad (6.2.12)$$

Hence the new interaction operator selects a particular direction in space, the magnetic quantization axis. This is a further reason why (6.1.1) cannot, 'a priori', be applied to transitions from (or to) individual m states.

(c) One of the requirements of the relativistic cross section formula must be that it gives back the non-relativistic formula when $v \ll c$. Comparison of (6.1.1) with (4.4.12a,b) shows that this requirement is not satisfied. We conclude that we must reapply Møller's methods for the case $(n\ell m \rightarrow \underline{\alpha})$ and that this reapplication must yield a formula which differs from (6.1.1).

3. An Outline of Møller's Method

Møller's adaptation (1932) of the Bethe approximation consists of a long article of which the text is in German and the

notation somewhat dated. For this reason, it seems pertinent to synopsise Møller's procedure here, noting the physical assumptions, approximations and limits of validity of the theory, and breaking off the section at that point where modification becomes necessary.

In common with the first Born approximation, the interaction between atom and electron is treated as a small perturbation which causes transitions between unperturbed eigenstates of the isolated systems. The non-relativistic Born theory employs a Coulomb interaction, whereas Møller also takes account of the spin interaction. Retardation and the relativistic increase of mass with velocity are also allowed for. As with the Born, the possibility of exchange is neglected.

Dirac plane waves are used to describe the free electron, but for the bound electron the approximate wave-functions of Darwin are employed. The condition of their validity is that $E_n \ll mc^2$, where n labels the discrete or continuum state in question and m is the rest mass of the electron.

To arrive at a plausible interaction operator, the following

procedure is adopted. Appropriate Dirac charge- and current-densities for the free electron are formed:

$$\begin{aligned} \rho^{(1)} &= -e \psi_{n_1}^*(x_1) \psi_{m_1}(x_1) \\ \underline{j}^{(1)} &= ec \psi_{n_1}^*(x_1) \underline{\alpha}^{(1)} \psi_{m_1}(x_1) \end{aligned} \quad (6.3.1)$$

where (1) labels the free electron, m_1 and n_1 the initial and final Dirac plane wave states, and where the components of $\underline{\alpha}^{(1)}$ are the Dirac current matrices. These charge- and current-distributions produce, according to Maxwell's theory, a scalar potential $\Phi^{(1)}$ and a vector potential $\underline{A}^{(1)}$ at the point x_2 given by

$$\begin{aligned} \Phi^{(1)}(x_2) &= \int \frac{[\rho^{(1)}(x_1)]}{|x_1 - x_2|} dx_1 \\ \underline{A}^{(1)}(x_2) &= \frac{1}{c} \int \frac{[\underline{j}^{(1)}(x_1)]}{|x_1 - x_2|} dx_1 \end{aligned} \quad (6.3.2)$$

The parentheses signify that for $\rho^{(1)}$ and $\underline{j}^{(1)}$ the retarded values, i.e. the values at time $t - \frac{|x_1 - x_2|}{c}$, are taken.

The interaction energy due to the effect of the fields $\underline{A}^{(1)}$ and $\Phi^{(1)}$ on the bound electron (2) at the point x_2 is, in the Dirac theory,

$$-e \left[\Phi^{(1)}(x_2) + \underline{\alpha}^{(2)} \cdot \underline{A}^{(1)}(x_2) \right] \quad (6.3.3)$$

Combination of (6.3.1), (6.3.2) and (6.3.3) shows that the desired interaction operator may be written

$$\frac{e^2}{|\chi_1 - \chi_2|} (1 - \alpha^{(1)} \cdot \alpha^{(2)}) \exp(i \frac{\Delta E}{\hbar} \frac{|\chi_1 - \chi_2|}{c}) \quad (6.3.4)$$

where $\Delta E = |E_m - E_n|$ is the magnitude of the energy transfer involved in the process. The factor $-\frac{e^2 \alpha^{(1)} \cdot \alpha^{(2)}}{|\chi_1 - \chi_2|}$ represents the spin interaction.

At this point the expressions for the Dirac and Darwin spinors and for the Dirac matrices are used explicitly. After some tedious calculation the expression

$$dQ(K) = \frac{8\pi a_0^2}{m_0^2/R_y} \cdot \frac{K dK}{[K^2 - (\frac{\Delta E}{\hbar c})^2]^2} \cdot \left| \varepsilon(K) + i \frac{\sqrt{\gamma^2 - 1}}{\gamma} \varepsilon'(K) \right|^2 \quad (6.3.5)$$

is obtained, where

$$\varepsilon(K) = \langle f | \exp(i \underline{k} \cdot \underline{r}) | i \rangle \quad (6.3.6)$$

and
$$\varepsilon'(K) = \langle f | \frac{1}{x} \exp(i \underline{k} \cdot \underline{r}) \frac{\partial}{\partial x} | i \rangle \quad (6.3.7)$$

In obtaining (6.2.5) the following inequalities are used:

$$K^2 \ll \chi^2 \quad (6.3.8)$$

$$K^2 \ll k_0^2 \quad (6.9)$$

so that terms of order $\frac{K^2}{\chi^2}$, $\frac{K^2}{k_0^2}$ may be neglected.

(6.3.8) follows from the use of Darwin wavefunctions for the bound and ejected electron, (6.3.9) from the requirements of 1st order perturbation theory. $\mathcal{E}'(K)$ derives from the spin interaction.

When $K^2 \ll \left(\frac{2mE_0}{\hbar^2}\right)$ we may make the Bethe approximation

$$|\mathcal{E}(K)|^2 = \frac{(Ka_0)^2}{\Delta E/R_y} f_{\Delta E}(0) \quad (6.3.10)$$

where $f_{\Delta E}(0)$ is the optical oscillator strength. Møller shows that the spin term $\mathcal{E}'(K)$ is appreciable when $K \ll \left(\frac{2mE_0}{\hbar^2}\right)^{1/2}$, i.e. for small momentum transfers. This is because the first term in the expansion of $\exp(i\mathbf{K}\cdot\mathbf{r})$ vanishes for $\mathcal{E}(K)$ due to the orthogonality of the wavefunctions whereas this is seen not to be so for $\mathcal{E}'(K)$.

Using the identity

$$-\langle f | \frac{\partial}{\partial x} | i \rangle = \frac{m \Delta E}{\hbar^2} \langle f | x | i \rangle \quad (6.3.11)$$

it can be shown that for small K we may write

$$\begin{aligned} X(K) &= \epsilon(K) + i \frac{\sqrt{\gamma^2 - 1}}{\gamma} \epsilon'(K) \\ &= \langle f | \underline{s} \cdot \underline{r} | i \rangle \end{aligned} \quad (6.3.12)$$

where \underline{s} is defined as a vector with components

$$s_x = K_x, \quad s_y = K_y, \quad s_z = K_z - \frac{\sqrt{\gamma^2 - 1}}{\gamma} \frac{\Delta E}{\hbar c} \quad (6.3.13)$$

(6.3.12) can be used in conjunction with (6.3.5) to find the contribution to the cross section in the range $K_{\min} \rightarrow K_0$, where

$$\begin{aligned} K_{\min} &= k_0 - k_1 \\ &\approx \left(\frac{\Delta E}{\hbar c} \right) \frac{\gamma}{\sqrt{\gamma^2 - 1}} \end{aligned} \quad (6.3.14)$$

and K_0 is given by (6.2.10). The contribution from the range $K_0 \rightarrow K_{\max}$ is evaluated by noting that here (6.3.5) reduces to

$$dQ(K) = \frac{8\pi a_0^2}{m v^2 / R_y} \cdot \frac{dK}{K^3} \cdot |\epsilon(K)|^2 \quad (6.3.15)$$

which is simply the non-relativistic expression.

Møller simplifies the calculation of the total cross section

$Q(n\ell \rightarrow n'\ell')$ by using the identity

$$\sum_m \sum_{m'} |X_{n\ell m \rightarrow n'\ell' m'}(K)|^2 = S^2 \mathcal{R}_{n,\ell'}^2 \quad (6.3.16)$$

Since here we are interested in orientations, (6.3.16) may not be used, and we thus diverge somewhat from Møller's procedure.

4. Adapting the Møller Formula

Due to the close analogy with equation (3.1.12) we can show that

$$\begin{aligned} & \int |X_{n\ell m \rightarrow n'\ell' m'}(K)|^2 d\omega(\hat{x}) \\ &= \sum_{\ell' m'} \sum_{\mu} S^2 |Y_{\ell' \mu}(\hat{x})|^2 \langle \ell' \mu | \begin{pmatrix} \ell & 1 & \ell' \\ m & \mu & -m' \end{pmatrix} \rangle^2 (2\ell'+1) \\ & \quad \cdot \mathcal{R}_{n,\ell'}^2 \end{aligned} \quad (6.4.1)$$

$$\begin{aligned} &= \sum_{\ell' m'} \ell' \left[S_x^2 \begin{pmatrix} \ell & 1 & \ell' \\ m & 0 & -m' \end{pmatrix}^2 + (S^2 - S_x^2) \right. \\ & \quad \left. \cdot \left\{ \begin{pmatrix} \ell & 1 & \ell' \\ m & 1 & -m' \end{pmatrix}^2 + \begin{pmatrix} \ell & 1 & \ell' \\ m & -1 & m' \end{pmatrix}^2 \right\} \right] (2\ell'+1) \mathcal{R}_{n,\ell'}^2 \end{aligned} \quad (6.4.2)$$

An expression for S^2 has been obtained by Møller. It is

$$S^2 = K^2 - \left(\frac{\Delta E}{\hbar c}\right)^2 - \frac{1}{8} \left(\frac{\Delta E}{\hbar c}\right)^2 \quad (6.4.3)$$

Thus we need only find an explicit expression for S_x^2 . From (6.3.13) we have

$$S_x^2 = \left(K_x - \frac{\sqrt{\gamma^2 - 1}}{\gamma} \cdot \frac{\Delta E}{\hbar c} \right)^2 \quad (6.4.4)$$

Thus on account of the inequality (6.3.9) we can show

$$S_x^2 \approx \frac{1}{\gamma^2(\gamma^2 - 1)} \left(\frac{\Delta E}{\hbar c} \right)^2 \quad (6.4.5)$$

Returning to (6.4.2) we have

$$\begin{aligned} & \int |X_{nlm \rightarrow x}(\mathbf{k})|^2 d\omega(\hat{\mathbf{x}}) \\ &= \sum_{l'm'} \left[\frac{1}{\gamma^2(\gamma^2 - 1)} \left(\frac{\Delta E}{\hbar c} \right)^2 \begin{pmatrix} l & 1 & l' \\ m & 0 & -m' \end{pmatrix}^2 \right. \\ & \quad + \left(K^2 - \left(\frac{\Delta E}{\hbar c} \right)^2 - \frac{1}{\gamma^2 - 1} \left(\frac{\Delta E}{\hbar c} \right)^2 \right) \\ & \quad \cdot \left. \left\{ \begin{pmatrix} l & 1 & l' \\ m & 1 & -m' \end{pmatrix}^2 + \begin{pmatrix} l & 1 & l' \\ m & -1 & -m' \end{pmatrix}^2 \right\} \right] \\ & \quad \cdot l'_> (2l' + 1) \mathcal{R}_{x, l'}^2 \end{aligned} \quad (6.4.6)$$

Using (6.3.5), (6.3.12) and (6.4.11) the integration over \mathbf{K}

may be performed analytically. The result is

$$\begin{aligned}
 Q(nlm \rightarrow \kappa) &= \frac{8\pi a_0^2}{m\nu^2 R_y} \cdot \left\{ \sum_{l'm'} R_{\kappa, l'}^2 \langle l' \rangle (2l'+1) \right. \\
 &\cdot \left[\left(\left(\frac{\Delta E}{\hbar c} \right)^2 / \gamma^2 (\gamma^2 - 1) (K_0^2 - \left(\frac{\Delta E}{\hbar c} \right)^2) - \left(1 - \frac{\nu^2}{c^2} \right) \right) \begin{pmatrix} l & 1 & l' \\ m & 0 & -m' \end{pmatrix}^2 \right. \\
 &+ \left. \left(\ln \frac{K_0^2 - \left(\frac{\Delta E}{\hbar c} \right)^2}{\left(\frac{\Delta E}{\hbar c} \right)^2 \frac{1}{\gamma^2 - 1}} + 1 - \frac{\left(\frac{\Delta E}{\hbar c} \right)^2}{(\gamma^2 - 1) (K_0^2 - \left(\frac{\Delta E}{\hbar c} \right)^2)} \right) \cdot \right. \\
 &\cdot \left. \left. \left\{ \begin{pmatrix} l & 1 & l' \\ m & 1 & -m' \end{pmatrix}^2 + \begin{pmatrix} l & 1 & l' \\ m & -1 & -m' \end{pmatrix}^2 \right\} \right] \\
 &+ \left. \int_{K_0}^{K_{\max}} \mathcal{E}(K) \frac{dK}{K^3} \right\}
 \end{aligned}$$

(6.4.7)

Now the integral over $K_0 \rightarrow K_{\max}$ may be obtained from earlier results (see Chapter 4). We evaluate the 3j-symbols, use the inequality $K_0^2 \gg \left(\frac{\Delta E}{\hbar c} \right)^2$ and obtain finally:

$$\begin{aligned}
& Q(nlm \rightarrow i) \\
&= \frac{2\pi e^4 \alpha^2}{R_y \cdot m v^2} \left\{ \left(\ln \frac{2c_i m v^2}{R_y} - \ln \left(1 - \frac{v^2}{c^2}\right) - 1 \right) \right. \\
&\quad \cdot \frac{1}{2} \left(\frac{(l+1)(l+2)+m^2}{(2l+3)(2l+1)} R_{x,l+1}^2 + \frac{l(l-1)+m^2}{(2l+1)(2l-1)} R_{x,l-1}^2 \right) \\
&\quad \left. + \left(1 - \frac{v^2}{c^2}\right) \left(\frac{(l+1)^2 - m^2}{(2l+3)(2l+1)} R_{x,l+1}^2 + \frac{l^2 - m^2}{(2l+1)(2l-1)} R_{x,l-1}^2 \right) \right\} \quad (6.4.8)
\end{aligned}$$

There are two checks on this equation: it reduces to (4.4.7) when $\frac{v}{c} \ll 1$, and to (5.1.1) when we sum over m . The factor C_i represents the contribution from the transitions with momentum transfers greater than $\hbar k_0$.

On insertion of the explicit values of the parameters $R_{x,d}$, $R_{x,s}$, C_i obtained in Chapter 4 we find

$$\begin{aligned}
Q(2p, 0 \rightarrow i) &= \frac{2\pi e^4 \alpha^2}{m v^2 \cdot R_y} \left\{ \left(\ln \frac{2m v^2}{R_y (1 - v^2/c^2)} + 10.392 \right) 0.45999 \right. \\
&\quad \left. + \left(1 - \frac{v^2}{c^2}\right) 0.67353 \right\} \quad (6.4.9a)
\end{aligned}$$

$$\begin{aligned}
Q(2p, \pm 1 \rightarrow i) &= \frac{2\pi e^4 \alpha^2}{m v^2 \cdot R_y} \left\{ \left(\ln \frac{2m v^2}{R_y (1 - v^2/c^2)} + 9.665 \right) 0.56676 \right. \\
&\quad \left. + \left(1 - \frac{v^2}{c^2}\right) 0.45999 \right\} \quad (6.4.9b)
\end{aligned}$$

Figure (6.1) exhibits the ratio of these two expressions,

Q_0/Q_1 , as a function of energy, for three different values of Z . For comparison, the corresponding non-relativistic expressions have also been included. Figure (6.1) makes it clear that the effect of the correction is to make the approach to the high energy limit more rapid, although still extremely slow, thus emphasizing that the high energy limit is of formal rather than of practical interest. The major correction is the so-called "relativistic rise" term,

$-\ln(1 - \frac{v^2}{c^2})$. According to Fano (1956), this term, which causes the total cross section to pass through a minimum before rising monotonically with further increase of energy, stems from virtual photons which give rise to forces

perpendicular to \mathbf{k} . Hence the fact that Q_0/Q_1 tends to the same high energy limit both relativistically and non-relativistically is not trivial. We recall that, for

those collisions which make the major contribution to the cross section at these energies (those of small $\hbar k$), $\hat{\mathbf{k}}$ tends with increase of energy to become parallel to the direction of coincidence, $\hat{\mathbf{k}}_0$. This is a purely

kinematic conclusion. The virtual photon forces identified by Fano, however, are a consequence of the special nature of the Møller interaction. The combination of these effects leads to the conclusion that the forces acting on the bound

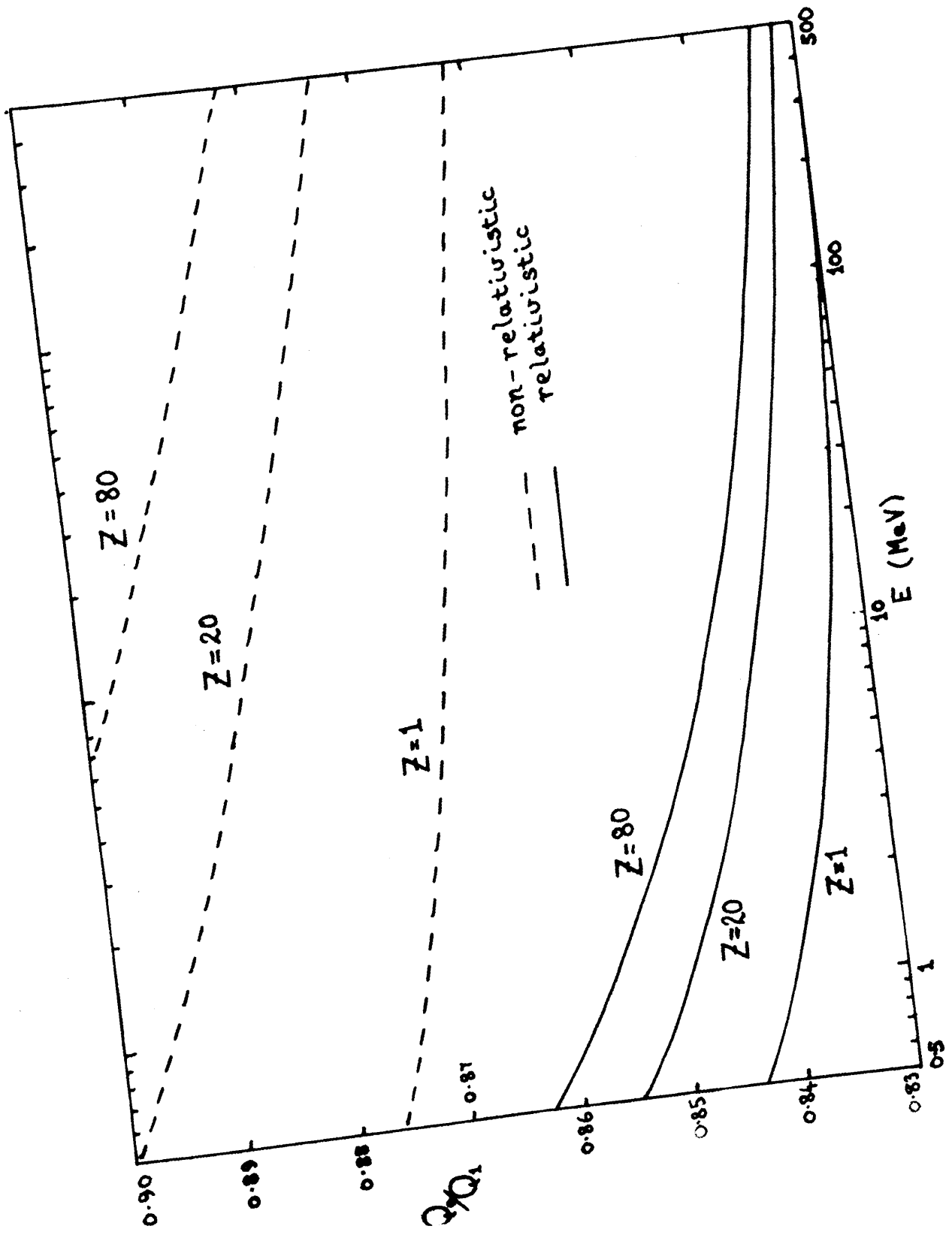


Fig. (6.1)

electron tend to become perpendicular to \mathbf{k}_0 in the limit of high energies, just as for the non-relativistic case.

CHAPTER 7

ANISOTROPY FOLLOWING INNER SHELL PHOTOIONIZATION

1. Introduction

It is known that there is a close connection between electron impact ionization in the limit of high energies and the process of photoionization. This connection is reflected in the presence of the optical oscillator strength in the Bethe asymptotic cross section formula (see, for example, Inokuti 1971). Hence one would expect the occurrence of anisotropic effects following electron ionization of inner shells to imply similar effects for photoionization. This fact has been realized by Flugge, Mehlhorn and Schmidt (hereafter abbreviated by FMS), who have recently (1972) calculated some Auger electron angular distributions following photoionization by unpolarized light. Notwithstanding the existence of these prior calculations of FMS, this chapter will be concerned with

- (a) the calculation of photoionization cross sections from the orbital designated by the set of quantum numbers $(n \ell j m_j)$;
- (b) the use of these to predict the asymmetry parameter of the resulting Auger electron angular distribution,

β , as a function of photon energy.

Before doing so, the obvious charge of redundancy must be countered.

(1) Explicit formulae will be given for any ($n \ell j m_j$) and for all possible light polarizations. FMS contains such formulae only for $\ell=1$, $j=3/2$, $|m_j|=3/2, 1/2$, and for unpolarized light. Thus their results represent a special case of the present calculation.

(2) By the manner in which FMS present and interpret their calculated data they give the impression that β is typically quite large, which is not in fact the case.

(3) In a simple physical argument, it is shown why the study of anisotropic effects following photoionization can be of more interest than similar studies with regard to photoexcitation.

2. Calculation and Results

The required photoionization cross sections are obtained by evaluating the expression

$$I^{\mu}(nljm_j) = \sum_{m_s'} \int |\langle \chi_{\mu, m_s'} | r C_{\mu}^1 | nljm_j \rangle|^2 d\omega(\hat{x}) \quad (7.2.1)$$

where $\frac{\hbar^2 k^2}{2m} = h\nu - E_{nlj}$ is the energy of the ejected photoelectron. Note that we integrate over all directions of ejection and sum over all final spin orientations. The index μ in the operator gives the polarization of the incident radiation. It will be apparent from (7.2.1) that the photoionization process is being described in the dipole approximation, which should hold for Z not too large.

Now the photoionization cross section will be proportional to (7.2.1), but since the proportionality constant is certainly independent of m_j , we can leave it out of consideration and need only evaluate for our purposes the quantity

$I^{\mu}(nljm_j)$. In the expression (3.1.17) we have

$I^{\mu}(nljm_j)$ in terms of 3j-symbols. It will be useful to write $I^{\mu}(nljm_j)$ in the general form

$$I^{\mu}(nljm_j) = A R_{\mu, l+1}^2 + B R_{\mu, l-1}^2 \quad (7.2.2)$$

where the $R_{\mu, l+1}$ are defined in (3.1.7) and A and B are functions of μ, l, j and m_j (not to be confused with the Einstein A and B coefficients). Calculation of

the $3j$ -symbols in (3.1.17) allows us to construct Table 7.1, which gives A and B for all μ , and for each of the two possibilities $j = l \pm \frac{1}{2}$. Note that an unpolarized beam may be represented by the incoherent addition of left- and right-circularly polarized beams.

For the specific case $j = \frac{3}{2}$, Table (7.1) gives

$$I^0\left(\frac{3}{2}, \frac{3}{2}\right) = I^0\left(\frac{3}{2}, -\frac{3}{2}\right) = \frac{9}{5} R_{xd}^2 \quad (7.2.3a)$$

$$I^0\left(\frac{3}{2}, \frac{1}{2}\right) = I^0\left(\frac{3}{2}, -\frac{1}{2}\right) = \frac{11}{5} R_{xd}^2 + 2R_{xs}^2 \quad (7.2.3b)$$

$$I^{+1}\left(\frac{3}{2}, \frac{3}{2}\right) = I^{-1}\left(\frac{3}{2}, -\frac{3}{2}\right) = \frac{18}{5} R_{xd}^2 \quad (7.2.4a)$$

$$I^{+1}\left(\frac{3}{2}, \frac{1}{2}\right) = I^{-1}\left(\frac{3}{2}, -\frac{1}{2}\right) = \frac{12}{5} R_{xd}^2 \quad (7.2.4b)$$

$$I^{+1}\left(\frac{3}{2}, -\frac{1}{2}\right) = I^{-1}\left(\frac{3}{2}, \frac{1}{2}\right) = \frac{7}{5} R_{xd}^2 + R_{xs}^2 \quad (7.2.4c)$$

$$I^{+1}\left(\frac{3}{2}, -\frac{3}{2}\right) = I^{-1}\left(\frac{3}{2}, \frac{3}{2}\right) = \frac{3}{5} R_{xd}^2 + 3R_{xs}^2 \quad (7.2.4d)$$

It can be checked that addition of (7.2.4a) to (7.2.4d) and

Polarization	$j = l + \frac{1}{2}$	$j = l - \frac{1}{2}$
	A	B
linear $\mu = 0$	$j^2 - m_j^2$	$(j+1)^2 - m_j^2$
right circular $\mu = +1$	$\frac{1}{2}(j+m_j+1) \cdot \left\{ j+m_j \left(\frac{j-1}{j+1} \right) \right\}$	$\frac{1}{2}(j-m_j) \cdot \left\{ j-m_j \left(\frac{j+2}{j+1} \right) \right\}$
left circular $\mu = -1$	$\frac{1}{2}(j-m_j+1) \cdot \left\{ j-m_j \left(\frac{j-1}{j+1} \right) \right\}$	$\frac{1}{2}(j+m_j) \cdot \left\{ j+m_j \left(\frac{j+2}{j+1} \right) \right\}$
zero (incoherent mixture of +1 and -1)	$\frac{1}{2}j(j+1) + \frac{1}{2}m_j^2 \left(\frac{j-1}{j+1} \right)$	$\frac{1}{2}j(j+1) + \frac{1}{2}m_j^2$

$\underbrace{\hspace{10em}}_{\text{All } \times 4j^2}$

$\underbrace{\hspace{10em}}_{\text{All } \times 4(j+1)^2}$

Table (r.1)

of (7.2.4b) to (7.2.4c) give expressions for unpolarized radiation which agree with FMS.

We turn now to the distribution of the Auger electrons ejected from the atom as a result of radiationless transitions into the vacancies left by photoionization. For the case where the residual ion is left with $J=0$ in the Auger shell, the distribution is particularly simple, and has been given by FMS:

$$I(\theta) \propto 1 + \beta P_2(\cos\theta) \quad (7.2.5)$$

where

$$\beta = \frac{I^u(\frac{3}{2}, \frac{1}{2}) - I^u(\frac{3}{2}, \frac{3}{2})}{I^u(\frac{3}{2}, \frac{1}{2}) + I^u(\frac{3}{2}, \frac{3}{2})} \quad (7.2.6)$$

Equations (7.2.3) and (7.2.4) give

$$\beta(\text{linear}) = \frac{0.2 R_{xd}^2 + R_{xs}^2}{2 R_{xd}^2 + R_{xs}^2} \quad (7.2.7)$$

$$\begin{aligned} \beta(\text{right circular}) &= \beta(\text{left circular}) \\ &= \beta(\text{unpolarized}) \\ &= (-0.5) \cdot \beta(\text{linear}) \end{aligned} \quad (7.2.8)$$

It is interesting that circularly polarized radiation produces the same Auger distribution as unpolarized radiation. This result is true for all j , as can readily be seen from Table (7.1). It arises from the independence of (7.2.6) of the sign of m_j . Note also that the expression (7.2.8) is exactly - 0.5 times that given by (7.2.7), so that the two distributions are opposite in sense, for all photon energies. This would seem to be a peculiarity of orbitals having $j = 3/2$.

Comments

It could be argued that the inclusion of all possible states of polarization is not really necessary, since an experimental measurement which uses unpolarized radiation will obtain information on the quantities $R_{K, l \pm 1}^2$ and hence the added practical complication of polarizing the radiation leads to no new information which could not have been obtained without recourse to this. However, there are several points to be made against this.

1) UV radiation from electron synchrotrons is at present being used in photoionization studies, and such radiation has a strong linear polarization. Thus the formula of FMS would be inapplicable to such a case.

2) The angular distributions resulting from the use of linearly polarized radiation are sometimes more anisotropic than those from unpolarized radiation, and may therefore be easier to measure.

3) Lastly, the use of polarized radiation provides a means of checking the information derived from unpolarized radiation.

FMS have calculated explicit values for the asymmetry parameter β for the cases Ca (3p subshell) and Mg (2p subshell). Of these, the former leads to larger β for all photon energies shown, and exhibits a steep maximum near threshold, in which β touches the extreme value - 0.5. Mg shows no maximum and is less than -0.1 for most of the energy range. FMS say that they select these two examples "to demonstrate the striking differences in the angular distribution of Auger electrons of different elements". They do not point^{out} however, that this striking difference can be readily correlated with the phenomenon observed in photoionization cross sections known as the Cooper minimum. In the case in point, this minimum is a result of the variation of the overlap, as a function of energy, of the χ_d with the 3p wave function. For a particular value of χ this results in the disappearance

of the quantity R_{Xd} . That this circumstance leads to a maximum in the Auger asymmetry parameter can be verified by reference to Table (7.1), using the fact that only the B coefficient of (7.2.2) takes part. Physically, it can readily be explained as follows. Given that the quantization axis is chosen along the wave vector of the photon, we see that angular momentum transfers to the atom are limited by the rule

$\Delta m \neq 0$. When to this is added the further restriction that only X_S states can be reached by photoionization, we see that we have the selection rule

$$Q(np, m=0 \rightarrow X_c) = 0 \quad (7.3.1)$$

where by X_c we have labelled the energy corresponding to the Cooper minimum. Hence only vacancies with $m \neq 0$ can be produced at the Cooper minimum, and the maximum in the asymmetry parameter is thus accounted for.

Hence one only expects large anisotropy in the region of a Cooper minimum. This is exemplified by the behaviour of β for the 2p subshell of Mg , which does not possess a Cooper minimum in its photoionization cross section. More generally, large anisotropy results only from photoionization of some subshells, only for photon energies in a certain range, and the behaviour of the $Mg\ 2p$ results of FMS may be regarded as more typical than that of the $Ca\ 3p$ results.

Many investigations have been carried out on the polarization of optical radiation from atoms excited by radiation which is itself polarized (see Mitchell and Zemansky, 1934; or more recently Kleinpoppen and Neugart, 1966). Typically one is exciting the atom to an upper state which has well-defined orbital angular momentum, and essentially one calculates the polarization of the de-excitation radiation from angular momentum conservation, a knowledge of radial wave functions thus being superfluous. The crucial difference in the ionization case is that continuum energy levels are degenerate with respect to orbital angular momentum, so that s, p, d, f... states are present at the same excitation energy. For each of these states of given ℓ it is possible to calculate the relative vacancy distribution in the residual ion over the substates, using only angular momentum conservation. However, to sum their contributions to the resultant vacancy distribution we must know the extent of the overlap of the final state wavefunction with the initial state wavefunction for each case.

To the extent that the dipole approximation is correct, one need only consider the two states given by $\ell' = \ell \pm 1$. In other words, the vacancy distribution depends on the ratio $R_{\ell\ell+1} / R_{\ell\ell-1}$, and thus contains information on the form of the radial wavefunctions. It is this feature of anisotropic phenomena following photoionization which could

render future experimental investigations particularly interesting.

CHAPTER 8

DIRECTIONAL CORRELATION IN INNER SHELL PHOTOIONIZATION

1. Theory

It is the intention of this chapter to demonstrate that when an atom de-excites following inner shell photoionization, the particle emitted - photon or Auger electron - is ejected in a direction which is strongly correlated with that of the primary photoelectron. It will be shown that the detailed form of the correlation is a function of parameters of basic theoretical interest - the radial dipole matrix elements, and the phase shifts of the partial (ejected electron) waves. For this reason, it is suggested that a coincidence experiment (electron-electron or electron-photon) could be expected to yield much worthwhile information.

We have seen in previous chapters how Auger angular distributions and X-ray polarizations depend on the ratios of the ionization cross sections $Q(n\ell m \rightarrow i)$ for different values of m . These ratios are not very large in general, and therefore do not lead to large anisotropy in the vacancy de-excitation process. However, it might happen

that the probability of ejection in a particular direction varies substantially, depending on which magnetic substate the electron initially occupies. Of course, an experiment on the angular distribution of photoelectrons will detect the sum of the contributions from the individual m states, and will give no information on the ratio of these contributions. To obtain such information, we must detect, in coincidence with the photoelectron, the particle which results from the filling of the vacancy caused by its ejection. If the ratio of the above-mentioned contributions is large, the angular distribution of the secondary particle may in general be expected to be highly anisotropic.

To put the foregoing argument on a more quantitative footing, we must first of all calculate the angular distribution of photoelectrons ejected from a bound state characterized by the quantum numbers $(n \ell m)$. Comparable calculations for the quantum numbers $(n \ell)$, summing over all orientations m , have been carried out by Zare and Cooper (1968). The atomic wavefunctions are calculated in the central field approximation, and the interaction between photon and atom is treated in the dipole approximation. The quantization axis is taken along the direction of the photon beam, and the beam is assumed to be unpolarized. This is achieved by calculating separately

the probabilities for right- and left-circular polarization and adding them incoherently.

The amplitude for photo-ejection from a bound state (nlm) by light of polarization μ is given by

$$\langle f | r C_{\mu}^1 | i \rangle = \sum_{l', m'} a(l', m') (-1)^{l'-m'+q} (l')^{\frac{1}{2}} \mathcal{R}_{\mu} \begin{pmatrix} l & 1 & l' \\ m & \mu & -m' \end{pmatrix} \quad (8.1.1)$$

where we have adopted the notation and procedure of Chapter 3. The dependence on direction of photo-ejection, it will be recalled, is contained in $a(l', m')$. The required angular distribution is proportional to

$$\begin{aligned} I^{\mu}(nlm; \theta) &= |\langle f | r C_{\mu}^1 | i \rangle|^2 \\ &= \sum_{l_1, l_2} a(l_1, m+\mu) a^*(l_2, m+\mu) \\ &\quad \cdot (-1)^{l_1+l_2+q_1+q_2} (l_1)^{\frac{1}{2}} (l_2)^{\frac{1}{2}} \mathcal{R}_{\mu} \mathcal{R}_{\mu} \\ &\quad \cdot \begin{pmatrix} l & 1 & l_1 \\ m & \mu & -m-\mu \end{pmatrix} \begin{pmatrix} l & 1 & l_2 \\ m & \mu & -m-\mu \end{pmatrix} \end{aligned} \quad (8.1.2)$$

The summations are limited by the requirements $l_1 = l \pm 1$, $l_2 = l \pm 1$ (triangular property of 3j-symbols).

For unpolarized radiation,

$$\begin{aligned}
I(nlm; \theta) &= \frac{1}{2} \left\{ |\langle f | r C_{+1}^1 | i \rangle|^2 + |\langle f | r C_{-1}^1 | i \rangle|^2 \right\} \\
&= \frac{1}{2} \sum_{l_1, l_2} (-1)^{l_1 + l_2 + g_1 + g_2} (l_1 >)^{\frac{1}{2}} (l_2 >)^{\frac{1}{2}} R_{\kappa l_1} R_{\kappa l_2} \\
&\quad \cdot \left\{ a(l_1, m+1) a^*(l_2, m+1) \begin{pmatrix} l & 1 & l_1 \\ m+1 & -m-1 & \end{pmatrix} \begin{pmatrix} l & 1 & l_2 \\ m+1 & -m-1 & \end{pmatrix} \right. \\
&\quad \left. + a(l_1, m-1) a^*(l_2, m-1) \begin{pmatrix} l & 1 & l_1 \\ m-1 & -m+1 & \end{pmatrix} \begin{pmatrix} l & 1 & l_2 \\ m-1 & -m+1 & \end{pmatrix} \right\}
\end{aligned}$$

(8.1.3)

After evaluating 3j-symbols and substituting the explicit expressions for the $a(l, m)$, we find

$$\begin{aligned}
&I(nlm; \theta) \\
&= \frac{1}{2} \left[\frac{R_{\kappa l+1}^2}{(2l+3)(2l+1)} \left\{ |Y_{l+1, m-1}(\hat{x})|^2 (l-m+1)(l-m+2) \right. \right. \\
&\quad \left. \left. + |Y_{l+1, m+1}(\hat{x})|^2 (l+m+1)(l+m+2) \right\} \right. \\
&\quad \left. + \frac{R_{\kappa l-1}^2}{(2l+1)(2l-1)} \left\{ |Y_{l-1, m-1}(\hat{x})|^2 (l+m)(l+m-1) \right. \right. \\
&\quad \left. \left. + |Y_{l-1, m-1}(\hat{x})|^2 (l-m)(l-m-1) \right\} \right]
\end{aligned}$$

$$\begin{aligned}
& + \frac{R_{x\ell+1} R_{x\ell-1}}{(2\ell+3)^{\frac{1}{2}}(2\ell+1)(2\ell-1)^{\frac{1}{2}}} \\
& \cdot \left\{ \left(Y_{\ell+1, m-1}^*(\hat{x}) Y_{\ell-1, m-1}(\hat{x}) e^{-i(\delta_{\ell+1} - \delta_{\ell-1})} + Y_{\ell-1, m-1}^*(\hat{x}) Y_{\ell+1, m-1}(\hat{x}) e^{i(\delta_{\ell+1} - \delta_{\ell-1})} \right) \right. \\
& \quad \cdot [(\ell-m+1)(\ell-m+2)(\ell+m)(\ell+m-1)]^{\frac{1}{2}} \\
& + \left(Y_{\ell+1, m+1}^*(\hat{x}) Y_{\ell-1, m+1}(\hat{x}) e^{-i(\delta_{\ell+1} - \delta_{\ell-1})} + Y_{\ell-1, m+1}^*(\hat{x}) Y_{\ell+1, m+1}(\hat{x}) e^{i(\delta_{\ell+1} - \delta_{\ell-1})} \right) \\
& \quad \cdot [(\ell+m+1)(\ell+m+2)(\ell-m)(\ell-m-1)]^{\frac{1}{2}} \left. \right\} \quad (8.1.4)
\end{aligned}$$

By squaring the well-known identity

$$\cos\theta Y_{\ell, m} = \left[\frac{(\ell+m+1)(\ell-m+1)}{(2\ell+3)(2\ell+1)} \right]^{\frac{1}{2}} Y_{\ell+1, m} + \left[\frac{(\ell+m)(\ell-m)}{(2\ell+1)(2\ell-1)} \right]^{\frac{1}{2}} Y_{\ell-1, m} \quad (8.1.5)$$

and rearranging terms, it is possible to eliminate cross terms between spherical harmonics appearing in (8.1.4).

We have then finally

$$\begin{aligned}
& I(n\ell m; \theta) \\
& = \frac{1}{2} \left[\frac{R_{x\ell+1}^2}{(2\ell+3)(2\ell+1)} \left\{ |Y_{\ell+1, m-1}(\hat{x})|^2 (\ell-m+1)(\ell-m+2) \right. \right. \\
& \quad \left. \left. + |Y_{\ell+1, m+1}(\hat{x})|^2 (\ell+m+1)(\ell+m+2) \right\} \right. \\
& + \frac{R_{x\ell-1}^2}{(2\ell+1)(2\ell-1)} \left\{ |Y_{\ell-1, m-1}(\hat{x})|^2 (\ell+m)(\ell+m-1) \right. \\
& \quad \left. + |Y_{\ell-1, m+1}(\hat{x})|^2 (\ell-m)(\ell-m-1) \right\}
\end{aligned}$$

$$\begin{aligned}
& + R_{x_{l+1}} R_{x_{l-1}} \cos(\delta_{l+1} - \delta_{l-1}) \\
& \cdot \left\{ \cos^2 \theta \left(|Y_{l,m-1}(\frac{\hat{r}}{R})|^2 + |Y_{l,m+1}(\frac{\hat{r}}{R})|^2 \right) \right. \\
& - \frac{(l+1)^2 - (m-1)^2}{(2l+3)(2l+1)} |Y_{l+1,m-1}(\frac{\hat{r}}{R})|^2 - \frac{(l+1)^2 - (m+1)^2}{(2l+3)(2l+1)} |Y_{l+1,m+1}(\frac{\hat{r}}{R})|^2 \\
& \left. - \frac{l^2 - (m-1)^2}{(2l+1)(2l-1)} |Y_{l-1,m-1}(\frac{\hat{r}}{R})|^2 - \frac{l^2 - (m+1)^2}{(2l+1)(2l-1)} |Y_{l-1,m+1}(\frac{\hat{r}}{R})|^2 \right\} \quad (8.1.6)
\end{aligned}$$

Below we evaluate (8.1.6) for the first few values of l :

$l=0$ (s-state):

$$I(ns; \theta) = \frac{1}{2} R_{xp}^2 \sin^2 \theta \quad (8.1.7a)$$

$l=1$ (p-state):

$$I(np, 0; \theta) = \frac{3}{2} R_{xd}^2 \sin^2 \theta \cos^2 \theta \quad (8.1.7b)$$

$$\begin{aligned}
I(np, \pm 1; \theta) &= \frac{1}{24} R_{xd}^2 [(3\cos^2 \theta - 1)^2 + 9\sin^4 \theta] \\
&+ \frac{1}{6} R_{xs}^2 \\
&+ \frac{1}{6} R_{xd} R_{xs} \cos(\delta_d - \delta_s) (3\cos^2 \theta - 1)
\end{aligned} \quad (8.1.7c)$$

$l=2$ (d-state):

$$\begin{aligned}
I(nd, 0; \theta) &= \frac{9}{40} R_{xf}^2 \sin^2 \theta (5\cos^2 \theta - 1)^2 \\
&+ \frac{1}{10} R_{xp}^2 \sin^2 \theta + \frac{3}{10} R_{xf} R_{xp} \cos(\delta_f - \delta_p) \\
&\quad \cdot \sin^2 \theta (5\cos^2 \theta - 1)
\end{aligned} \quad (8.1.7d)$$

$$\begin{aligned}
I(nl, \pm 1; \theta) = & \frac{3}{40} R_{xf}^2 \cos^2 \theta [(5 \cos^2 \theta - 3)^2 + 25 \sin^4 \theta] \\
& + \frac{3}{10} R_{xp}^2 \cos^2 \theta \\
& + \frac{3}{10} R_{xp} R_{xf} \cos(\delta_f - \delta_p) \\
& \cdot \cos^2 \theta (5 \cos^2 \theta - 3)
\end{aligned}$$

(8.1.7e)

$$\begin{aligned}
I(nl, \pm 2; \theta) = & \frac{3}{160} R_{xf}^2 \sin^2 \theta [(5 \cos^2 \theta - 1)^2 + 25 \sin^4 \theta] \\
& + \frac{3}{10} R_{xp}^2 \sin^2 \theta \\
& + \frac{3}{20} R_{xf} R_{xp} \cos(\delta_f - \delta_p) \sin^2 \theta (5 \cos^2 \theta - 1)
\end{aligned}$$

(8.1.7f)

The $I(nl; \theta)$ which Cooper and Zare calculate can all be cast in the form $a + b \cos^2 \theta$, irrespective of the values of n and l . This is because summation over m renders all subshells spherically symmetric, so that asymmetry enters only through the incident photon. The $I(nlm; \theta)$, on the other hand, become increasingly complex functions of θ as l increases, reflecting the increasing complexity of the angular wavefunction.

For inner shells, and particularly for the heavier atoms, one must take account of fine structure. This means that the initial bound state of the electron should be described in the coupled representation $(nljm_j)$. It can be shown, by a straight-forward extension of the algebra of Chapter 3, that for the present case

$$\begin{aligned}
 & |\langle f | r C_{\mu}^1 | i \rangle |_{\text{coupled}}^2 \\
 &= \sum_{m, m_s} [j] \begin{pmatrix} l & s & j \\ m & m_s & -m_j \end{pmatrix}^2 |\langle f | r C_{\mu}^1 | i \rangle |_{\text{uncoupled}}^2
 \end{aligned}
 \tag{8.1.8}$$

Hence we may write

$$\begin{aligned}
 & I(nljm_j; \theta) \\
 &= \frac{1}{2} \sum_{m, m_s} \begin{pmatrix} l & s & j \\ m & m_s & -m_j \end{pmatrix}^2 [j] I(nlm; \theta)
 \end{aligned}
 \tag{8.1.9}$$

As stated earlier, we can gain information about the $I(nljm_j; \theta)$, and hence the $I(nlm; \theta)$, by observing the angular distribution of the secondary particle, which can either be a photon or an Auger electron. A comprehensive review of the Auger effect is given by Burhop (1952).

To render the discussion more specific, we consider an Auger transition of the type $L_3 M_{2,3} M_{2,3} (^2 S_0)$ where the Auger electron is emitted as a single $p_{3/2}$ -wave. For the case where one does not detect the direction of the initial photoelectron, the angular distribution can be written

$$I(\theta_A) \propto 1 + \beta P_2(\cos \theta_A) \quad (8.1.10)$$

where we have used θ_A for the direction of ejection of the Auger electron to avoid confusion with θ , that of the photoelectron. $P_2(\cos \theta_A)$ is a Legendre polynomial and

$$\beta = \frac{Q(\frac{3}{2}, \frac{1}{2}) - Q(\frac{3}{2}, \frac{3}{2})}{Q(\frac{3}{2}, \frac{1}{2}) + Q(\frac{3}{2}, \frac{3}{2})} \quad (8.1.11)$$

β is called the asymmetry parameter of the distribution and the $Q(j, m_j)$ are abbreviations for the total ionization cross sections $Q(nl; m_j \rightarrow X)$.

If the angle of ejection of the photoelectron is measured in coincidence with that of the Auger electron, we may define by extension an asymmetry parameter which is a function of θ :

$$\beta(\theta) = \frac{I(\frac{3}{2}, \frac{1}{2}; \theta) - I(\frac{3}{2}, \frac{3}{2}; \theta)}{I(\frac{3}{2}, \frac{1}{2}; \theta) + I(\frac{3}{2}, \frac{3}{2}; \theta)} \quad (8.1.12)$$

where $I(j, m_j; \theta)$ is in abbreviated form the $I(nl; j, m_j; \theta)$ which was defined in (8.1.9).

2. Results

We have taken theoretical values for the $R_{\kappa l+1}$ from two sources. Firstly, we have used the results of Burgess (1964), which apply to hydrogenic systems, and which should therefore give good results when applied to the inner shells of the heavier atoms (although it should be remembered that in this region the dipole approximation will be suspect). Secondly, the results of McGuire (1970) have been employed. McGuire has calculated the $R_{\kappa l+1}$ for selected values of κ for the elements He to Xe. Details of his method of calculation are given elsewhere (McGuire, 1968). Briefly, he approximates the quantity $-rV(r)$ by a series of straight lines, adjusting the parameters of the straight lines to give approximately the same bound state energy eigenvalues as those obtained by Herman and Skillman (1963) using the Hartree-Fock-Slater approach. He then uses the discrete and continuum orbitals of the model to obtain photoionization cross sections.

The theoretical $R_{\kappa l+1}$ values can be used to evaluate the $I(nlm; \theta)$ given in (8.1.7a - f). The case $I(ns; \theta)$ is somewhat trivial: here we have a $\sin^2 \theta$ distribution for all $R_{\kappa p}$. For the case $I(np, 0; \theta)$ we have a

$\sin^2\theta \cos^2\theta$ distribution for all R_{xp} , but for $I(np, \pm 1; \theta)$ we have two competing outgoing channels and therefore the detailed form of the distribution depends on the ratio R_{xd}/R_{xs} and on the phase shift difference $(\delta_d - \delta_s)$. Figure (8.1) shows $I(2p, 0; \theta)$ and $I(2p, \pm 1; \theta)$, using Burgess's data, for zero energy of ejection. $I(2p, \pm 1; \theta)$ was calculated using the extreme values of 0 and π for the phase shift difference. It is interesting that the ratio

$$\frac{I(2p, 0; \theta_{\text{magic}})}{I(2p, \pm 1; \theta_{\text{magic}})} \quad (8.2.1)$$

(where $\theta_{\text{magic}} = \cos^{-1}(\frac{1}{\sqrt{3}}) \approx 55^\circ$ is the so-called "magic angle") does not depend on the phase shift difference but only on the ratio R_{xd}/R_{xs} .

The picture is not appreciably altered for ejection energies greater than threshold, for a hydrogenic system, because of the slow, monotonic variation of R_{xd}/R_{xs} with κ . However, a very different picture can be seen for the lighter atoms on the basis of McGuire's data. We consider the particular case of photoionization from the 3p-subshell of Ca. Figure (8.2) shows the situation at threshold. Here,

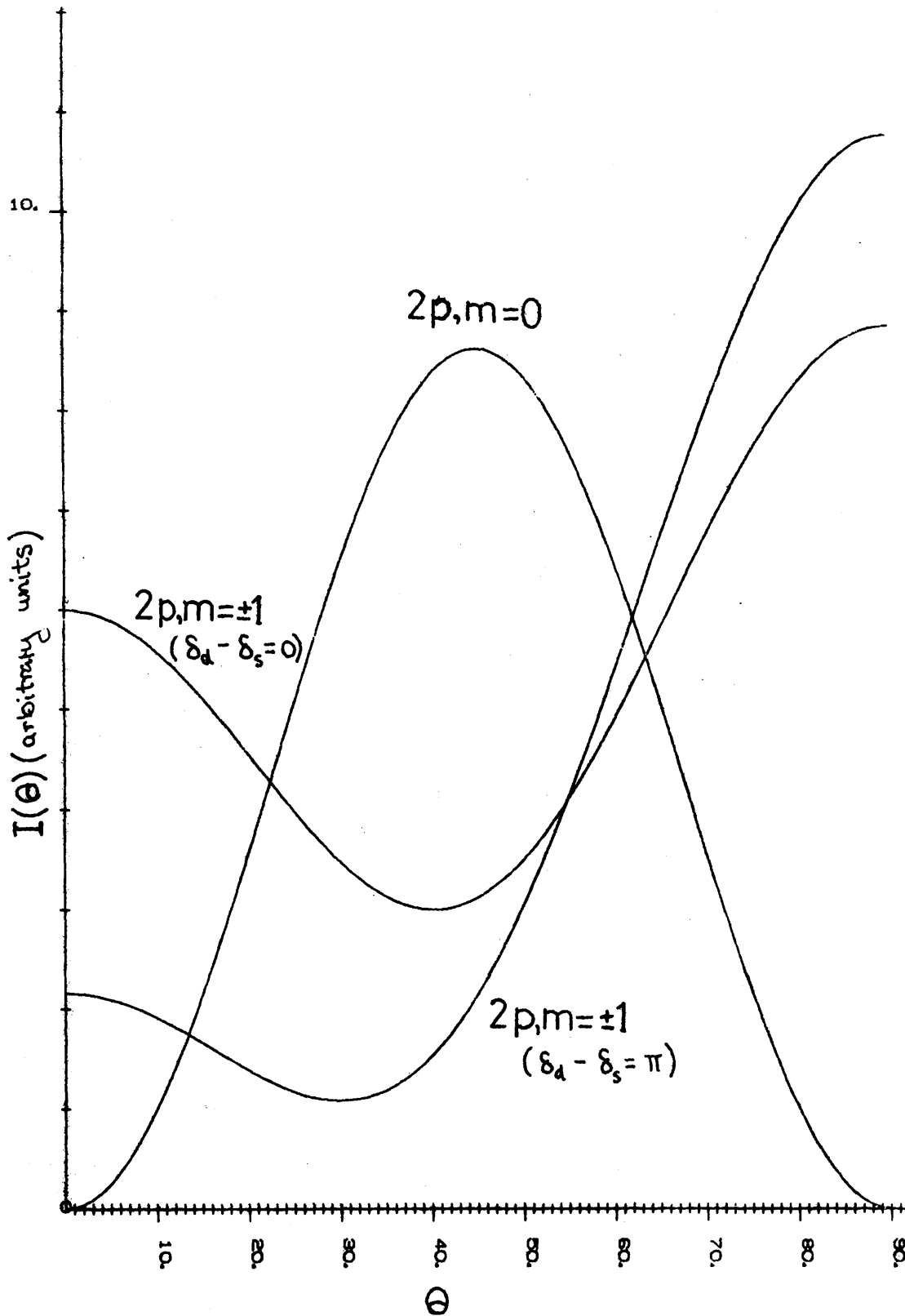


Fig. (8.1) Angular distribution of photoelectrons ejected from the hydrogenic states $(2p, 0)$, $(2p, \pm 1)$ with

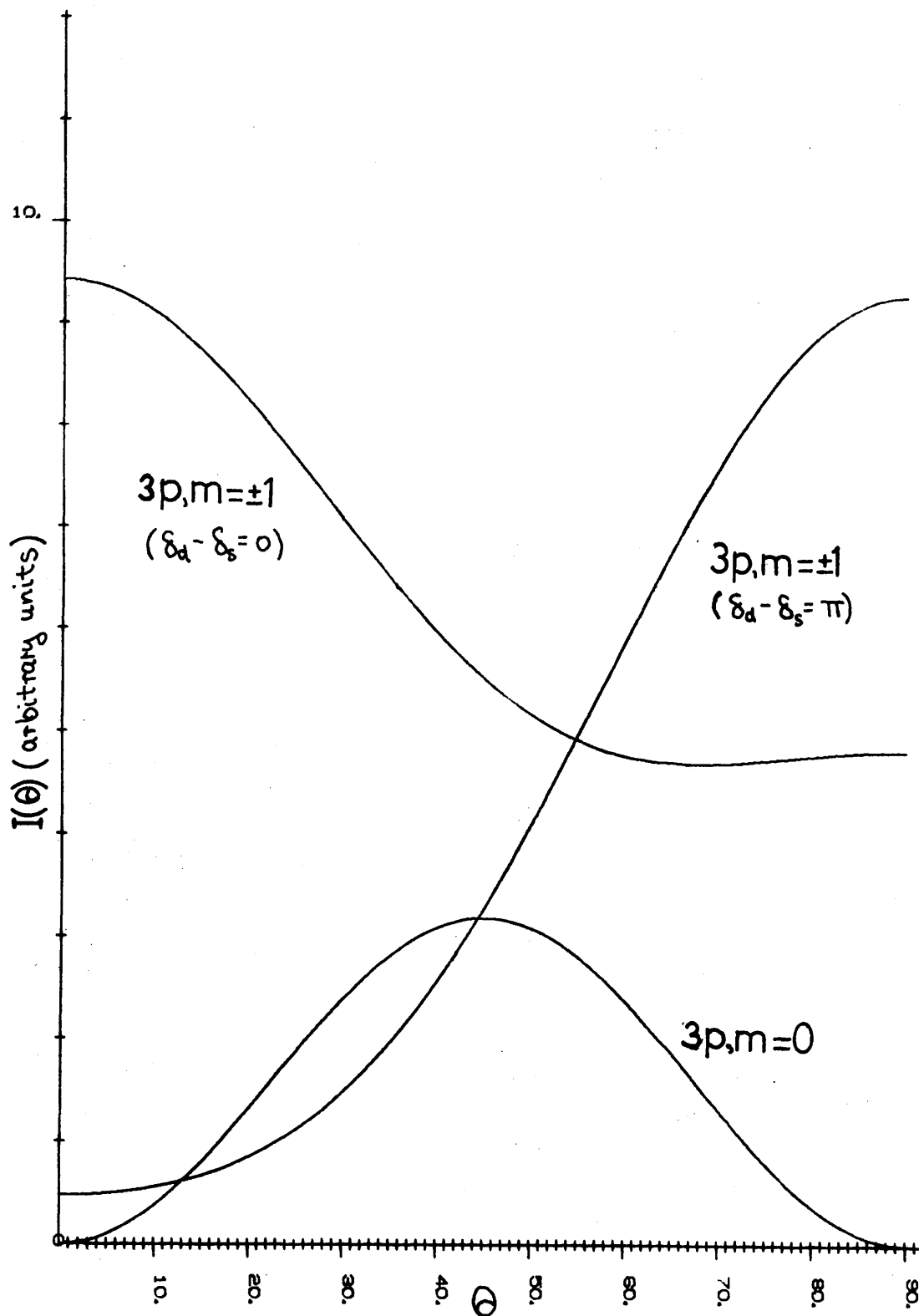


Fig. (8.2)

Angular distribution of photoelectrons ejected from Ca states $(3p, 0)$, $(3p, \pm 1)$ with zero energy.

$R_{xd}/R_{xs} \approx 1$, and $I(3p, \pm 1; \theta)$ is extremely sensitive to the phase shift difference. Furthermore, the distributions vary rapidly as the total photoionization cross section goes through what has become known as the "Cooper minimum". Such minima are associated with a change in sign of R_{xd} as X varies, so that for a particular value of X we have $R_{xd} = 0$. Inspection of (8.1.7b) and (8.1.7c) shows that $I(n p, 0; \theta) = 0$ and $I(n p, \pm 1; \theta) = \text{constant}$ at the Cooper minimum. For energies well above the minimum, we have $R_{xd} \gg R_{xs}$ as in the Coulomb case, so that here the distributions look much like those of Figure (8.1). Incidentally, for the 2p-subshell of Ca McGuire's data give a picture which approaches more nearly to the hydrogenic case, as one would expect of an inner subshell. The most important feature of these results, then, is that the ratio $I(n p, 0; \theta) / I(n p, \pm 1; \theta)$ is far from being unity for most angles θ , and is a rapidly-varying function of θ . Thus encouraged, we insert the data of Figure (8.1) into the formulae (8.1.9) and (8.1.12) and obtain the corresponding behaviour of $\beta(\theta)$ as a function of θ . We see that the magnitude of $\beta(\theta)$ varies considerably and that its sign changes twice in the region $\theta = 0$ to $\theta = \pi/2$ (Figure (8.3)).

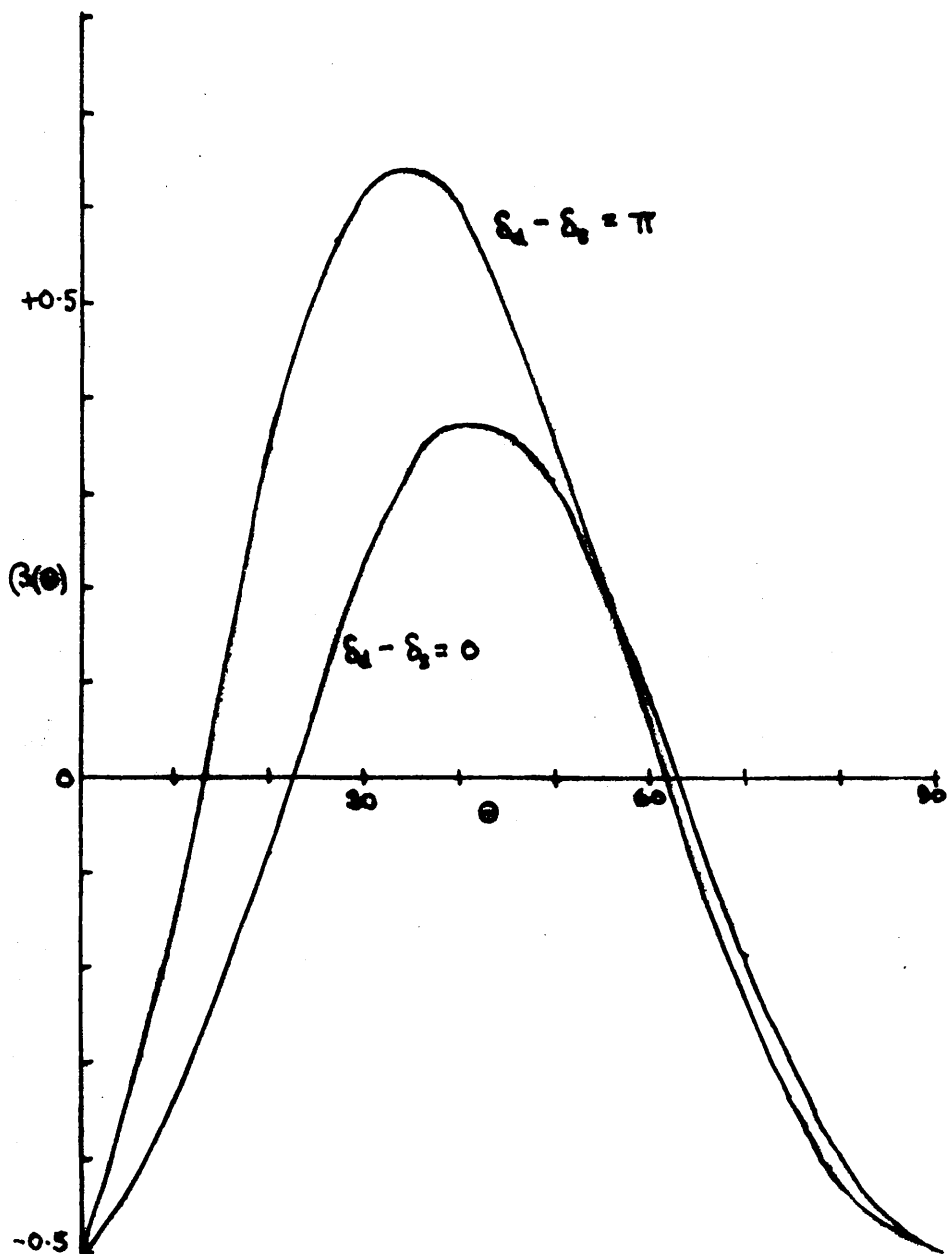
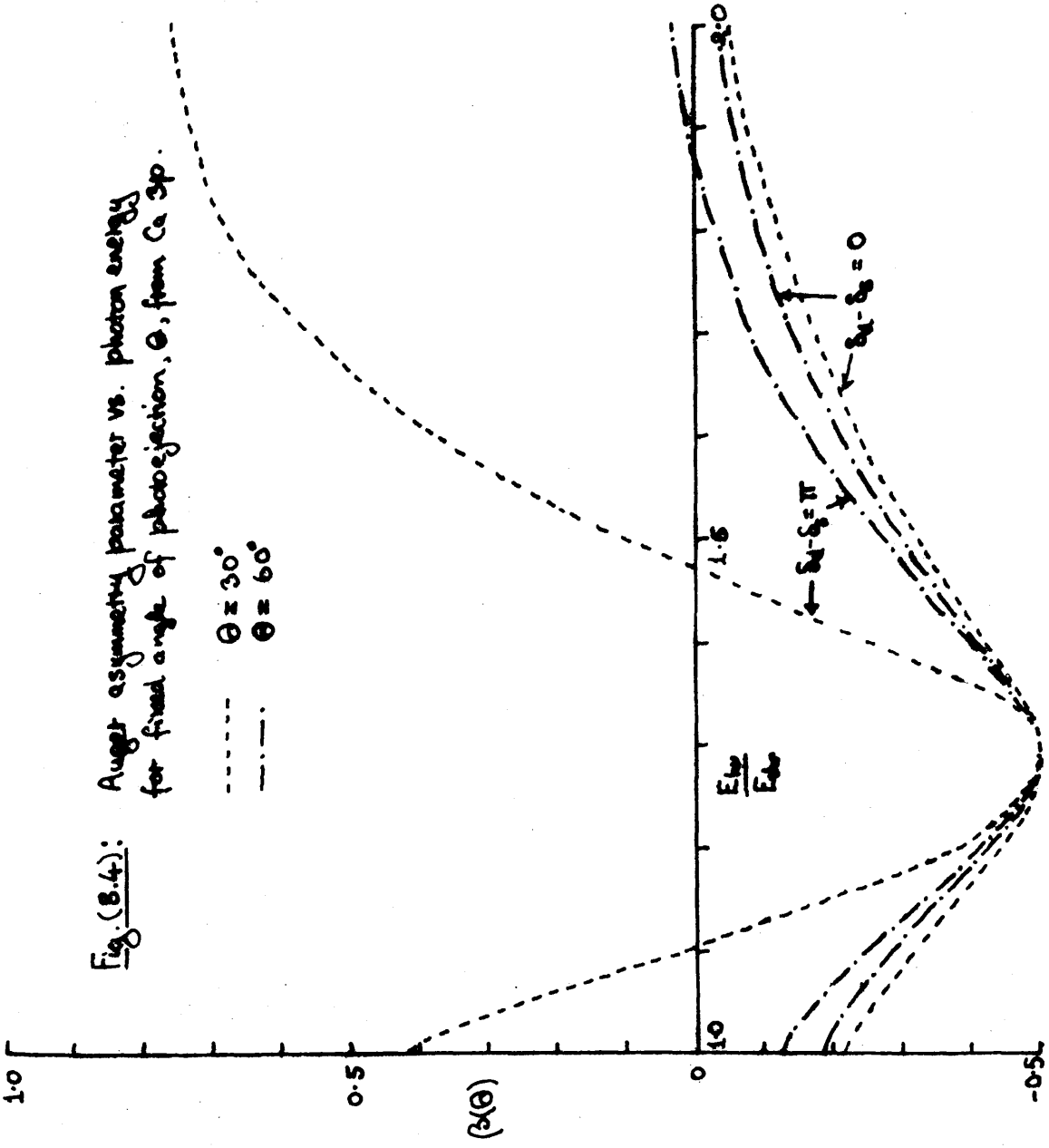


Fig. (8.3) Auger asymmetry parameter $\beta(\theta)$ vs. θ , angle of photoejection, using data of Fig(8.1).

Fig. (B.4): Auger asymmetry parameter vs. photon energy for fixed angle of photoejection, θ , from Ca 3p.

--- $\theta = 30^\circ$
 - - - $\theta = 60^\circ$



In figure (8.4) we have shown $\beta(\theta)$ for various angles as a function of the photon energy, using the data of McGuire for the Ca 3p-subshell. Notice that $\beta(\theta) = -0.5$ at the energy of the Cooper minimum, independently of θ , Also, $\beta(90^\circ) = \beta(0^\circ) = -0.5$ independently of R_{xd} , R_{xs} , ξ_d and ξ_s , and hence independently of photon energy.

This chapter has indicated that some interesting results might be expected from an experiment which detected in coincidence a photoelectron and the resultant Auger electron (or photon). Coincidence experiments are relatively recent in the field of atomic physics, due to the difficulty of using the counting techniques - responsible for their success in nuclear physics - in the detection of low energy particles. However, the use of the coincidence technique is increasing (Erhardt, 1971) and has already had some important successes.

Thus the experiment proposed here is put forward in the realization that it may not be feasible for technical reasons, but in the expectation that such problems could be solved in the near future.

CHAPTER 9

CORRELATION BETWEEN SPIN POLARIZATION AND ANGLE OF PHOTOEJECTION

1. General Case: Arbitrary Angle of Ejection

In recent years, the study known as photoelectron spectroscopy has come into being. Experimental techniques have developed to such an extent that not only total photoabsorption cross sections, but also the individual subshell contributions and angular distributions may be measured. The recent paper of Kennedy and Manson (1972) contains many useful references in this field. Thus it is now possible to measure the energy and direction of the ejected electron; the only parameter which remains unmeasured is its spin orientation. This chapter will show that, following photoionization by circularly polarized light, the electrons originating from a particular fine structure state are in general partially spin-polarized, the degree of spin polarization depending strongly on the angle of ejection. Thus the spin polarization depends on the same basic theoretical parameters - radial dipole matrix elements, phase shifts - as does the angular distribution. We shall see, however, that the spin polarization has the added interest that for certain

directions of ejection it is possible to predict the degree of polarization purely from angular momentum conservation and independently of the details of radial wavefunctions.

The premises of the calculation are identical to the foregoing part of this thesis - wavefunctions are calculated in the central field approximation, and the interaction between photon and atom is restricted to the dipole term. The matrix element required is

$$\langle \chi_{\tilde{\kappa}, m_s'} | r C_{+1}^1 | n l j m_j \rangle \quad (9.1.1)$$

where $\hbar \tilde{\kappa}$ is the momentum and m_s' the spin component of the ejected electron, and the operator describes the electric dipole interaction with a right circularly polarized beam of radiation. The corresponding cross section for photoejection in the direction θ (the polar angle with respect to the photon momentum as Z-axis) is

$$I_{\chi, m_s'}(\theta) = \frac{4\pi^2 \alpha a_0^2}{3} N_{nlj} \frac{(\epsilon - \epsilon_{nlj})}{(2j+1)} \cdot \sum_{m_j} |\langle \chi_{\tilde{\kappa}, m_s'} | r C_{+1}^1 | n l j m_j \rangle|^2 \quad (9.1.2)$$

where ϵ_{nlj} is the binding energy in rydbergs of an electron in the bound state $(n l j)$; $\epsilon = \epsilon_{nlj} + \frac{\hbar^2 \tilde{\kappa}^2}{2m} \cdot R_y^{-1}$; α is the fine structure constant; a_0 the Bohr radius; and

is the number of electrons occupying the initial state. It will be found convenient to cast $I_{x,m'_s}(\theta)$ in the form

$$I_{x,m'_s}(\theta) = \frac{\sigma_{\text{tot}}(m'_s)}{4\pi} (1 + \beta(m'_s) P_2(\cos\theta)) \quad (9.1.3)$$

where

$$\sigma_{\text{tot}}(m'_s) = \int_{-1}^{+1} I_{x,m'_s}(\theta) d(\cos\theta) \quad (9.1.4)$$

$P_2(x) = \frac{1}{2}(3x^2 - 1)$ and β is called the asymmetry parameter of the distribution. Now the calculation of (9.1.1), and hence of (9.1.3), is essentially similar to that outlined in Chapter 3, except that no integration over angle of ejection is performed. After employing the identities

$$\sum_m |Y_{l,m}|^2 = \frac{2l+1}{4\pi} \quad (9.1.5)$$

and

$$\sum_m m^2 |Y_{l,m}|^2 = \frac{l(l+1)(2l+1)}{8\pi} \sin^2\theta \quad (9.1.6)$$

the following expressions are obtained:

Case (i) $j = l + \frac{1}{2}$

$$\sigma_{\text{tot}}(+\frac{1}{2}) = \frac{\pi^2}{3} \alpha_0^2 [N_{nl, l+\frac{1}{2}} (\epsilon - \epsilon_{nl, l+\frac{1}{2}}) / (2l+2)] \cdot [(3l+2) R_{X, l+1}^2 + l R_{X, l-1}^2]$$

(9.1.7)

$$\beta(+\frac{1}{2}) = \frac{-(l+2)(3l+1)R_{x,l+1}^2 + l(l-1)R_{x,l-1}^2 + 6l^2 R_{x,l+1} R_{x,l-1} \cos(\delta_{l+1} - \delta_{l-1})}{(2l+1) [(3l+2)R_{x,l+1}^2 + lR_{x,l-1}^2]}$$

(9.1.7b)

$$\sigma_{\text{tot}}(-\frac{1}{2}) = \frac{\pi^2}{3} \alpha a_0^2 [N_{nl,l+\frac{1}{2}} (\epsilon - \epsilon_{nl,l+\frac{1}{2}}) / 2l+2] \cdot [(l+2)R_{x,l+1}^2 + 3lR_{x,l-1}^2]$$

$$\beta(-\frac{1}{2}) = \frac{(l+2)(l-1)R_{x,l+1}^2 - 3l(l-1)R_{x,l-1}^2 + 6l(l+2)R_{x,l+1} R_{x,l-1} \cos(\delta_{l+1} - \delta_{l-1})}{(2l+1) [(l+2)R_{x,l+1}^2 + 3lR_{x,l-1}^2]} \quad (9.1.7c)$$

(9.1.7d)

Case (ii) $j = l - \frac{1}{2}$

$$\sigma_{\text{tot}}(+\frac{1}{2}) = \frac{\pi^2}{3} \alpha a_0^2 [N_{nl,l-\frac{1}{2}} (\epsilon - \epsilon_{nl,l-\frac{1}{2}}) / 2l] \cdot [(l+1)R_{x,l+1}^2 + (3l+1)R_{x,l-1}^2] \quad (9.1.8a)$$

$$\beta(+\frac{1}{2}) = \frac{(l+1)(l+2)R_{x,l+1}^2 - (l-1)(3l+2)R_{x,l-1}^2 + 6(l+1)^2 R_{x,l+1} R_{x,l-1} \cos(\delta_{l+1} - \delta_{l-1})}{(2l+1) [(l+1)R_{x,l+1}^2 + (3l+1)R_{x,l-1}^2]} \quad (9.1.8b)$$

$$\sigma_{\text{tot}}(-\frac{1}{2}) = \frac{\pi^2}{3} \alpha a_0^2 [N_{nl,l-\frac{1}{2}} (\epsilon - \epsilon_{nl,l-\frac{1}{2}}) / 2l] \cdot [3(l+1)R_{x,l+1}^2 + (l-1)R_{x,l-1}^2]$$

(9.1.8c)

$$\beta(-\frac{1}{2}) = \frac{-3(l+1)(l+2)R_{X,l+1}^2 + (l-1)(l+2)R_{X,l-1}^2 + 6(l-1)R_{X,l+1}R_{X,l-1}\cos(\delta_{l+1}-\delta_{l-1})}{(2l+1)[3(l+1)R_{X,l+1}^2 + (l-1)R_{X,l-1}^2]}$$

(9.1.8d)

A useful check on these equations is to sum over spin orientations. For both Case (i) and Case (ii) one obtains

$$\sigma_{\text{tot}} = \frac{4\pi\alpha_0^2}{3} [N_{nlj}(\epsilon - \epsilon_{nlj})/2j+1] \cdot [(l+1)R_{X,l+1}^2 + lR_{X,l-1}^2]$$

(9.1.9a)

and

$$\beta = (-\frac{1}{2}) \cdot \frac{(l+1)(l+2)R_{X,l+1}^2 + l(l-1)R_{X,l-1}^2 - 6l(l+1)R_{X,l+1}R_{X,l-1}\cos(\delta_{l+1}-\delta_{l-1})}{(2l+1)[(l+1)R_{X,l+1}^2 + lR_{X,l-1}^2]}$$

(9.1.9b)

which agrees with the Bethe-Cooper-Zare formula for the photoelectron angular distribution.

Before evaluating the above results numerically, we wish to consider the special case where the photoelectron is ejected along the direction of the quantization axis (forward or backward ejection). Of course, this can be obtained by setting $\theta=0^\circ$ or $\theta=180^\circ$ in the general formula. However, the following section will show that for such a case the spin polarization can be obtained simply from angular momentum conservation. This has also the virtue of providing a

further check for the algebra of the present section.

2. Special Case: Ejection Along Quantization Axis.

For the particular case of forward (or backward) ejection, we shall show that the spin polarization can be obtained independently of any detailed knowledge of atomic wave-functions. Now as a result of our choice of quantization axis, we have

$$m' = 0 \quad (9.2.1)$$

where m' is the orbital angular momentum component along this axis of the ejected electron. If the photon responsible for the transition is right circularly polarized, we know that

$$\Delta m = m' - m = +1 \quad (9.2.2)$$

As a result of combining the last two relations, the selection rule

$$m = -1 \quad (9.2.3)$$

is obtained. In the presence of a spin-orbit interaction,

m is no longer a good quantum number and we specify the orbital occupied by the bound electron by the set $(nlj m_j)$.

We may expand this bound state thus:

$$|n\ell j m_j\rangle = \sum_{m, m_s} \begin{pmatrix} \ell & s & j \\ m & m_s & -m_j \end{pmatrix} [j]^{\frac{1}{2}} (-1)^{\ell+s-m_j} \cdot |n\ell m\rangle \chi_{m_s}^s \quad (9.2.4)$$

If the spin component of the ejected electron is m_s^i , the orthonormality of the spin functions and the selection rule (9.2.3) limit the contribution to the transition amplitude to one term in the expansion (9.2.4), this term being

$$\begin{pmatrix} \ell & s & j \\ -1 & m_s^i & -m_j \end{pmatrix} [j]^{\frac{1}{2}} (-1)^{\ell+s-m_j} |n\ell -1\rangle \chi_{m_s^i}^s \quad (9.2.5)$$

Hence the spin polarization

$$P = 100 \frac{I(+\frac{1}{2}) - I(-\frac{1}{2})}{I(+\frac{1}{2}) + I(-\frac{1}{2})} \quad (9.2.6)$$

can be replaced for this special case by

$$P = 100 \frac{\begin{pmatrix} \ell & s & j \\ -1 & +\frac{1}{2} & +\frac{1}{2} \end{pmatrix}^2 - \begin{pmatrix} \ell & s & j \\ -1 & -\frac{1}{2} & +\frac{3}{2} \end{pmatrix}^2}{\begin{pmatrix} \ell & s & j \\ -1 & +\frac{1}{2} & +\frac{1}{2} \end{pmatrix}^2 + \begin{pmatrix} \ell & s & j \\ -1 & -\frac{1}{2} & +\frac{3}{2} \end{pmatrix}^2} \quad (9.2.7)$$

Since $s = \frac{1}{2}$, we have the two possibilities $j = \ell \pm \frac{1}{2}$.

Using explicit expressions for the 3j-symbols, we find

$$P = 100 \cdot \begin{cases} -1/\ell+1 & (j = \ell + \frac{1}{2}) \\ 1/\ell & (j = \ell - \frac{1}{2}) \end{cases} \quad (9.2.8)$$

Remembering the statistical weight factor $(2j+1)$, we note that the contributions from the states $j = l \pm \frac{1}{2}$ are such as to cancel each other out. The values $l = 1$, $j = \frac{1}{2}$ are of particular interest in that they lead to $P = 100\%$.

3. Results

The percentage spin polarization of electrons ejected with momentum $\hbar k$ at an angle θ may be defined as

$$P(\theta) = 100 \frac{I_{X,+\frac{1}{2}}(\theta) - I_{X,-\frac{1}{2}}(\theta)}{I_{X,+\frac{1}{2}}(\theta) + I_{X,-\frac{1}{2}}(\theta)} \quad (9.3.1)$$

To obtain explicit numerical values of $P(\theta)$, we must now choose an atomic system, specify the subshell from which the electron is to be ejected, and obtain theoretical values for the radial dipole matrix elements and phase shifts needed. The choice of atom was dictated as follows. The formulae (9.1.7a,b,c,d) and (9.1.8a,b,c,d) were obtained by neglect of coupling of the bound electron to other electrons. This is justified for either a single electron in an otherwise empty subshell or an electron in a closed subshell (Pauli vacancy principle). We opt for the latter since the fine structure splitting is so small in the former case as to make experimental energy discrimination unlikely. The noble gases were chosen because of the availability of a recent

calculation (Kennedy and Manson, 1972) which provides the requisite theoretical data for these elements, for both outer and inner subshells; and also because they are simple to deal with experimentally, being monatomic gases at room temperature. Figure 9.1 shows the percentage spin polarization $P(\theta)$ as a function of the angle of photo-ejection θ from the $4^2p_{1/2}$ -subshell of Kr, each curve corresponding to a different photon energy. Note that $P(0^\circ) = 100\%$, in agreement with Section 9.2, for all energies. Note also the interesting behaviour which occurs at the energy of the Cooper minimum, discussed in previous chapters. At this energy, only the contribution from the outgoing S-wave is present, and this is accompanied by the complete suppression of the spin orientation $m_s = -\frac{1}{2}$, so that we have $P = 100\%$ for all angles of ejection.

Figure (9.2) shows the corresponding situation for the inner $3^2p_{1/2}$ -subshell of Kr. The important difference here is that there is no Cooper minimum present, so that the change in P with photon energy is much less marked.

The picture for the other noble gases is similar to that given above for Kr.

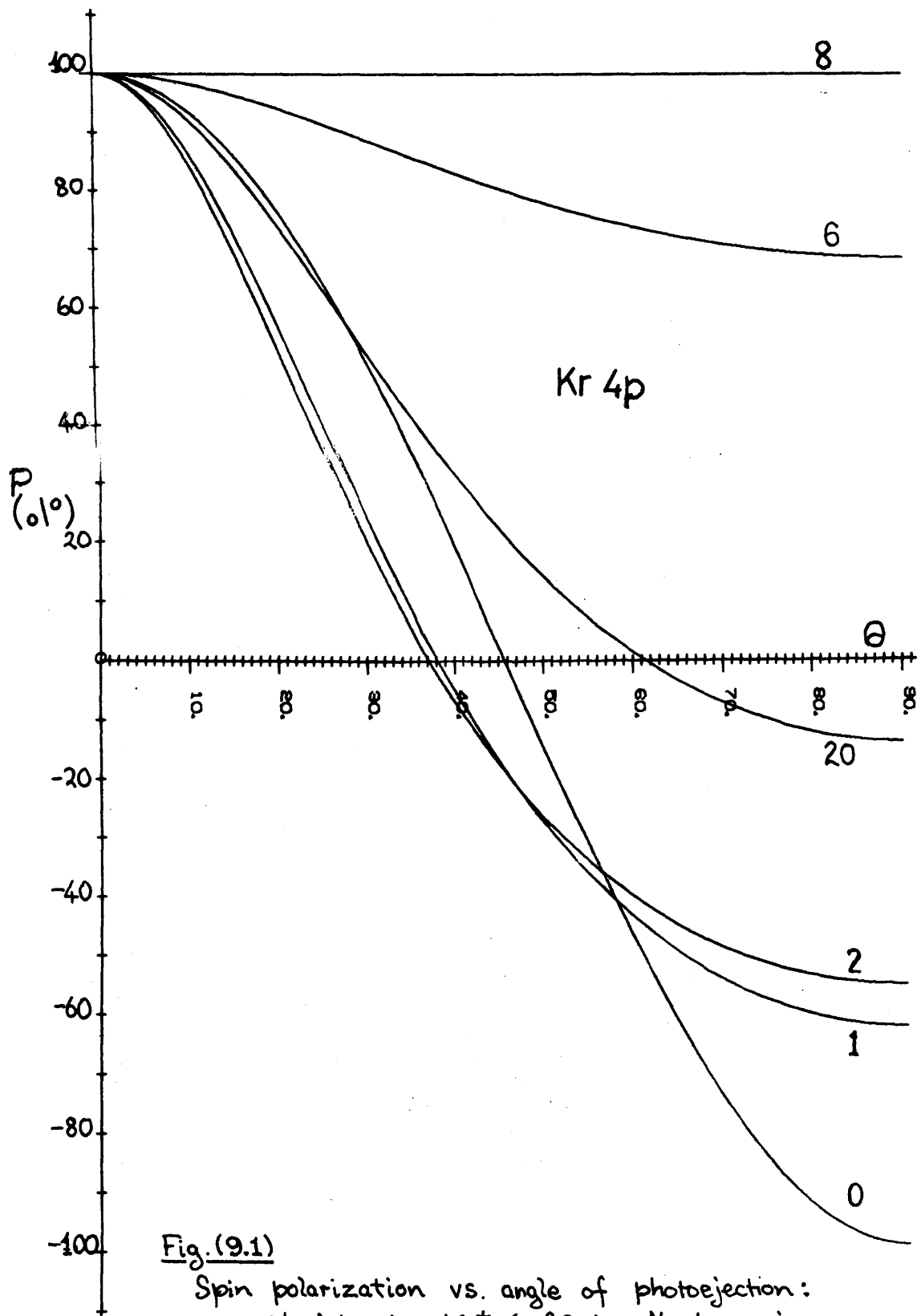


Fig. (9.1)

Spin polarization vs. angle of photoejection:
 residual ion is $\text{Kr}^+ (4^2P_{1/2})$. Numbers give
 ejection energy in rydbergs.

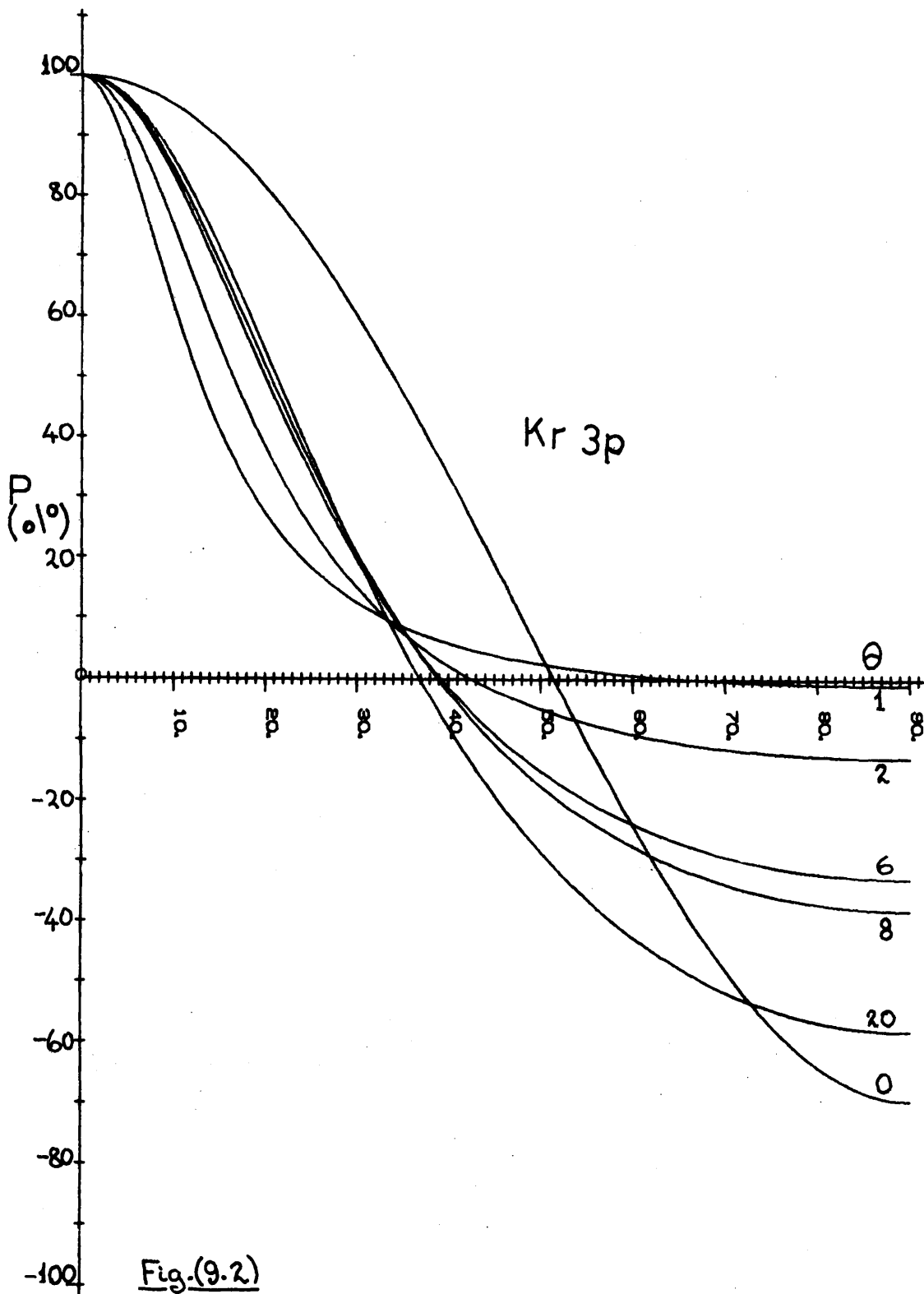


Fig.(9.2)

Spin polarization vs. angle of photoejection:
 residual ion is $\text{Kr}^+ (3^2P_{1/2})$. Numbers give
 ejection energy in rydbergs.

Photoejection from a closed p-subshell leaves the residual ion in either of the states $p_{\frac{1}{2}, \frac{3}{2}}$. In the presence of a spin-orbit interaction, these two states are separated in energy: hence, for ionization with photons of a sharp wavelength, the photoelectrons will consist of two groups, differing in energy by the amount of the fine structure splitting. The problem of observing the spin polarization of these groups separately can be dealt with in two ways. Firstly, the photon wavelength can be arranged so that only the higher energy $p_{\frac{3}{2}}$ group is obtained. In this connection, we note that the energy resolution necessary to achieve this is available, as shown by Berkowitz et al, (1966) who have studied the angular distribution of the two groups of photoelectrons for the noble gases. Secondly, both groups can be excited, and subsequently separated by using their different mean velocities to deflect them through different angles. This, however, could prove difficult and lead to losses in intensity.

It seems unlikely that the process dealt with in this chapter will provide a serious rival to the existing methods of providing intense beams of spin-polarized electrons; however, it could provide an interesting extension to photoelectron spectroscopy as a means of gaining information on both bound and continuum atomic wavefunctions.

APPENDIX

THE FORM OF ANISOTROPIES IN THE HIGH-ENERGY
LIMIT OF THE BORN APPROXIMATION

In the course of calculating the angular distribution of products in the electron impact dissociation of H_2^+ , Zare (1967) makes some general assertions concerning the form of anisotropies in the high energy limit of the Born approximation. In particular, he claims that the work of Percival and Seaton (1958) (henceforth referred to as PS) on the polarization of atomic line radiation contains an error in this respect. We shall show that (a) Zare's general argument contains a fallacy; (b) the results of PS are correct; and (c) the rapidity with which the high energy limit is approached depends on whether or not the transition in question is optically allowed.

It is well known that the physical reason for the variation of such anisotropies as a function of impact energy is the energy dependence of the direction of momentum transfer to the atom \hat{k} (momentum transfer $\hbar k$). The customary approach is to consider that \hat{k} is parallel to the incident beam at threshold and perpendicular at the high energy limit, varying monotonically between these two

extremes. Hence PS simplify their calculation by setting

θ_K (the angle between \hat{K} and \hat{k}_0 , where $\hbar k_0$ is the momentum of the incoming electron) equal to $\pi/2$. Zare contends that this substitution is in general unjustified. He correctly notes that, as $K \rightarrow K_{min}$ (the kinematic lower limit), $\theta_K \rightarrow 0^\circ$ even for k_0 very large. Since the momentum transfer integrand in the Born approximation weights strongly small values of K close to K_{min} , the form of the anisotropy even at high energies may be substantially less than the limiting form predicted by putting $\theta_K = \pi/2$. This is in agreement with the conclusions of § 4.3. However, Zare extends his argument in the following manner:

"It might be wondered whether the $\sin^2 \theta$ limiting form (Zare is referring to the dissociation of H_2^+) would be reached, provided we were to consider still higher energies than that shown in Figure 7. However, this is not the case, as can be demonstrated in the following manner. Let us calculate the fractional contribution to the total integral made by those values of θ' (our θ_K) that are less than or equal to θ'_{magic} (θ'_{magic} is the "magic angle" of 54.7° introduced by Van Vleck (1925))
 such values of $\theta' \leq \theta'_{magic}$, corresponding to the limits of integration from K_{min} to $\sqrt{3} K_{min}$, cause peaking

along k_0 and thus oppose the formation of a $\sin^2\theta$ distribution. In the high-energy limit, the integrand of (52) will be dominated by some leading inverse power of K , so that the indefinite integral has the functional form $-\beta K^{-n}$ where, in general, $n > 0$. The fraction ξ of the total integral for which $\theta' \leq \theta'_{\text{magic}}$ is thus given by

$$\xi(\theta' \leq \theta'_{\text{magic}}) = \frac{(-\beta K^{-n})_{K_{\text{min}}}^{\sqrt{3} K_{\text{min}}}}{(-\beta K^{-n})_{K_{\text{min}}}^{K_{\text{max}}}} \quad (54)$$

which is seen to be independent of the bombardment energy E_0 ."

Zare concludes that if $n \geq 2$, the angular distribution need never be reversed in sense. Since the above argument is quite general, Zare goes on to say that the performance of the integral over K in PS Equations (6.13), (6.14) and (6.15) is incorrect in the general case, and leads to the wrong high-energy limit of the line polarization P , unless the integrand in question varies as K^{-1} or slower.

The flaw in Zare's argument is contained in the statement: "In the high-energy limit, the integrand of (52) will be dominated by some leading inverse power of K ". This is not the case, for the coefficient β of such an inverse power of K will be shown to be itself a function of the collision

energy, so that although Zare's equation (54) is quite correct, the contribution from such a term tends rapidly to zero as $k_0 \rightarrow \infty$.

We shall demonstrate this for the case dealt with by PS; namely, the excitation $1s \rightarrow nlm$ in the Born approximation. Restating PS equation (6.13) in altered notation, we have:

$$Q(1s \rightarrow nlm) = \frac{4\pi}{(2l+1)k_0 k_1} \int_{k_{\min}}^{k_{\max}} |P_l^{iml}(\cos\theta_k)|^2 I_{ne}(k) K dk \quad (\text{A.1})$$

where

$$I_{ne}(k) = \frac{4k_1}{k^4 k_0} (2l+1) |\langle nlm | j_l(kr) | 1s \rangle|^2 \quad (\text{A.2})$$

in which

$$j_l(kr) = \left(\frac{\pi}{2kr}\right)^{\frac{1}{2}} J_{l+\frac{1}{2}}(kr) \quad (\text{A.3})$$

Now since

$$Q(1s \rightarrow nl) = \frac{2\pi}{k_0 k_1} \int_{k_{\min}}^{k_{\max}} I_{ne}(k) K dk \quad (\text{A.4})$$

we have

$$\frac{Q(1s \rightarrow nlm)}{Q(1s \rightarrow nl)} = \left(\frac{2}{2l+1}\right) \cdot \frac{\int_{k_{\min}}^{k_{\max}} |P_l^{iml}(\cos\theta_k)|^2 I_{ne}(k) K dk}{\int_{k_{\min}}^{k_{\max}} I_{ne}(k) K dk} \quad (\text{A.5})$$

By setting $\Theta_k = \frac{\pi}{2}$ PS obtain from this

$$\lim_{k_0 \rightarrow \infty} \left[\frac{Q(1s \rightarrow nlm)}{Q(1s \rightarrow n\ell)} \right] = \left(\frac{2}{2\ell+1} \right) |P_\ell^{lm}(0)|^2 \quad (\text{A.6})$$

Now the Bethe cross section (4.3.1) is the asymptotic form of the Born approximation as k_0 becomes large; PS do not make it clear whether (A.6) should apply in the Bethe region or whether it is intended as a purely formal high-energy limit. The procedure we follow is equivalent to performing the Bethe approximation on the expression (A.5).

In § 4.3 we saw that Θ_k is significantly different from $\frac{\pi}{2}$ only if $k_{\min} \leq k \leq k_0$, k_0 being the "momentum cut-off factor" introduced by Bethe (1930). Hence for

$k_0 \leq k \leq k_{\max}$, the approximation represented by (A.6) is certainly justified in the Bethe approximation, and we need only consider the behaviour of the integrand in (A.5) in the lower region of momentum transfers. This region is defined such that the inequality

$$Kr \ll 1 \quad (\text{A.7})$$

holds for all τ contributing appreciably to the integration implied in (A.2).

Thus $j_\ell(Kr)$ can be replaced by the leading term, of order

$(Kr)^{\ell}$, in its expansion, and we find

$$\left[\frac{Q(1S \rightarrow n\ell m)}{Q(1S \rightarrow n\ell)} \right]_{K \leq K_0} \approx \left(\frac{2}{2\ell+1} \right) \frac{\int_{K_{min}}^{K_0} |P_{\ell}^{lm}(\cos\theta_K)|^2 K^{2\ell-3} dK}{\int_{K_{min}}^{K_0} K^{2\ell-3} dK} \quad (A.8)$$

Now at high energies

$$K_{min} \approx \frac{m\Delta E}{\hbar^2 K_0} \quad (A.9)$$

and thus we may write, using (4.3.2),

$$\cos \theta_K \approx \frac{K}{2K_0} + \frac{K_{min}}{K} \quad (A.10)$$

for such energies. The first of the two terms on the right side of (A.10) is certainly much smaller than unity for $K \ll K_0$, so that the substitution

$$P_{\ell}^{lm}(\cos\theta_K) \approx P_{\ell}^{lm}\left(\frac{K_{min}}{K}\right) \quad (A.11)$$

should lead to no serious error in evaluating (A.8). Hence we make the substitution $x = K_{min}/K$ and find

$$\left[\frac{Q(1S \rightarrow n\ell m)}{Q(1S \rightarrow n\ell)} \right]_{K \leq K_0} \approx \left(\frac{2}{2\ell+1} \right) \frac{\int_{K_{min}/K_0}^1 |P_{\ell}^{lm}(x)|^2 x^{-2\ell+1} dx}{\int_{K_{min}/K_0}^1 x^{-2\ell+1} dx} \quad (A.12)$$

The energy dependence in (A.12) is thus confined to the lower limit of integration, making it clear, in view of (A.9), that the dominant term at high energies will come from the leading inverse power of x in the integrand, and not, as stated by

Zare, from that of K.

Now the associated Legendre function $P_l^{lm}(\alpha)$ is the product of $(1-\alpha)^{\frac{1}{2}m}$ and a polynomial of degree $(l-m)$; hence the coefficient of the leading inverse power of α in the upper integral in (A.12) is just

$|P_l^{lm}(0)|^2$, so that

$$\lim_{k_0 \rightarrow \infty} \left[\frac{Q(1S \rightarrow nlm)}{Q(1S \rightarrow nl)} \right]_{k \leq k_0} = \left(\frac{2}{2l+1} \right) |P_l^{lm}(0)|^2 \quad (\text{A.13})$$

and we have thus vindicated the use of (A.6) by PS as a formal high-energy limit. Also, because of its similarity in structure, one can easily show that the expression (52) of Zare's paper (for the angular distribution of products following the dissociation of H_2^+) must eventually reach the $\sin^2 \theta$ form corresponding to $\theta_k = \frac{\pi}{2}$.

The question remains as to whether the PS values calculated by using (A.6) are attained in the region of energies for which the Bethe approximation is valid, or whether they represent a merely formal high-energy limit, unattainable except for collision energies which require the modification of the Bethe formula itself due to the onset of relativistic effects. Now for optically-disallowed excitations ($l \geq 2$ in the above formulae) the contribution from distant collisions

(represented by (A.12)) is relatively unimportant (see, for example, Inokuti (1971) p.307). Hence, one may substitute

$\theta_K = \frac{\pi}{2}$ for such excitations throughout the Bethe region of validity, and the line polarization following a transition from such an excited state will reach the value P_0 predicted by PS throughout this region (neglecting any other depolarizing phenomena). For an optically-allowed transition, the contribution of the distant collisions is predominant at high energies, and one cannot neglect the contribution represented by (A.12). We shall find it convenient to use the formula of Vriens and Carrière (1970) for the polarization:

$$P = \frac{100 P_0 (3 \overline{\cos^2 \theta_K} - 1)}{200 - P_0 (1 - \overline{\cos^2 \theta_K})} \quad (\text{A.14})$$

where

$$\overline{\cos^2 \theta_K} = \frac{\int_{K_{\min}^2}^{K_{\max}^2} \cos^2 \theta_K f_n(K) \frac{d(K^2)}{K^2}}{\int_{K_{\min}^2}^{K_{\max}^2} f_n(K) \frac{d(K^2)}{K^2}} \quad (\text{A.15})$$

and $f_n(K)$ is the generalized oscillator strength for the transition. The relation between $f_n(K)$ and the Born matrix element is given in Chapter 5. P_0 is the threshold polarization; values of P_0 have been tabulated for a wide range of transitions by PS.

Now (A.15) can be rewritten as

$$\overline{\cos^2 \Theta_K} = \frac{\int_{k_{\min}^2}^{k_0^2} \cos^2 \Theta_K f_n(k) \frac{d(k^2)}{k^2} + \int_{k_0^2}^{k_{\max}^2} \cos^2 \Theta_K f_n(k) \frac{d(k^2)}{k^2}}{\int_{k_{\min}^2}^{k_{\max}^2} f_n(k) \frac{d(k^2)}{k^2}} \quad (\text{A.16})$$

From the definition of the parameter k_0 , we can make the substitution $f_n(k) \approx f_n(0)$ in the first integral in the numerator, $f_n(0)$ being the optical oscillator strength; from our kinematic analysis of the behaviour of \hat{K} (Chapter 4) we can set $\Theta_K = \frac{\pi}{2}$ in the second integral, the contribution from which thereby vanishes. We have therefore

$$\begin{aligned} \overline{\cos^2 \Theta_K} &\approx \frac{f_n(0) \int_{k_{\min}^2}^{k_0^2} \cos^2 \Theta_K \frac{d(k^2)}{k^2}}{\int_{k_{\min}^2}^{k_{\max}^2} f_n(k) \frac{d(k^2)}{k^2}} \quad (\text{A.17}) \\ &= \left\{ f_n(0) + O(E^{-1} \ln E) \right\} / \int_{k_{\min}^2}^{k_{\max}^2} f_n(k) \frac{d(k^2)}{k^2} \end{aligned}$$

Now the evaluation of the denominator is equivalent to the performance of the Born approximation; it must be evaluated separately for each collision energy of interest, since the limits k_{\min} , k_{\max} are themselves functions of energy. However, it has been amply demonstrated (see Inokuti, 1971) that the Bethe asymptotic cross section, which is a function of the parameters $f_n(0)$ and C_n (the latter to be defined) has virtually all the physical content of the Born approximation, at least to terms of order E^{-1} . The Bethe procedure gives:

$$\int_{k_{\min}^2}^{k_{\max}^2} f_n(k) \frac{d(k^2)}{k^2} = f_n(0) \ln(4c_n E/R_y) \quad (\text{A.18})$$

where c_n is defined by

$$\begin{aligned} \ln [c_n (\Delta E/R_y)^2] &= \int_0^{\infty} [f_n(k)/f_n(0)] \frac{d(k^2)}{k^2} \\ &\quad - \int_0^{\infty} \{1 - [f_n(k)/f_n(0)]\} \frac{dk^2}{k^2} \end{aligned} \quad (\text{A.19})$$

substitution of (A.18) in (A.17) gives

$$\overline{\cos^2 \theta_k} = [\ln(4c_n E/R_y)]^{-1} \quad (\text{A.20})$$

and thus

$$P = \frac{100P_0 [3 - \ln(4c_n E/R_y)]}{(200 - P_0) \ln(4c_n E/R_y) + P_0} \quad (\text{A.21})$$

The formula (A.21) gives the polarization of any line in terms of the two parameters P_0 and c_n . As mentioned before, P_0 has been tabulated by PS; equation (A.19) shows that c_n depends only on the shape of the generalized oscillator strength $f_n(k)$ and hence on the shape of the differential cross section.

We shall test the validity of the assumptions on which (A.21) is based by evaluating the polarization of the helium line ($3^1P \rightarrow 2^1S$) following the electron impact excitation

($1^1S \rightarrow 3^1P$). For this line there are experimental data (Moustafa Moussa, 1967) available, and also a Born approximation calculation (Vriens and Carrière, 1970). The latter calculation takes a truncated series expansion for $f_n(K)$ of the Lassette type (Lassette, 1965) and determines the expansion coefficients by fitting to the definitive $f_n(K)$ obtained by Kim and Inokuti (1968). It then calculates both excitation cross section and polarization using the expansion. We use the value

$$\ln C_{3^1P} = -1.833 \quad (\text{A.22})$$

given by Kim and Inokuti, so that any difference between the two calculations cannot be ascribed to the use of different wavefunctions. The results are shown in Figure (A.1). We see that the present results converge on those of Vriens and Carrière with increasing energy, so that by $E = 3\text{keV}$ the two curves are indistinguishable. Both curves are in reasonable agreement with experiment, considering that the latter is uncorrected for the depolarizing effect of cascade population of the upper level. Since the validity of the Born itself is questionable below 400eV , one sees that the use of (A.21) represents a simple and worthwhile alternative to more elaborate Born calculations, which require a numerical integration for each value of E of interest. Furthermore, an estimate of P made with an empirically-determined C_n may be

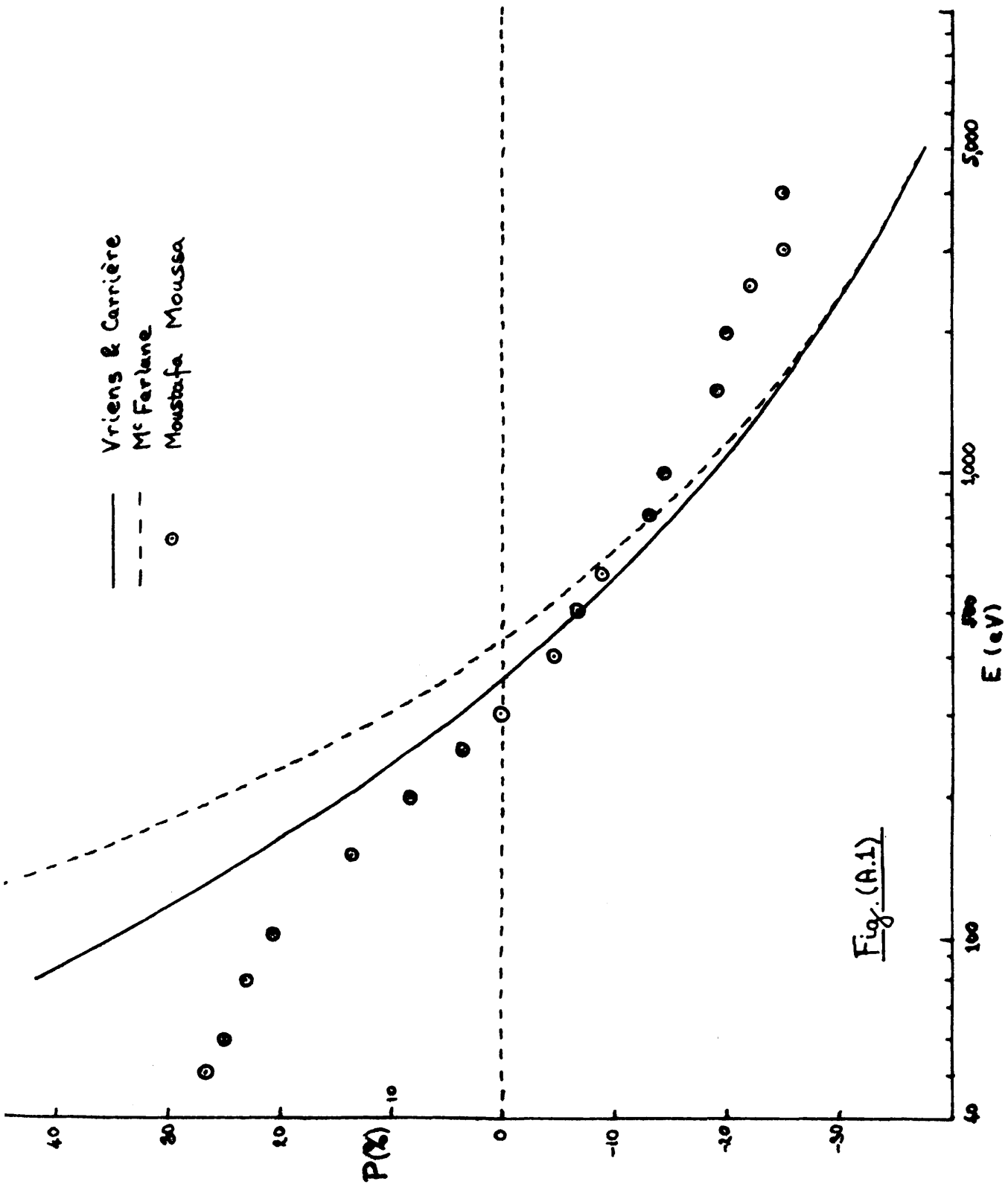


Fig. (A.1)

more accurate than a full Born calculation with inadequate wavefunctions.

It is interesting to note that the formula (A.21) requires a correlation between the shape of the differential cross section at a particular (moderate to high) energy and the polarization of radiation from the subsequent transition. It is possible that this could be exploited both experimentally and theoretically.

The thesis of Moustafa Moussa (1967) contains some calculations on the high energy tendency of the polarization. However, these are unsupported by any kinematic analysis such as is employed here, and consequently Moustafa Moussa is able to deal only with the low momentum transfer range ($K < K_0$). Hence his conclusions, although correct, remain qualitative.

We conclude with a summary of the appendix:

a) The argument about the high energy limit of anisotropies is more subtle than it appears at first sight - as witness the inadequacy of its treatment by Zare and also, differently, by PS.

- b) The limiting values P_{∞} given by PS are formally correct, but practically wrong for optically-allowed excitations, for which case the approach to the limit is extremely slow, so that $P \ll P_{\infty}$, even for very fast electrons (see Figure (A.1)). This stricture does not apply to optically-disallowed excitations.
- c) A compact formula giving P as a function of impact energy has been obtained. The excellent agreement with the full Born calculation of Vriens and Carriere for $E > 1 \text{ keV}$ suggests the correctness of the kinematic argument on which the formula is based.
- d) The dependence of the formula for P on the parameter C_n , which can be obtained independently from total and differential cross sections, both theoretical and experimental, implies an interesting cross-correlation among these different types of high energy data.
- e) The generality of the kinematic procedure for \tilde{K} suggests its possible extension to other types of anisotropic process following on electron impact, e.g. the angular distribution of products after molecular dissociation; or the direction of ejection of secondary electrons after ionization.

REFERENCES

Banks, D., Vriens, L. and Bensen, T.F.M., 1969, J.Phys.B:
Atom.Molec. Phys. 2, 976-83.

Berkowitz, J., Ehrhardt, H. and Tekaas, T., 1967, Z.Phys.,
69-116.

Bethe, H.A., 1930, Ann.der Phys. 5, 325-400.

Bethe, H.A., 1933, Handbuch der Physik 24, 273-560.

Bethe, H.A., and Salpeter, E.E., 1957, Encyclopaedia of
Physics 35 ed. S. Flügge (Berlin: Springer-Verlag) 88-436.

Burgess, A., 1964, M.R.A.S. 69, 1-20.

Burgess, A., and Percival, I.C., 1968, Advances in Atomic and
Molecular Physics, eds. Bates and Estermann (New York: Academic
Press) 120-22.

Burhop, E.H.S., 1940, Proc. Camb.Phil.Soc. 36, 43-9.

Burhop, E.H.S., 1952, The Auger Effect and Other Radiationless
Transitions (London: Cambridge University Press).

Cleff, B. and Mehlhorn, W., 1971, Phys.Lett. 37A, 3-4.

Cooper, J., and Zare, R.N., 1968, Lectures in Theoretical Physics XIc, eds. Geltman, Mahanthappa and Brittin (New York: Gordon and Breach), 317-337.

Coster, D., and Mulder, F.P., 1926, Z.Phys. 38, 264- .

Edmonds, A.R., 1960, Angular Momentum in Quantum Mechanics (Princeton N.J.: Princeton University Press).

Ehrhardt, H., 1971, Atomic Physics 2, eds. Woodgate and Sandars (London: Plenum Press) 141-154.

Feynman, R.P., and Hibbs, 1965, Quantum Mechanics and Path Integrals.

Fano, U., 1956, Phys.Rev. 102, 385-7.

Flügge, S., Mehlhorn, W., and Schmidt, V., 1972, Phys.Rev.Letts. 29, 7-9.

Herman, F. and Skillman, S., 1963, Atomic Structure Calculations (Englewood Cliffs, N.J.: Prentice-Hall).

Hidy, J., Henins, A. and Bearden, J.A., 1970, Phys.Rev.A, 2, 1708-11.

Inokuti, M., 1971, Rev. Mod. Phys, 43, 297-347.

Kennedy, D.J., and Manson, S.T., 1972, Phys. Rev. A5, 227-247.

Kim, Y.-K., and Inokuti, M., 1968, Phys.Rev. 175, 176- .

Kleinpoppen, H., 1969, Physics of the One- and Two-Electron Atoms, eds. Bopp and Kleinpoppen (Amsterdam: North Holland) 612-31).

Kleinpoppen, H., and Neugart, R., 1967, Z. Phys. 198, 321-328.

Lassetre, E.N., 1965, J. Chem. Phys. 43, 4479- .

Mandl, F., 1952, AERE Report T/R 1006.

Massey, H.S.W., and Mohr, C.B.O., 1933, Proc.Roy.Soc. A, 140, 613- .

McCrea, D., and McKirgan, T.V.M., 1960, Proc.Phys.Soc. 75, 235-42.

McFarlane, S.C., 1972, J. Phys. B.: Atom.Molec. Phys. 5, 1906-15.

McGuire, E.J., 1968, Phys. Rev. 175, 20-30.

McGuire, E.J., 1970, Sandia Laboratories Report SC-RR-70-721.

Mehlhorn, W., 1968, Phys. Lett. 26A, 166-7.

Messiah, A., 1961, Quantum Mechanics, (Amsterdam; North Holland).

Miller, W.F., and Platzman, R.L., 1957, Proc. Phys. Soc. 70,
299-303.

Mitchell, A.C.G., and Zemansky, M.W., 1934, Resonance Radiation
and Excited Atoms (Cambridge: University Press).

Moiseiwitsch, B.L., and Smith, S.J., 1968, Rev. Mod. Phys. 40,
238-

Møller, C., 1932, Ann. der Phys. 14, 531-585.

Mott, N.F., and Massey, M.S.W., 1965, Theory of Atomic
Collisions (Oxford: Clarendon Press).

Moustafa Moussa, H.R., 1967, Ph.D. Thesis, University of
Leiden (unpublished).

Omidvar, K., 1965, Phys. Rev. 140, A26-37.

Percival, I.C., and Seaton, M.J.. 1958, Phil. Trans. Roy. Soc.

A. 251, 113-38.

Schram, B.L., and Vriens, L., 1965, Physica, 31, 1431-6.

Swan, P., 1955, Proc. Phys. Soc. A68, 1157-60.

Van der Tuuk, J.H., 1927, Z. Phys. 44, 737- .

Van Vleck, J.M., 1925, Proc. Natl. Acad. Sci. (U.S.) 11, 612- .

Vriens, L., and Bensen, T.F.M., 1968, J. Phys. B., Atom. Molec.

Phys. 1, 1223-9.

Vriens, L., Case Studies in Atomic Collision Physics I, eds.

McDaniel and McDowell (Amsterdam: North Holland), 335-98.

Vriens, L., and Carrière, J.D., 1970, Physica 49, 517-531.

Zare, R.N., 1967, J. Chem. Phys. 47, 204-215.

The polarization of characteristic x radiation excited by electron impact†

SC McFARLANE

Department of Physics, University of Stirling, Stirling, Scotland

MS received 25 May 1972

Abstract. Using hydrogenic wavefunctions, the cross sections for ionization of an atom from the magnetic substates of the L_3 level are calculated in (i) the Bethe approximation; and (ii) the first Born approximation. Calculation (ii) differs from previous work of a similar nature in that it takes as axis of quantization the direction of the incident electron beam.

Hence the polarization of the resulting characteristic x radiation is estimated; it is found to be small in comparison with the degree of polarization which typically results from the excitation of optical lines, in marked disagreement with a previous calculation.

1. Introduction

When atomic line radiation is excited by a collimated beam of electrons, it is in general polarized. This is well known from observation and has been accounted for satisfactorily within the framework of quantum mechanics. The field is the subject of a recent review article by Kleinpoppen (1969). The electron beam introduces a large degree of anisotropy into the process which manifests itself in the non-uniform angular distribution of the emitted radiation. Hence, when a collimated beam is used to excite the characteristic x rays of an atom, the question arises as to whether this radiation also is polarized. The purpose of the present study is to look at the latter process in more detail and to give some kind of quantitative indication of the extent of the polarization to be expected in a given line.

There has been, to the author's knowledge, only one published experimental study of x ray polarization—that of Hrdý *et al* (1970) on the L_{α_1} x rays of mercury. They claim good agreement with the only previous theoretical work, due to Mehlhorn (1968). But there are strong reasons for believing the results of Mehlhorn to be erroneous; these will be discussed in detail later.

The basic premise of the theory presented here is the same as that of the Oppenheimer-Penney theory of the polarization of optical line radiation; that one may calculate separately the probability of collisionally exciting a state with a particular orbital angular momentum component along a fixed direction, and the probability of emission of a polarized photon in the subsequent transition from that state. Percival and Seaton (1958) showed that in certain circumstances, this assumption leads to ambiguities, and presented a more sophisticated theory which successfully resolved these ambiguities.

† This work was first reported on at the 3rd National Atomic and Molecular Physics Conference, University of York, April 1971.

Nevertheless, we shall retain the assumption in what follows, on the grounds that the inequality

$$\text{fine structure splitting} \gg \text{line width} \gg \text{hyperfine structure splitting} \quad (1)$$

is generally true of x ray spectra, and that therefore the ambiguity should not arise in practice.

Hence we can separate the problem into two parts—the collisional and the radiative, the former presenting the greater difficulty. The bulk of discussion in this paper will concern the collision problem, but § 2 deals with the question of threshold polarization which for optical lines may be calculated without knowledge of cross sections. § 3 deals with the calculation of the ionization cross section from any state designated by the quantum numbers (nlm) in the Bethe approximation, whereas § 4 uses the Born approximation to calculate the cross sections for ionization from the states $(2p, m = 0)$ and $(2p, m = \pm 1)$ using hydrogenic wavefunctions. The Bethe approximation is, of course, much cruder than the Born. The advantages of its use lie in its simplicity and its generality (it applies to any values of (nlm)). Also, it supplies a formal high energy limit on the Born calculation, and a simple physical picture which helps to explain the results.

Section 5 gives the results of these calculations and § 6 comments on their significance.

2. Threshold polarization

In electron impact excitation, it is well known that the threshold polarization can be calculated without any knowledge of cross sections. Thus the question presents itself where this can be done for excitation of x ray levels by electron impact.

We consider, for the moment, the process to be simply one of ionization. Before the collision takes place, the incident electron has zero orbital angular momentum component along the quantization axis, by definition. Also, the shell which is to be ionized is initially complete, and therefore has zero orbital angular momentum component ($M_L = 0$). Hence the total component is initially zero (ignoring any component which may exist in an outer shell, which takes no part in the ionization process). After the collision, at the energy of the ionization threshold, the scattered and ejected electrons have zero velocity and therefore zero orbital angular momentum. Hence only vacancy states with $M_L = 0$ can be excited, and we have a very similar threshold selection rule to that for optical excitation, that is

$$\sigma(n, L, M_L \neq 0) = 0. \quad (2)$$

However, the process is *not* simply one of ionization. It is possible to create a vacancy in an inner shell by exciting an electron to a discrete unfilled level. Because of the narrowness of the energy range occupied by such levels, the probability of this process is in general small compared with that of ionization, and if we use a collisional approximation such as the Born, which is in any case only valid for high impact energies, the error in ignoring excitation to discrete levels should be negligible. But as we approach the ionization threshold, the discrete excitations will become increasingly important, and the above threshold law will therefore be invalid.

Strictly speaking, then, the threshold energy will be the energy required to excite an electron to the first unoccupied outer level. Only if this level is an S state ($L = 0$) will the selection rule (2) still obtain. For $L \neq 0$, we have merely $\Delta M_L = 0$ for the transition, a restriction which will not lead to large ratios between the cross sections for producing

vacancy states with different M_L . Even if the first unoccupied outer level should be an S state, the situation is complicated by the fact that the outer energy levels may be sufficiently close compared with the energy resolution of the incident electron beam that any large threshold polarization is effectively smeared out.

This very qualitative account is meant to indicate the more complicated nature of the threshold region in the x ray case and to guard against the facile application of a threshold selection rule derived from the optical excitation case. The remainder of this paper will deal with the region well above threshold, where these strictures do not apply.

3. The Bethe approximation

At sufficiently high energies of impact, the bulk of all ionizing collisions are due to small angle, 'glancing' collisions, that is collisions involving small momentum transfer, \mathbf{K} . This justifies replacing the exponential in the Born matrix element by its first two terms (see Mott and Massey 1965 p 497).

$$\exp(i\mathbf{K} \cdot \mathbf{r}) \simeq 1 + i\mathbf{K} \cdot \mathbf{r} \quad (3)$$

so that

$$|\langle \kappa l' m' | \exp(i\mathbf{K} \cdot \mathbf{r}) | nlm \rangle|^2 \simeq |\langle \kappa l' m' | (\mathbf{K} \cdot \mathbf{r}) | nlm \rangle|^2 \quad (4)$$

where (nlm) are the quantum numbers of the initial atomic state and $(\kappa l' m')$ those of a state in the continuum. Strictly speaking, the continuum state should represent the ejection of an electron in a particular direction. It can be demonstrated by expanding such a state in spherical harmonics that one arrives at the same result as in equation (6) below.

To measure the polarization we must choose our z axis along the direction of the incident electron. With this choice we have

$$\mathbf{K} \cdot \mathbf{r} = Kr(\cos \lambda \cos \theta + \sin \lambda \sin \theta \cos \phi) \quad (5)$$

where (θ, ϕ) are the polar angles of the vector \mathbf{r} and λ is the angle between \mathbf{K} and the quantization axis. We may arbitrarily set the azimuthal angle of \mathbf{K} equal to zero in these axes.

Substitution of (5) into (4) and summation over the angular momentum quantum numbers of the final state gives

$$\begin{aligned} & \sum_{l'm'} |\langle \kappa l' m' | (\mathbf{K} \cdot \mathbf{r}) | nlm \rangle|^2 \\ &= K^2 \cos^2 \lambda \{ |\langle \kappa l + 1 m | r \cos \theta | nlm \rangle|^2 + |\langle \kappa l - 1 m | r \cos \theta | nlm \rangle|^2 \} \\ & \quad + \frac{1}{2} K^2 \sin^2 \lambda \{ |\langle \kappa l + 1 m + 1 | r \sin \theta e^{i\phi} | nlm \rangle|^2 + |\langle \kappa l + 1 m - 1 | r \sin \theta e^{-i\phi} | nlm \rangle|^2 \\ & \quad + |\langle \kappa l - 1 m + 1 | r \sin \theta e^{i\phi} | nlm \rangle|^2 + |\langle \kappa l - 1 m - 1 | r \sin \theta e^{-i\phi} | nlm \rangle|^2 \}. \quad (6) \end{aligned}$$

The angular parts of these matrix elements can be evaluated simply (see Bethe and Salpeter 1957 p 432). Now we make the additional approximation $\lambda = \frac{1}{2}\pi$, that is the momentum transfer takes place perpendicular to the direction of incidence; this should hold good in the limit of high energies. Thus we find for the total ionization cross

section, on performing the integration over K ,

$$\sigma_{nlm}^i = \frac{4\pi a_0^2}{(T/Ry)} \left(\int_0^\infty \mathcal{R}_{nl}^{\kappa l+1} d\kappa \frac{(l+1)(l+2)+m^2}{2(2l+3)(2l+1)} + \int_0^\infty \mathcal{R}_{nl}^{\kappa l-1} d\kappa \frac{(l-1)(l+m^2)}{2(2l+1)(2l-1)} \right) \ln\left(\frac{4T}{Ry}\right) \tag{7}$$

where $\mathcal{R}_{nl}^{\kappa l'} = |\int_0^\infty R_{n'l'}(r)R_{nl}(r)r^3 dr|^2$, the R 's being the appropriate radial eigenfunctions. T is the kinetic energy of the incident electron and Ry the Rydberg energy.

We are concerned here with the ratio of the cross sections for ionization from different substates corresponding to the same subshell defined by the values of n and l . From (7) we can write such a ratio

$$\frac{\sigma_{nlm'}^i}{\sigma_{nlm}^i} = \frac{\int_0^\infty \mathcal{R}_{nl}^{\kappa l'+1} d\kappa \frac{(l+1)(l+2)+m'^2}{2(2l+3)(2l+1)} + \int_0^\infty \mathcal{R}_{nl}^{\kappa l'-1} d\kappa \frac{(l-1)(l+m'^2)}{2(2l+1)(2l-1)}}{\int_0^\infty \mathcal{R}_{nl}^{\kappa l+1} d\kappa \frac{(l+1)(l+2)+m^2}{2(2l+3)(2l+1)} + \int_0^\infty \mathcal{R}_{nl}^{\kappa l-1} d\kappa \frac{(l-1)(l+m^2)}{2(2l+1)(2l-1)}} \tag{8}$$

Note that, in the high energy limit, this ratio is independent of incident electron energy. To evaluate the ratio for given values of n , l , and m in a particular atom, we must first make some assumptions about the form of the radial atomic wavefunctions. We shall postpone consideration of this until § 5.

4. The Born approximation

The Born amplitude for a transition from an initial state to a final state is proportional to the matrix element (sometimes called the atomic form factor)

$$\langle f | \exp(i\mathbf{K} \cdot \mathbf{r}) | i \rangle. \tag{9}$$

In the ionization process we wish to consider, i is a state labelled by the quantum numbers n , l and m , where the axis of quantization is as defined above. For the innermost shells of the heavier atoms, the deviation of the potential from Coulomb shape is small, and to a good approximation we may use hydrogenic eigenstates with the appropriate screening. f is a state of the continuous spectrum in which the atomic electron is moving in a particular direction in the field of a charge $+Z'e = +(Z-s)e$, where Z is the nuclear charge and s the screening factor for the subshell. From general symmetry considerations we can say that the 2p state is the first state, going out from the nucleus, capable of giving rise to polarized x rays. Calculations of cross sections for ionization from the 2p state of a hydrogen like system in the Born approximation have been carried out by several investigators (Burhop 1940, Mandl 1952, Swan 1955, McCrea and McKirgan 1960, and Omidvar 1965). However, in all of these the quantization axis is taken as parallel to the momentum transfer vector. This is done to simplify the evaluation of the matrix element (9), since $\exp(i\mathbf{K} \cdot \mathbf{r})$ becomes simply $\exp(iKr \cos \theta)$. As long as the cross section is averaged over m , this procedure leads to no difficulty. But if we are interested in a particular value of m , the total cross section is physically meaningless, since \mathbf{K} , the quantization axis, is itself a function of incident electron energy.

In what follows, a method is shown of relating ionization cross sections from particular magnetic substates to a fixed axis of quantization along the direction of the

incident beam of electrons. To avoid confusion, we shall label magnetic quantum states taken with respect to axis \mathbf{K} by μ , those taken with respect to \mathbf{k} (the wavevector of the incident electron) by m . If we consider these two sets of axes as coinciding when one set is rotated in the appropriate direction through an angle about their common y axis, we obtain the following relation between the two sets of quantum states $|nlm\rangle$ and $|nl\mu\rangle$:

$$|nlm\rangle = \sum_{\mu} \mathcal{D}_{m\mu}^{(l)}(0\lambda 0) |nl\mu\rangle \quad (10)$$

where the rotation matrix element $\mathcal{D}_{m\mu}^{(l)}(\alpha\beta\gamma)$ is as defined by Edmonds (1960).

Hence we have

$$\langle f | \exp(i\mathbf{K} \cdot \mathbf{r}) |nlm\rangle = \sum_{\mu} \mathcal{D}_{m\mu}^{(l)}(0\lambda 0) \langle f | \exp(i\mathbf{K} \cdot \mathbf{r}) |nl\mu\rangle. \quad (11)$$

The cross section is proportional to

$$|\langle f | \exp(i\mathbf{K} \cdot \mathbf{r}) |nlm\rangle|^2 = \sum_{\mu, \mu'} \mathcal{D}_{m\mu}^{*(l)} \mathcal{D}_{m\mu'}^{(l)} \langle nl\mu' | \exp(-i\mathbf{K} \cdot \mathbf{r}) |f\rangle \langle f | \exp(i\mathbf{K} \cdot \mathbf{r}) |nl\mu\rangle. \quad (12)$$

The differential cross sections for the cases $(2p, 0)$ and $(2p, \pm 1)$ which Burhop and others calculate are in effect the diagonal elements of the matrix defined by the right hand side of equation (12) (apart, that is, from the rotation matrix elements). We have to evaluate also the off-diagonal elements. As it happens, a detailed consideration of the matrix elements shows that these off-diagonal terms vanish when one integrates over all directions of ejection of the atomic electron. So we may write

$$\int |\langle f | \exp(i\mathbf{K} \cdot \mathbf{r}) |nlm\rangle|^2 d\omega(\hat{\mathbf{K}}) = \sum_{\mu} |\mathcal{D}_{m\mu}^{(l)}(0\lambda 0)|^2 \int |\langle f | \exp(i\mathbf{K} \cdot \mathbf{r}) |nl\mu\rangle|^2 d\omega(\hat{\mathbf{K}}) \quad (13)$$

or, alternatively,

$$f_E(K; nlm) = \sum_{\mu} |\mathcal{D}_{m\mu}^{(l)}(0\lambda 0)|^2 f_E(K; nl\mu) \quad (14)$$

where

$$f_E(K; nlm) = \frac{E/Ry}{(Ka_0)^2} \int |\langle f | \exp(i\mathbf{K} \cdot \mathbf{r}) |nlm\rangle|^2 d\omega(\hat{\mathbf{K}}) \quad (15)$$

is the generalized oscillator strength, E being the energy transfer in the collision. Note that in this case $f_E(K)$, usually valuable precisely because of its independence of incident particle energy, is here dependent on the energy of the collision through the angle λ , which is itself related to the energy:

$$\cos^2 \lambda = \frac{\{(Ka_0)^2 + E/Ry\}^2}{4(Ka_0)^2 T/Ry}. \quad (16)$$

We use $f_E(K)$ here for the sake of brevity.

For the $2p$ state, evaluating the rotation matrix elements yields the relations

$$f_E(K; 2p, m = 0) = \cos^2 \lambda f_E(K; 2p, \mu = 0) + \sin^2 \lambda f_E(K; 2p, \mu = \pm 1) \quad (17a)$$

and

$$f_E(K; 2p, m = \pm 1) = \frac{1}{2}(1 + \cos^2 \lambda) f_E(K; 2p, \mu = \pm 1) + \frac{1}{2} \sin^2 \lambda f_E(K; 2p, \mu = 0). \quad (17b)$$

The $f_E(K)$ for a hydrogenic system of effective charge Z' are of the general form

$$f_E(K; nl\mu) = \xi_{nlm} \left\{ 1 - \exp\left(-\frac{2\pi Z'}{\kappa a_0}\right) \right\}^{-1} \times \exp\left\{-\frac{2Z'}{\kappa a_0} \arctan\left(\frac{2\kappa a_0/nZ'}{Q - (\kappa a_0/Z')^2 + 1/n^2}\right)\right\} \quad (18)$$

where $Q = (\kappa a_0/Z')^2$ and κh is the momentum of the ejected electron. We obtain from the work of Banks *et al* (1969) in conjunction with that of Vriens and Bensen (1968), the expressions

$$\xi_{2p,\mu=0} = \frac{4\epsilon}{15\{(\epsilon - Q)^2 + Q\}^5} \{7(\epsilon - Q)^4 + (64Q + 4)(\epsilon - Q)^3 + (192Q^2 + 54Q)(\epsilon - Q)^2 + 80Q^2(\epsilon - Q) + 15Q^2\} \quad (19a)$$

and

$$\xi_{2p,\mu=\pm 1} = \frac{4\epsilon}{15\{(\epsilon - Q)^2 + Q\}^4} \{4(\epsilon - Q)^2 + (28Q + 3)(\epsilon - Q) + 24Q^2 + 18Q\} \quad (19b)$$

where $\epsilon = E/Z'^2 R_y$. Hence by means of equations (16), (17a), (17b), (18), (19a) and (19b) we have defined $f_E(K; 2p, m = 0)$ and $f_E(K; 2p, m = \pm 1)$ in terms of Q, ϵ and $t (= T/Z'^2 R_y)$. To obtain the total cross section we require the relation

$$\sigma = \frac{4\pi a_0^2}{tZ'^2} \int_{Q_{\min}}^{Q_{\max}} \int f_E(K) \frac{dQ}{Q} \frac{d\epsilon}{\epsilon} \quad (20)$$

where

$$Q_{\min} = 2t - \epsilon - 2t(1 - \epsilon/t)^{1/2} \quad (21a)$$

and

$$Q_{\max} = 2t - \epsilon + 2t(1 - \epsilon/t)^{1/2} \quad (21b)$$

from the kinematics of the collision process.

The double integration in (20) must be performed numerically for each value of t of interest. The resulting total cross sections are shown in the following section.

5. Results

5.1. Bethe approximation

Equation (8) becomes for the particular case of an initial 2p state:

$$\frac{\sigma_{2p0}^i}{\sigma_{2p\pm 1}^i} = \frac{\int \mathcal{R}_{2p}^{\kappa d} d\kappa \cdot \frac{1}{5}}{\int \mathcal{R}_{2p}^{\kappa d} d\kappa \cdot \frac{7}{30} + \int \mathcal{R}_{2p}^{\kappa s} d\kappa \cdot \frac{1}{6}} \quad (22)$$

To obtain a numerical value for the ratio we must make some assumption about the wavefunctions. If we take them to be hydrogenic and use the data of Bethe and Salpeter

(1957 p 350) for the radial matrix elements, we find

$$\frac{\sigma_{2p0}^i}{\sigma_{2p\pm 1}^i} = 0.814. \quad (23)$$

This ratio is independent of both t and Z' . The percentage polarization of radiation is defined as

$$P = 100 \frac{I^{\parallel} - I^{\perp}}{I^{\parallel} + I^{\perp}}$$

where I^{\parallel} is the intensity of radiation with electric vector aligned parallel to the quantization axis, and I^{\perp} the intensity with electric vector perpendicular to the same axis, the direction of observation in both cases being at right angles to the axis. Now I^{\parallel} and I^{\perp} depend on the optical transition probabilities and on the population of atoms with vacancies in the different substates, the latter being proportional to the ionization cross sections for these substates. Since there is a substantial spin-orbit interaction, the substates in question are designated by the quantum numbers n, l, j, m_j . The ionization cross sections for these substates must therefore be expressed in terms of those for substates designated by n, l, m . This may be done using vector coupling coefficients. When these coefficients are evaluated, together with the appropriate optical transition probabilities, for the particular case of ionization from the L_3 sublevel, the resulting expressions for P are as follows:

$$P(L_l) = P(M_1 \rightarrow L_3) = 300 \frac{\sigma_0 - \sigma_1}{5\sigma_0 + 7\sigma_1} \quad (24a)$$

$$P(L_{\alpha_1}) = P(M_5 \rightarrow L_3) = 100 \frac{\sigma_0 - \sigma_1}{7\sigma_0 + 13\sigma_1} \quad (24b)$$

$$P(L_{\alpha_2}) = P(M_4 \rightarrow L_3) = 300 \frac{\sigma_1 - \sigma_0}{4\sigma_0 + 11\sigma_1} \quad (24c)$$

where we have used the abbreviations $\sigma_0 = \sigma_{2p0}^i$ and $\sigma_1 = \sigma_{2p\pm 1}^i$. Thus, in the limit of high energies

$$P_{\infty}(L_l) = -5.04\% \quad (25a)$$

$$P_{\infty}(L_{\alpha_1}) = -1.00\% \quad (25b)$$

$$P_{\infty}(L_{\alpha_2}) = +3.91\%. \quad (25c)$$

These polarization are small, whereas P_{∞} for many optical transitions is large. It is possible to gain some physical insight into this result as follows.

As the collision energy becomes large, the momentum transfer is virtually at right angles to the direction of incidence. This means that any transitions which result from the collision must obey the selection rule

$$\Delta m = \pm 1. \quad (26)$$

This is true for both optical excitation and inner shell ionization. In the latter case, the only transitions into the continuum in the Bethe limit are those which are optically allowed. This situation is illustrated in figure 1. In (a) we see that, notwithstanding the selection rule, transitions from all magnetic substates into the continuum are possible.

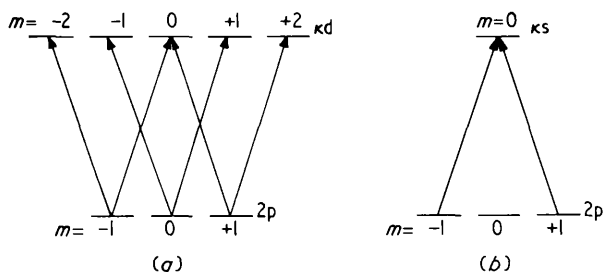


Figure 1. Bound-free transitions from the 2p level in the Bethe limit. The selection rule $\Delta m = \pm 1$ means that, in case (b) the ionization cross section from the state $(2p, m = 0)$ is zero.

In (b), however, transitions from the state $(2p, m = 0)$ are forbidden. In this case the vacancy distribution after the collision will be highly unequal and the polarization of the characteristic x rays large. That the polarization is in fact small is a result of the inequality

$$\int \mathcal{R}_{nl}^{\kappa l+1} d\kappa \gg \int \mathcal{R}_{nl}^{\kappa l-1} d\kappa \quad (27)$$

where the radial eigenfunctions are hydrogenic.

5.2. Born approximation

The total cross sections $\sigma(2p, m = 0)$ and $\sigma(2p, m = \pm 1)$, as calculated from the expression (20) above, are shown in figure 2. They are given in scaled units of $\pi a_0^2/Z^4$. The cross sections intersect at around 16 times the threshold energy. They intersect again on the low energy side of the peak, as can be seen more clearly in figure 3, which gives the

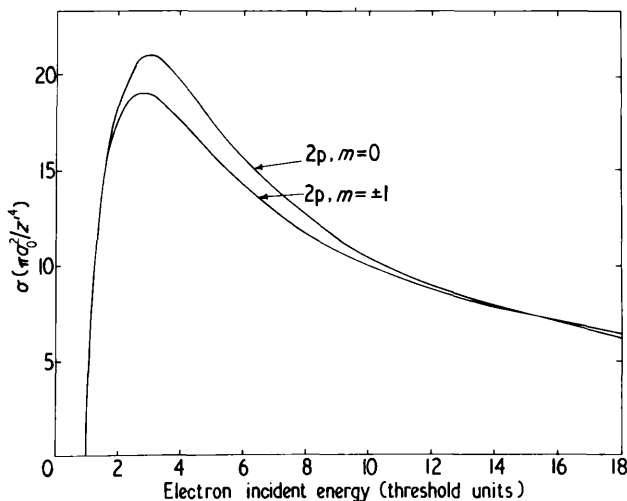


Figure 2. Ionization cross sections from the hydrogenic states $(2p, m = 0)$ and $(2p, m = \pm 1)$ in the Born approximation, referred to a quantization axis aligned parallel to the direction of electron incidence.

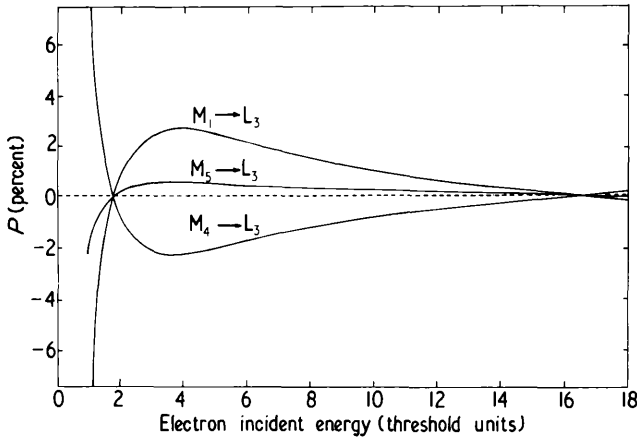


Figure 3. Percentage polarization of the lines $L_{\alpha_1}(M_5 \rightarrow L_3)$, $L_{\alpha_2}(M_4 \rightarrow L_3)$ and $L_I(M_1 \rightarrow L_3)$ as a function of electron incident energy. The calculation uses the cross section data shown in figure 2.

polarization of the lines L_I , L_{α_1} , and L_{α_2} as a function of collision energy. There seems to be no physical justification for this low velocity behaviour, which can probably be safely ascribed to the inadequacy of the Born approximation in this region.

At this point we should mention that figures 2 and 3 are in sharp disagreement with the published results of Mehlhorn (1968). Mehlhorn's calculated polarizations are substantially larger for all incident electron energies shown, do not change sign anywhere in this range, and appear to be tending to very different high energy limits. It appears that Mehlhorn's results can be accounted for on the assumption that his collision cross sections are referred to a momentum transfer quantization axis. This has been confirmed by Mehlhorn (private communication).

In further support of the present results, two checks have been carried out. The cross section ratio for the Bethe limit was obtained by setting $K = 0$ in equation (20) and performing the integration over ϵ . The result was

$$\frac{\sigma(2p, m = 0)}{\sigma(2p, m = \pm 1)} = 0.81161 \tag{28}$$

in good agreement with (23). Also, the corresponding expressions for $f_E(K)$ in the binary encounter (classical impulse) theory (see Burgess and Percival 1968, or Vriens 1969) were calculated for the particular case $\lambda = \frac{1}{2}\pi$ and checked with the previous unpublished calculations of Banks (1968 private communication). They are:

$$f_E(K; 2p, m = 0) = \frac{16}{5\pi} \frac{\epsilon Q^{5/2}}{\{(\epsilon - Q)^2 + Q\}^4} \tag{29a}$$

and

$$f_E(K; 2p, m = \pm 1) = \frac{8}{5\pi} \frac{\epsilon Q^{5/2} \{9(\epsilon - Q)^2 + Q\}}{\{(\epsilon - Q)^2 + Q\}^5}. \tag{29b}$$

Setting $\lambda = \frac{1}{2}\pi$ in equations (17a) and (17b), it can be shown graphically that they agree well with (29a) and (29b) respectively, in the limit of large Q and ϵ , as the work of Vriens and Bonsen (1968) shows they must.

6. Comments

Both Bethe and Born calculations concur in suggesting that the polarization of characteristic x radiation resulting from electron impact is small over the intermediate to high range of collision energies. However, in the Bethe case we saw that this conclusion is a result of the inequality (27), and such radial matrix elements tend to be highly sensitive to the form of the wavefunctions, so that a small deviation from the Coulomb shape which we assume might lead to significantly different results.

In appraising the validity of the foregoing simple theory, it should be remembered that it neglects several effects which may have an important influence. Firstly, it takes no account of the phenomenon of radiationless or Auger transitions (see Burhop 1952), which may seriously alter the primary vacancy distribution due to the collision, and hence the polarization. Secondly, it ignores the effect of focussing and acceleration by the highly charged nucleus on the incoming electron, which must pass close to the nucleus to ionize from an inner shell. Thirdly, and perhaps most importantly, the theory makes no allowance for the effects of relativity. Even for Z as low as 30, the velocity of an L shell electron is $\sim 0.1c$, and for the Born to be valid the incident electron must be at least two or three times faster. It is hoped to take some account of relativity in a future paper.

Acknowledgments

The author would like to thank Professor I C Percival for initiating this research and for many extremely helpful discussions, Mr J Wilson for his help in programming the numerical work, and the Science Research Council for providing a Research Studentship.

References

- Banks D, Vriens L and Bensen T F M 1969 *J. Phys. B: Atom. molec. Phys.* **2** 976–83
 Bethe N A and Salpeter E E 1957 *Encyclopedia of Physics* Vol 35 ed S Flügge (Berlin: Springer-Verlag)
 Burgess A and Percival I C 1968 *Advances in Atomic and Molecular Physics* eds Bates and Estermann (New York: Academic Press) 120–22
 Burhop E H S 1940 *Proc. Camb. Phil. Soc.* **36** 43–9
 ——— 1952 *The Auger Effect and Other Radiationless Transitions* (London: Cambridge University Press)
 Edmonds A R 1960 *Angular Momentum in Quantum Mechanics* (Princeton NJ: Princeton University Press)
 Hrdý J, Henins A and Bearden J A 1970 *Phys. Rev. A* **2** 1708–11
 Kleinpoppen H 1969 *Physics of the One- and Two-Electron Atoms* eds Bopp and Kleinpoppen (Amsterdam: North-Holland) 612–31
 Mandl F 1952 *AERE Report T/R1006*
 McCrea D and McKirgan T V M 1960 *Proc. Phys. Soc.* **75** 235–42
 Mehlhorn W 1968 *Phys. Lett.* **26A** 166–7
 Mott N F and Massey H S W 1965 *Theory of Atomic Collisions* (Oxford: Clarendon Press)
 Omidvar K 1965 *Phys. Rev.* **140** A26–37
 Percival I C and Seaton M J 1958 *Phil. Trans. R. Soc. A* **251** 113–38
 Swan P 1955 *Proc. Phys. Soc.* **A68** 1157–60
 Vriens L and Bensen T F M 1968 *J. Phys. B: Atom. molec. Phys.* **1** 1123–9
 Vriens L 1969 *Case Studies in Atomic Collision Physics I* eds McDaniel and McDowell (Amsterdam: North-Holland), 335–98